

INVESTIGATIONS OF A FOUR-STROKE
FLEXIBLE VALVE TIMINGS SYSTEM



MUHAMMAD HAZIQ ADHAM BIN ROSLI

اونيورسيتي مليسيا قهغ

UNIVERSITI MALAYSIA PAHANG

MASTER OF SCIENCE

UNIVERSITI MALAYSIA PAHANG

UNIVERSITI MALAYSIA PAHANG

DECLARATION OF THESIS AND COPYRIGHT

Author's Full Name : MUHAMMAD HAZIQ ADHAM BIN ROSLI

Date of Birth : 4TH NOVEMBER 1994

Title : INVESTIGATIONS OF A FOUR-STROKE
FLEXIBLE VALVE TIMINGS SYSTEM

Academic Session : SEMESTER 2 2020/2021

I declare that this thesis is classified as:

- CONFIDENTIAL (Contains confidential information under the Official Secret Act 1997)*
- RESTRICTED (Contains restricted information as specified by the organization where research was done)*
- OPEN ACCESS I agree that my thesis to be published as online open access (Full Text)

I acknowledge that Universiti Malaysia Pahang reserves the following rights:

1. The Thesis is the Property of Universiti Malaysia Pahang
2. The Library of Universiti Malaysia Pahang has the right to make copies of the thesis for the purpose of research only.
3. The Library has the right to make copies of the thesis for academic exchange.

Certified by:



(Student's Signature)



(Supervisor's Signature)

MUHAMMAD HAZIQ ADHAM BIN
ROSLI
941104-07-5037
Date: 22/03/21

Ts. Dr. MOHD RAZALI BIN
HANIPAH
Date: 22/03/21

NOTE : * If the thesis is CONFIDENTIAL or RESTRICTED, please attach a thesis declaration letter.

SUPERVISOR'S DECLARATION

I hereby declare that I have checked this thesis and in my opinion, this thesis is adequate in terms of scope and quality for the award of the degree of Master of Science.



(Supervisor's Signature)

Full Name : Ts. Dr. MOHD RAZALI BIN HANIPAH
Position : SENIOR LECTURER
Date : 22/03/2021



UMP

اونيورسيتي ملايسيا قهغ

UNIVERSITI MALAYSIA PAHANG

STUDENT'S DECLARATION

I hereby declare that the work in this thesis is based on my original work except for quotations and citations which have been duly acknowledged. I also declare that it has not been previously or concurrently submitted for any other degree at Universiti Malaysia Pahang or any other institutions.



(Student's Signature)

Full Name : MUHAMMAD HAZIQ ADHAM BIN ROSLI

ID Number : MMA18002

Date : 22/03/2021

UMP

اونيورسيتي ملايسيا قهغ

UNIVERSITI MALAYSIA PAHANG

INVESTIGATIONS OF A FOUR-STROKE FLEXIBLE VALVE TIMINGS
SYSTEM

The logo of the University of Malaysia Pahang (UMP) is a shield-shaped emblem. It features a central white diamond with a yellow diamond inside it, surrounded by a blue and green circular swirl. The shield is divided into four quadrants: top-left is teal, top-right is light blue, bottom-left is light blue, and bottom-right is teal. The letters 'UMP' are written in white across the center of the shield.

MUHAMMAD HAZIQ ADHAM BIN ROSLI

Thesis submitted in fulfillment of the requirements
for the award of the degree of
Master of Science

اونيورسيتي ملايسيا قهغ

UNIVERSITI MALAYSIA PAHANG

College of Engineering

UNIVERSITI MALAYSIA PAHANG

MARCH 2021

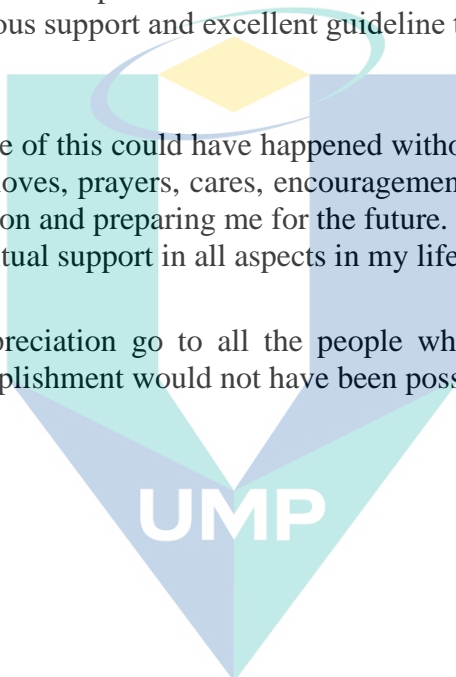
ACKNOWLEDGEMENTS

First and foremost, praises and thanks to God, the Almighty, for his showers of blessings, providing me this opportunity, and granting the capability for me to accomplish this project and thesis. This thesis appears in its current form due to assistance and guidance from several people that continuously giving me immeasurable support throughout the progress of this project. I would therefore like to express my sincere and deep appreciation to these individuals for their goodwill.

I would like to deliver my sense of gratitude to both of my Master Degree's supervisors Dr. Mohd Razali Bin Hanipah from Universiti Malaysia Pahang for giving me consultations, continuous support and excellent guideline throughout the entire project's period.

Most importantly, none of this could have happened without my family. I am extremely grateful to have their loves, prayers, cares, encouragements, supports and sacrifices for the sake of my education and preparing me for the future. I would like to thank them for their material and spiritual support in all aspects in my life.

My gratitude and appreciation go to all the people who have supported directly or indirectly. This accomplishment would not have been possible without each of them.



اونيورسيتي مليسيا قهغ

UNIVERSITI MALAYSIA PAHANG

ABSTRAK

Teknologi pemasaan injap berubah-ubah (VVT) telah berjaya menunjukkan keberkesanan meningkatkan prestasi enjin pembakaran dalaman (IC). VVT menawarkan kawalan tambahan pada pernafasan enjin agar keadaan operasi enjin dapat disesuaikan dengan lebih tepat, menjadikan output dan prestasi diperkuat. Bagaimana pun, masih terdapat ruang untuk penambahbaikan dalam teknologi VVT ini. Tujuan penyelidikan ini ialah untuk melakukan siasatan ke atas enjin empat lejang menggunakan alat berangka satu dimensi dibentangkan. Falsafah lejang masukan dan ekzos untuk pemasaan injap berubah-ubah telah diselidiki melalui teknik pengoptimuman. Akhir sekali, prestasi enjin ditingkatkan dengan strategi pemasaan injap fleksibel (FVT) menggunakan alat statistik. Tujuan utamanya adalah untuk menunjukkan peningkatan prestasi enjin dapat dicapai dengan pelaksanaan strategi FVT. Model asas dibangunkan dengan menggunakan alat simulasi numerik satu dimensi berdasarkan spesifikasi enjin petrol empat lejang 65cc. Nilai pekali aliran masukan dan ekzos diperoleh dari eksperimen bangku aliran dengan nilai tertinggi masing-masing 0.397 dan 0.441. Dengan menggunakan spesifikasi dan parameter sebenar enjin, penilaian simulasi telah dijalankan. Model asas disahkan berdasarkan perbandingan spesifikasi dari data pengeluaran. Prestasi model enjin asas disiasat. Model ini menjalani pengubahsuaian prestasi untuk mendapatkan garis kuasa dan tork yang optimum untuk keseluruhan tahap kelajuan mesin. Pengoptimuman prestasi dilakukan melalui reka bentuk eksperimen (DOE) menggunakan matriks faktorial penuh dengan sasaran untuk meningkatkan prestasi model asas. Ini diperoleh melalui variasi masa injap masukan dan ekzos serta peningkatan maksimum menggunakan eksperimen faktorial penuh dengan tiga peringkat. Eksperimen DOE telah mengenal pasti beberapa profil FVT yang optimum. Hasilnya menunjukkan peningkatan daya brek hingga 11.49% dengan nilai maksimum dihasilkan ialah 2.52kW lebih berbanding model asa dengan nilai maksimum 2.3kW. Kecekapan isi padu ditingkatkan menghasilkan peningkatan BMEP dengan lebih dari 10%. Penggunaan bahan bakar dan kadar pelepasan gas juga menerima penambahbaikan dengan ketara menggunakan dengan pelaksanaan FVT. Beberapa strategi FVT telah dikenal pasti sebagai pemboleh ubah bermanfaat untuk meningkatkan prestasi enjin. EIVC dan EEVC menunjukkan impak positif pada kelajuan enjin yang lebih rendah, sementara LIVC, EIVO, dan LEVC pada kelajuan yang lebih tinggi. LEVO dan kenaikan injap masukan yang lebih tinggi bermanfaat pada semua kelajuan. LIVO dan EEVO tidak menunjukkan kesan positif terhadap prestasi enjin. Kesimpulannya, kajian ini telah menunjukkan potensi strategi FVT yang tinggi yang dapat meningkatkan prestasi enjin pada semua tahap kelajuan.

ABSTRACT

Variable valve timing (VVT) technology has been successful in enhancing internal combustion (IC) engine performance. VVT offers additional control on engine breathing so that the engine operating conditions may be tailored more precisely; hence, output and performance are amplified. VVT is one of the best ways to be implemented as it is cheap at cost and feasible without adding too much weight to the car. However, in VVT, there is a challenge within in order to provide the optimum valve lift profile. In this research, an investigation of a four-stroke spark ignition engine using a numerical tool is presented. The objectives carried in this research is, to investigate the engine performance characteristic of a four-stroke spark-ignition engine using a numerical tool by using real time data from benchwork experiment, to investigate the intake and exhaust performance characteristics for variable valve timing through optimization technique of improving engine performance and efficiency, to improve engine performance of flexible valve timing (FVT) strategies in tool using statistical analysis and design of experiment. The primary goal is to show engine performance boosting could be achieved by the implementation of FVT strategies. A numerical baseline model was developed using numerical simulation tool based on a 65cc four-stroke gasoline engine. The flow coefficient values of intake and exhaust ports were obtained from flow bench experiments with the highest value of 0.397 and 0.441 respectively. A simulation assessment has been conducted using the real specifications and parameters of an actual engine. The baseline model was validated against manufacturer specifications. The engine performances of the baseline model were investigated. This model undergone performance tuning to obtain the optimum power and torque curves for the whole engine speed range. Performance optimization was conducted through design of experiments (DOE) using full factorial matrix with the target of boosting the performance of the baseline model. This was obtained through the variation of intake and exhaust valves timing as well as maximum lift using a full factorial experiment with three levels. The DOE experiments have identified several optimum FVT profiles. The result has shown an increase of up to 11.49% in brake power with maximum 2.52kW produced compared to the baseline model with maximum value of 2.3kW. Volumetric efficiency is improved resulting in BMEP amplification with more than 10%. Fuel consumption and gas emissions rate are also improved significantly using the FVT application. Few FVT strategies have been identified as beneficial variables to boost engine performance. EIVC and EEVC are advantageous at lower engine speed, while LIVC, EIVO, and LEVC are advantageous at higher speed. LEVO and higher intake valve lift are beneficial at all speeds. LIVO and EEVO show no positive impact on engine performance. In conclusion, this study has shown high potential of FVT strategies which can improve engine performance over the whole range of engine speeds.

TABLE OF CONTENT

DECLARATION

TITLE PAGE

ACKNOWLEDGEMENTS **ii**

ABSTRAK **iii**

ABSTRACT **iv**

TABLE OF CONTENT **v**

LIST OF TABLES **viii**

LIST OF FIGURES **ix**

LIST OF SYMBOLS **xii**

LIST OF ABBREVIATIONS **xiii**

CHAPTER 1 INTRODUCTION **1**

1.1 Background of research 1

1.2 Problem statement 2

1.3 Objectives 4

1.4 Project scope 4

1.5 Summary 5

CHAPTER 2 LITERATURE REVIEW **6**

2.1 The internal combustion engine 6

2.1.1 Four-stroke engine cycle 7

2.1.2 Otto cycle 8

2.1.3 Atkinson and Miller cycles 10

2.2	The combustion process in an SI engine	15
2.3	Motion inside the cylinder	16
2.4	Engine performance parameters	17
2.4.1	Engine parameters	17
2.4.2	Performance parameters	21
2.4.3	Emissions	29
2.5	Poppet valve system	33
2.6	Variable valve timing	36
2.6.1	Valve overlap	38
2.6.2	Variable valve actuation	39
2.6.3	Applications of VVT	44
2.7	Design of Experiment	46
2.7.1	Factorial and Fractional Designs	48
2.8	Summary	50
CHAPTER 3 METHODOLOGY		51
3.1	Overview of Research	51
3.2	One-dimensional Simulation Tool	54
3.3	Baseline Engine Specifications	54
3.4	One-dimensional Modelling	55
3.5	Valve Lift Profile of Baseline Model	57
3.6	Valve Flow Coefficient	58
3.7	Flexible Valve Timing Strategies	59
3.8	Design of Experiment	62
CHAPTER 4 RESULTS AND DISCUSSION		64

4.1	Baseline port flow performance	64
4.2	Baseline model performance	67
4.3	FVT model optimization	71
4.3.1	Maximum BMEP as model response	73
4.3.2	Maximum volumetric efficiency as model response	74
4.3.3	Minimum BSFC as model response	76
4.3.4	Minimum CO emission as model response	77
4.3.5	Model response performances comparison	78
4.3.6	Response surface correlation for engine performance	82
4.3.7	Valve events sensitivity against engine response (Volumetric Efficiency)	88
4.3.8	Summary of ANOVA	90
4.4	FVT profiles for various engine speed	91
4.5	FVT Model Performance Result	95
CHAPTER 5 CONCLUSION		109
5.1	Conclusion	109
5.2	Future recommendations	111
REFERENCES		112
APPENDIX A PORT FLOW ASSESSMENT		120
APPENDIX B		121
APPENDIX C		122
APPENDIX D		123

LIST OF TABLES

Table 2.1	Variable valve timings targets and impacts	37
Table 2.2	Summary and comparison of the current variable valve control technologies in the market	41
Table 3.1	Baseline Engine Specifications	55
Table 3.2	Part Specifications of 1-D Baseline Model	56
Table 3.3	Valve Lift Profile Parameters of Baseline Model	57
Table 3.4	Design of Experiment Matrix	63
Table 4.1	Summary of performances result for maximum BMEP as the model response.	73
Table 4.2	Summary of performance result for volumetric efficiency as the model response.	75
Table 4.3	Summary of erformance result for minimum BSFC as the model response.	76
Table 4.4	Summary of performance result for CO emission as the model response.	77
Table 4.5	ANOVA Table for Engine Performance (Volumetric Efficiency)	90
Table 5.1	Intake Valve Flow Coefficient	120
Table 5.2	Exhaust Valve Flow Coefficient	120
Table 5.3	FVT Valve Lift Profile Parameters	121
Table 5.4	FVT Valve Lift Events Modifcation Attribute	122
Table 5.5	Summary of Positive Impact of Valve Timing Strategies on FVT Engine Performance	123
Table 5.6	Summary of Positive Impact of Valve Timing Strategy on Engine Performance	123

اونیورسیتی ملیسیا قهغ

UNIVERSITI MALAYSIA PAHANG

LIST OF FIGURES

Figure 2.1	Four-stroke cycle.	7
Figure 2.2	Actual (a) and ideal (b) four-stroke cycles with p-V diagrams.	9
Figure 2.3	p-V (a) and T-s (b) diagrams of ideal otto cycle.	10
Figure 2.4	Early (a) and late (b) intake valve closing.	12
Figure 2.5	A comparison of the standard Otto cycle with the Miller cycle.	13
Figure 2.6	A p–V diagram comparison of the Otto cycle and the Miller cycle	14
Figure 2.7	Cylinder geometry definitions for an engine with a flat top piston.	18
Figure 2.8	SI Wiebe combustion sub-model.	19
Figure 2.9	Heat release system.	20
Figure 2.10	Work per cycle calculation and IMEP representation from p-V diagram.	21
Figure 2.11	Forces acting on the crankshaft.	25
Figure 2.12	Variation in pollutant concentration with air-fuel-ratio	32
Figure 2.13	NO _x , HC and CO emissions over air-fuel ratio	33
Figure 2.14	Conventional valve cam timing system	34
Figure 2.15	Valve timing diagram for a four-stroke engine	35
Figure 2.16	p-V diagram for gas exchange processes	36
Figure 2.17	Variable valve timing philosophies.	38
Figure 2.18	Influence of valve overlap at (a) full-load and (b) idle.	39
Figure 2.19	Possibilities to influence engine characteristics by means of VVA	40
Figure 2.20	Combustion chamber volume at TDC and BDC	45
Figure 2.21	Full factorial (a) and one-half factorial (b) in three dimensions.	49
Figure 3.1	Methodology Flowchart	53
Figure 3.2	Engine Components Layout	54
Figure 3.3	Engine Structure of Baseline Model	55
Figure 3.4	One-dimensional Schematic of Baseline Model	56
Figure 3.5	Valve Lift Profile of Baseline Model	57
Figure 3.6	Engine Head Part for Flow Assessment	58
Figure 3.7	Engine head setup for flow coefficient experiments.	59
Figure 3.8	Flexible Valve Timing Strategies	61
Figure 3.9	DOE Strategy of 3 Level Full Factorial Experiment	62
Figure 4.1	Volume Flow Rate of Intake Port	64
Figure 4.2	Volume Flow Rate of Exhaust Port	64

Figure 4.3	Flow Coefficient of Intake Port	65
Figure 4.4	Flow Coefficient of Exhaust Port	65
Figure 4.5	Discharge Coefficient of Intake Port	66
Figure 4.6	Discharge Coefficient of Exhaust Port	66
Figure 4.7	Valve Flow Coefficient of Intake and Exhaust Valve of Baseline Model	67
Figure 4.8	Power Curve Validation from Tool Simulation	68
Figure 4.9	Valve Lift Profile and Volumetric Flow Rate	69
Figure 4.10	BMEP, Volumetric Efficiency, BSFC and Emissions of Baseline model	70
Figure 4.11	FVT Model Optimization Flowchart	72
Figure 4.12	Summary of performances result for maximum BMEP as the model response.	74
Figure 4.13	Summary of performance result for volumetric efficiency as the model response.	75
Figure 4.14	Summary of performance result for minimum BSFC as the model response.	76
Figure 4.15	Summary of performance result for minimum CO emission as the model response.	78
Figure 4.16	BMEP performance curve comparison	79
Figure 4.17	Volumetric efficiency performance curve comparison	80
Figure 4.18	BSFC performance curve comparison	81
Figure 4.19	CO performance curve comparison	82
Figure 4.20	Response Surface of BSFC (a) and CO (b) against BMEP and Volumetric Efficiency at 1000 RPM	83
Figure 4.21	Response Surface of BSFC (a) and CO (b) against BMEP and Volumetric Efficiency at 2000 RPM	83
Figure 4.22	Response Surface of BSFC (a) and CO (b) against BMEP and Volumetric Efficiency at 3000 RPM	84
Figure 4.23	Response Surface of BSFC (a) and CO (b) against BMEP and Volumetric Efficiency at 4000 RPM	84
Figure 4.24	Response Surface of BSFC (a) and CO (b) against BMEP and Volumetric Efficiency at 5000 RPM	85
Figure 4.25	Response Surface of BSFC (a) and CO (b) against BMEP and Volumetric Efficiency at 6000 RPM	85
Figure 4.26	Response Surface of BSFC (a) and CO (b) against BMEP and Volumetric Efficiency at 7000 RPM	86
Figure 4.27	Response Surface of BSFC (a) and CO (b) against BMEP and Volumetric Efficiency at 8000 RPM	87

Figure 4.28	Response Surface of BSFC (a) and CO (b) against BMEP and Volumetric Efficiency at 9000 RPM	87
Figure 4.29	Response Surface of BSFC (a) and CO (b) against BMEP and Volumetric Efficiency at 10 000 RPM	88
Figure 4.30	Main Effect Value of Valve Events against Engine Speed	89
Figure 4.31	Interaction Effect Value of Four Significant Interaction against Engine Speed	90
Figure 4.32	FVT Valve Lift Profile Curve from 1000 RPM to 2000 RPM	92
Figure 4.33	FVT Valve Lift Profile Curve at 3000 RPM	92
Figure 4.34	FVT Valve Lift Profile Curve from 4000 RPM to 5000 RPM	93
Figure 4.35	FVT Valve Lift Profile Curve at 6000 RPM	94
Figure 4.36	FVT Valve Lift Profile Curve at 7000 RPM above	95
Figure 4.37	Brake Mean Effective Pressure (BMEP) of FVT Model	96
Figure 4.38	Net Indicated Mean Effective Pressure (IMEP720) of FVT Model	97
Figure 4.39	Pumping Mean Effective Pressure (PMEP) of FVT Model	98
Figure 4.40	Brake Torque of FVT Model	99
Figure 4.41	Brake Power of FVT Model	100
Figure 4.42	Brake Power (HP) of FVT Model	100
Figure 4.43	Volumetric Efficiency of FVT Model	101
Figure 4.44	Brake Thermal Efficiency of FVT Model	102
Figure 4.45	Indicated Efficiency of FVT Model	103
Figure 4.46	Brake Specific Fuel Consumption (BSFC) of FVT Model	104
Figure 4.47	Air-Fuel Ratio of FVT Model	105
Figure 4.48	Carbon Monoxide Emission of FVT Model	106
Figure 4.49	Hydrocarbon Emission of FVT Model	107
Figure 4.50	Nitrogen Oxide Emissions of FVT Model	108

LIST OF SYMBOLS

ω	Angular Momentum
η	Efficiency
Θ	Degree of Angle
ρ	Density
τ	Torque
C_v	Flow Coefficient
G	Specific Gravity of Fluid
m_f	Mass of Fuel Consumption
\dot{m}_a	Actual Mass Flow Rate
\dot{m}_t	Theoretical Mass Flow Rate
n_c	Number of Cylinder
n_r	Number of Crankshaft Rotation

UMP

اونيورسيتي ملايسيا قهغ

UNIVERSITI MALAYSIA PAHANG

LIST OF ABBREVIATIONS

ABDC	After Bottom Top Dead Centre
AFR	Air-to Fuel Ratio
ATDC	After Top Dead Centre
BBDC	Before Bottom Top Dead Centre
BDC	Bottom Top Dead Centre
BMEP	Brake Mean Effective Pressure
BSFC	Brake Specific Fuel Consumption
BTDC	Before Top Dead Centre
CA	Crank Angle
CAD	Crank Angle Degree
CI	Compression Ignition
CO	Carbon Monoxide
CR	Compression Ratio
CV	Calorific Value
EEVC	Early Exhaust Valve Closing
EEVO	Early Exhaust Valve Opening
EGR	Exhaust Gas Recirculation
EIVC	Early Intake Valve Closing
EIVO	Early Intake Valve Opening
EV	Exhaust Valve
EVC	Exhaust Valve Closing
EVO	Exhaust Valve Opening
EVMAX	Maximum Exhaust Valve Lift
FMEP	Friction Mean Effective Pressure
HCCI	Homogeneous Charge Compression Ignition
HP	Horsepower
IMEP	Indicated Mean Effective Pressure
IV	Intake Valve
IVC	Intake Valve Closing
IVO	Intake Valve Opening
IVMAX	Maximum Intake Valve Lift

kW	kilowatts
LEVC	Late Exhaust Valve Closing
LEVO	Late Exhaust Valve Opening
LIVC	Late Intake Valve Closing
LIVO	Late Intake Valve Opening
MEP	Mean Effective Pressure
NEDC	New European Driving Cycle
NO _x	Nitrogen Oxide
p-V	Pressure-Volume
RPM	Revolution per Minute
SI	Spark Ignition
TDC	Top Dead Centre
TDCF	Top Dead Centre Firing
T-s	Temperature-Entropy
VD	Valve Diameter
VL	Valve Lift
VVA	Variable Valve Actuation
VVT	Variable Valve Timing
$W_{\text{Compression}}$	Compression Work
W_{Pumping}	Pumping Work
W_{Net}	Net Work
WOT	Wide Open Throttle

اونیورسیتی ملیسیا قهغ

UNIVERSITI MALAYSIA PAHANG

CHAPTER 1

INTRODUCTION

1.1 Background of research

The emissions regulation standards have been continuously improved due to increasing environmental concerns. It drives automotive manufacturers to produce cars that meet those standards. According to International Council on Clean Transportation in their policy update 2019, new cars CO₂ emissions, on average, have to reduce by 15% by 2025 and by 37.5% by 2030, relative to a 2021 baseline. Expressed in NEDC terms, using the current 2021 CO₂ target of 95 g/km as the baseline, these reductions would translate into a target value of 81 g/km (2025) and 59 g/km (2030) (ICCT 2019).

In addition, internal combustion engines are driven towards extinction as the demand for electric-powered vehicles has increased significantly. Thus, various means of improvement have been devised over the years in the area of internal combustion engines such as forced induction system, high end technology of injection system and combustion profile, weight reduction, cylinder deactivation and alternative fuel for combustion.

Several advanced combustion strategies were introduced to face the challenges of the energy conservation and emission reduction for internal combustion (IC) engines. One of the main strategies to improve the combustion processes of internal combustion engines (ICEs) is to discover useful ways to decrease exhaust emissions without major modifications to the design (Jabbar, Vaz et al. 2016).

Variable valve timing (VVT) has been identified as one of the crucial technologies to enhance internal combustion engine performance. VVT offers additional control means the engine operating conditions may be tailored more precisely; hence output and performance were amplified (Ma 1988). The flexibility of the valve timing

adjustment, duration, lift, or a combination of these could possibly result in an improvement to the performance, fuel economy and emissions of the SI engine (Turner, Kenchington et al. 2004, Lee and Chang 2017), improved engine braking, residual exhaust control, and cylinder deactivation (Halderman and Mitchell 2014).

The advantages of employing VVT are not limited to increased efficiency and reduced exhaust emissions, it also brings an augmentation to the engine performance without the help of any additional devices unless the Variable Valve Actuation (VVA) system to initiate the VVT mechanism. In addition, VVT is proven to improve the engine breathing in a wide range of speeds or conditions, leads to better performance, high efficiency and reduced emissions.

However, there are several limitations in VVT implementation, which make VVT an inadequate technique to achieve the optimum performance of the engines. This issue is due to the actuation system that is limited to a few valve profiles rather than providing wide variety of valve profiles that optimize the engine performance according to engine speeds and engine loads.

In this research, flexible valve timing (FVT) strategies are proposed as the solution in performance-boosting and utilize the full potential of valve lift profile variation technique as used in VVT, by providing extensive valve lift profiles throughout the whole range of engine speed to increase the performance. The superiority of the FVT system is aimed towards a fully flexible control of the intake and exhaust valve individually without any dependency on a camshaft. FVT is a camless technology to improve engine breathing, thus improve efficiency, performance, emissions and fuel consumption. The FVT consists of 12 strategies, which explained further in chapter 3. By using one or more of the FVT combination, a refined and tuned engine performance is achievable.

1.2 Problem statement

Since the emission regulation standards have continuously tightened from time to time by reason of environmental concern, it alerts automotive industry player to produce a car that is able to meet the standard set. The urge to this matter caused many consequences to the conventional IC engine in order to achieve the target. Electric powered cars, hybrid cars, engine downsizing and vehicle weight reduction have been

implemented in the production in order to meet the standards. Despite that, every approach carries a different kind of disadvantages which need to be recovered with another approach. VVT is one of the best ways to be implemented as it is cheap at cost and feasible without adding too much weight to the car. However, in VVT, there is a challenge within in order to provide the optimum valve lift profile.

From the past decade only Koenigsegg (Hoglund, Carlson et al. 2017) has ever produced an engine without a camshaft by patenting their internal combustion with pneumatic valve return spring. This FREEVALVE technology, according to Koenigsegg, can vary the valve opening point, valve closing point, and valve maximum lift depends on the engine speed and other few conditions. However, it has been seen that by using pneumatic valve return spring, the valve lift profile produced is square-shaped rather than a cam-shaped curve due to its law of actuation. Furthermore, a pneumatic spring will have to synchronize with engine speed and this matter will cause a complication when implemented at higher engine speed.

FVT is a method to encounter these problems. In FVT, an optimum valve lift profile will be determined at every level of engine speed. This study is aimed to conduct a numerical investigation of the impact of FVT on a downsized engine which focused on the study of determining the best strategy of valve timing to be used in different level of the speed range. The flexibility of the valve timing adjustment, duration, lift, or a combination of these could result in an improvement to the performance, fuel economy and emissions of the SI engine (Turner, Kenchington et al. 2004). The only challenge is to increase valve timing precision.

1.3 Objectives

Three objectives were defined in this project:

1. To evaluate the engine performance behaviour of a four-stroke spark-ignition engine using a validated one-dimensional numerical model from flowbench experiments.
2. To obtain the intake and exhaust performance characteristics for variable valve timing through multi-objective optimization technique.
3. To improve the engine performance output of the flexible valve timing (FVT) strategies using statistical analysis and design of experiment.

1.4 Project scope

In order to achieve the list of objectives above, there are a few constraints of scopes that must be achieved. The scopes of this project are:

1. A 65cc single cylinder four-stroke, air-cooled, normally aspirated is used as the baseline.
2. One-dimensional numerical model construction with actual geometrical dimensional and cam profile of the baseline engine.
3. A portflow performance assessment on the intake and exhaust flow coefficients data as model tuning.
4. The study focused on six valve timing variables and 12 strategies for flexible valve timing.
5. The design of experiment is three-level full factorial approach.

6. The objectives for engine output performance multi-objective optimization are to maximize brake mean effective pressure and volumetric efficiency while minimizing brake specific fuel consumption and carbon monoxide emission.

1.5 Summary

In this chapter, the introduction of this research and background of study has been presented. Problem statement and objectives of this study have been stated. The research scope has been clearly outlined. The next chapter covers the literature review for this research which mainly on the theoretical ideas of internal combustion engine, valve timing technology and studies, including previous work on the related topic.

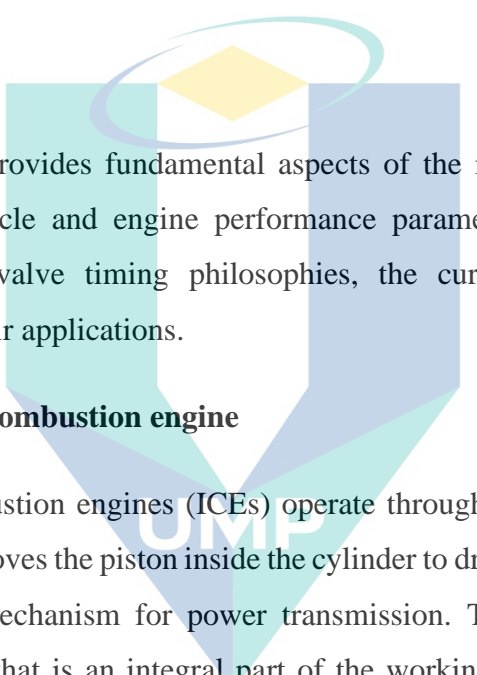


اونيورسيتي مليسيا قهغ

UNIVERSITI MALAYSIA PAHANG

CHAPTER 2

LITERATURE REVIEW



This chapter provides fundamental aspects of the internal combustion engine, four-stroke engine cycle and engine performance parameters. The literature review covers the variable valve timing philosophies, the current state of the art, key manufacturers and their applications.

2.1 The internal combustion engine

Internal combustion engines (ICEs) operate through the combustion of the air-fuel mixture, which moves the piston inside the cylinder to drive the crankshaft connected to the crank slider mechanism for power transmission. The fuel is ignited inside a combustion chamber that is an integral part of the working fluid flow circuit (Knight 2004). The expansion of the high temperature and high-pressure gases produced by combustion applies direct force to the piston head of the engine. The combustion pressure transferred the force to the piston to move downward, converting chemical energy into useful mechanical energy and produce work (Van Basshuysen and Schäfer 2004). ICEs are widely used in many applications such as road vehicles, boats, ships, airplanes, trains and stationary power plants.

A spark-ignition engine is an internal combustion engine, generally known as a petrol engine, where the air-fuel mixture is ignited by a spark plug during the combustion process. Whereas, the combustion process in compression ignition or Diesel engine is initiated by compression of the cylinder charge.

2.1.1 Four-stroke engine cycle

For the ICE to run continuously, a reciprocation motion must be sustained. This is possible through a four-stroke cycle that utilizes four distinct piston strokes, which are intake, compression, power, and exhaust, to complete one operating cycle. A stroke refers to the full travel of the piston from the top dead centre (TDC) to bottom dead centre (BDC). The piston makes two complete passes in the cylinder to complete one operating cycle. One cycle requires two revolutions of the crankshaft, which will add up to 720 angles of degree rotation.

Figure 2.1 shows the processes involve in one complete cycle of a four-stroke SI engine. In intake stroke, the intake valve opens to induct fuel and air mixture into the cylinder. A vacuum effect is created when the piston moves from TDC to BDC, drawing air into the combustion chamber.

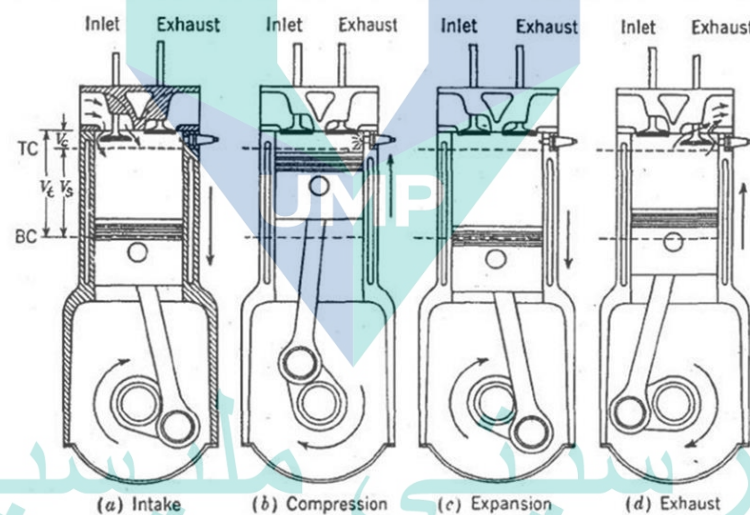


Figure 2.1 Four-stroke cycle.

Source: Jacobs (2017)

The exhaust valve remains closed throughout the stroke. In compression stroke, both the intake and exhaust valves are closed, sealing the cylinder and as the piston moves towards TDC, it compresses the trapped fuel-air mixture resulting in increase of pressure in the cylinder. The spark plug is ignited just before TDC, which ignites the compressed mixture to initiate the combustion process. In power stroke, both valves remain closed initially, the cylinder pressure increases and pushing the piston towards BDC to produce work. But when the piston almost at BDC, the exhaust valve opens to release the pressure

to reduce pumping work. The cylinder is still filled by the exhaust gases at a lower pressure at BDC. This process is called exhaust blowdown (Çengel and Boles 2014), and most combustion gases leave the cylinder by the time the piston reaches BDC. In exhaust stroke, burned fuel from combustion becomes useless after the completion of the expansion stroke and is made to escape through the exhaust valve to the atmosphere. The piston moves from BDC to TDC and the exhaust gases are driven out of the engine cylinder. This removal of gas is accomplished during this stroke.

2.1.2 Otto cycle

Otto cycle is named after Nikolaus A. Otto, a German engineer who had successfully built a four-stroke engine in 1876 in Germany using the cycle proposed by Frenchman Beau de Rochas (Çengel and Boles 2014) to represent an ideal thermodynamics cycle for spark-ignition reciprocating engines. This cycle is shown in Figure 2.2 (b), in comparison with the actual four-stroke cycle in Figure 2.2 (a). The ideal Otto cycle consists of four internally reversible processes represents isentropic compression (1-2), constant-volume heat addition (2-3), isentropic expansion (3-4), and constant-volume heat rejection (4-1). This curve represents what internal combustion engine ultimate performance goal, i.e., to match as close to the ideal cycle as possible.

اونيورسيتي ملايسيا قهغ

UNIVERSITI MALAYSIA PAHANG

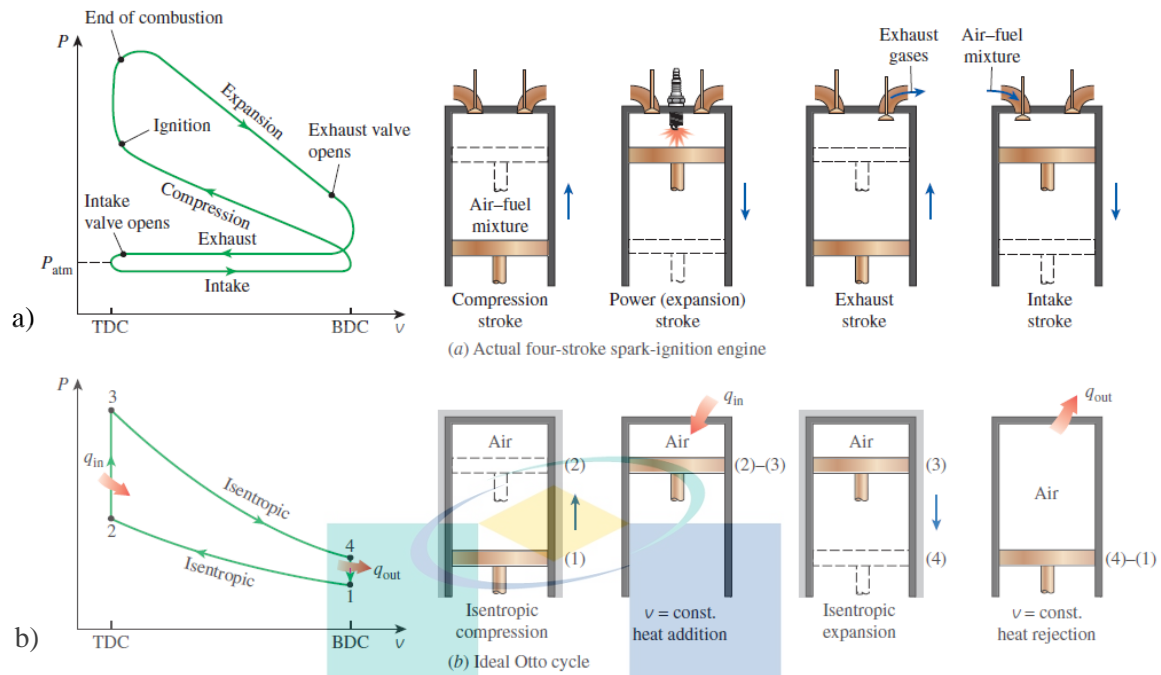


Figure 2.2 Actual (a) and ideal (b) four-stroke cycles with p-V diagrams.
Source: Çengel and Boles (2014)

Figure 2.3 shows p-V and T-s Diagrams of the ideal Otto cycle. In process 1-2, the piston moves from BDC to TDC position. Air undergoes isentropic compression thus, volume decreases, pressure and temperature increase. As this is an isentropic process, entropy remains constant. Process 2-3 represents an isochoric heat addition process; when the piston is at TDC, heat is added at constant volume. Temperature, pressure, and entropy increase. In process 3-4, air undergoes isentropic expansion, the piston is pushed from TDC to BDC position and increases the cylinder volume. Pressure and temperature decrease with entropy remains constant. In process 4-1, heat is rejected at constant volume, subsequently, pressure, temperature, and entropy fall.

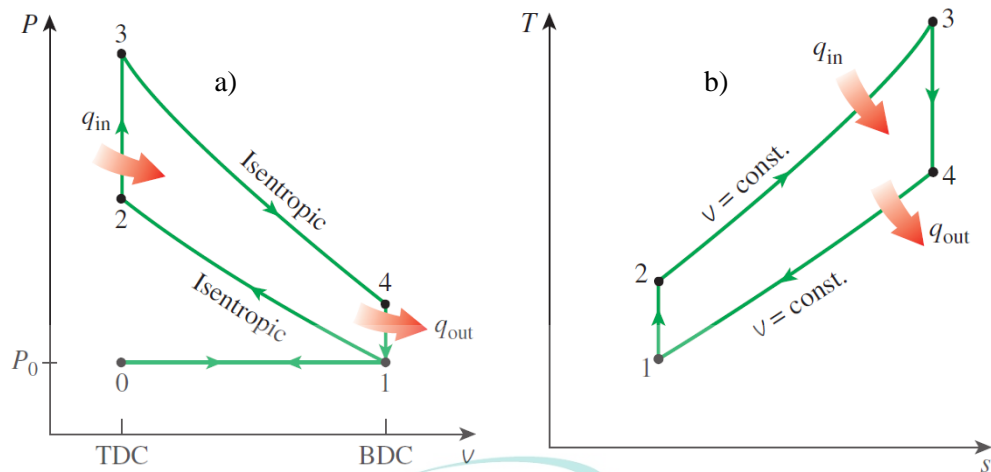


Figure 2.3 p-V (a) and T-s (b) diagrams of ideal otto cycle.

Source: Çengel and Boles (2014)

In addition, there are some differences between ideal and the actual cycle; pumping work exists in the actual cycle, which is the nett work done during exhaust and intake strokes. Furthermore, differences exist between exhaust and inlet pressure levels resulting in blowdown losses due to the early opening of the exhaust valve. Consequently, this has contributed to a loss of work output during the expansion stroke. Finally, the blow-by losses are caused by the leakage of combustion gases through piston rings and other crevices and frictional losses also found in the actual four-stroke engine cycle.

2.1.3 Atkinson and Miller cycles

Engine cycles in which the effective compression ratio is smaller than the effective expansion ratio is known as over-expanded cycles. Over-expanded cycles are commonly referred to as Miller or Atkinson invented by Ralph Miller (Miller 1956) and James Atkinson (Atkinson 1887), respectively.

In modern applications, over-expanded cycles are implemented with either early or late intake valve closing (EIVC or LIVC). The primary effect of EIVC and LIVC is a reduction in temperature at the end of the compression stroke. The lower temperature enables the use of higher geometric compression ratios that produce longer expansion ratios and better efficiency (Boretti and Scalzo 2011). The additional expansion would increase the amount of power in the expansion stroke, leading to an increase in engine thermal efficiency (Pulkrabek 1997). This is achievable through some mechanical

linkages which produce greater expansion ratio than the compression ratio, resulting in higher engine efficiency (Wang and Hou 2005).

In the Atkinson engine, the piston is not directly connected to the crankshaft like the typical four-stroke engine. It is connected through a mechanical linkage consist of a four-bar mechanism. In this way, the engine could implement longer expansion and exhaust strokes than its intake and compression strokes during its operating cycle. Higher thermal efficiency is achieved and a shorter compression stroke compared to the expansion stroke reduces the compression ratio (Zhao 2017).

Hou (2007) stated the Atkinson cycle has greater work output and higher thermal efficiency than the Otto cycle at the same operating conditions (Hou 2007). Pertl, Trattner et al. (2012) present a 15% increase in indicated engine efficiency of the Atkinson principle realized via crank train kinematics at Wide Open Throttle (WOT) operation. An increment of thermal efficiency of the small spark-ignition gas engine compared with the conventional engines due to the implementation of the Atkinson cycle was discovered (Shojaeefard and Keshavarz 2015).

Proposed variable Atkinson cycle hydraulic actuated valvetrain was realized for partial engine load operations, contributing to an average saving on the resulted BSFC at approximately 16.1 g/kW·h over the entire sampled speed-load map (Li, Khajepour et al. 2018).

Miller on the other hand was primarily interested in using intake valve closing timing to limit TDC temperatures. The Miller cycle is originated from the Atkinson cycle but it is actually a modified Otto cycle, as is called the Otto-Atkinson cycle in some literature (Luria, Taitel et al. 1982). Figure 2.4 shows the patented late and early valve timing diagrams for the Miller cycle.

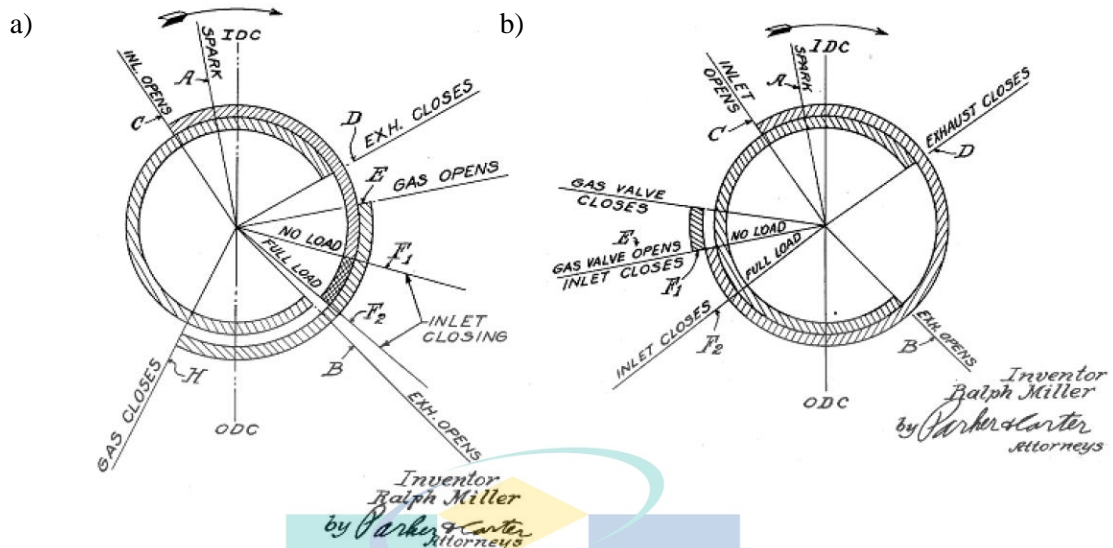


Figure 2.4 Early (a) and late (b) intake valve closing.
Source: Miller (1956)

He described variable intake valve timing mechanisms that allowed IVC to vary with engine load to control the in-cylinder temperature at the end of the compression stroke. While Miller mentions both early and late intake valve closings, he seemed to prefer closing the intake valve early while the cylinder volume was still increasing because additional expansion after intake valve closing could further cool the intake charge (Miller 1947). He referred to this as “internal cooling”. However, both EIVC and LIVC techniques lead to a smaller effective compression ratio.

A comparison of the standard Otto cycle with the Miller cycle is shown in Figure 2.5. For the Otto cycle, the compression ratio is identical to the expansion ratio, while in Miller cycle, the compression ratio is lower than the expansion ratio. Miller cycle inherits the additional intake blow-back at the beginning of the compression stroke that causes reverse flow out of the cylinder. From the p–V diagram of the Miller cycle, a higher engine-efficiency is expected with an increased expansion-ratio because more heat is changed to mechanical power (Wang, Lin et al. 2008). This was the primary idea behind the Miller cycle.

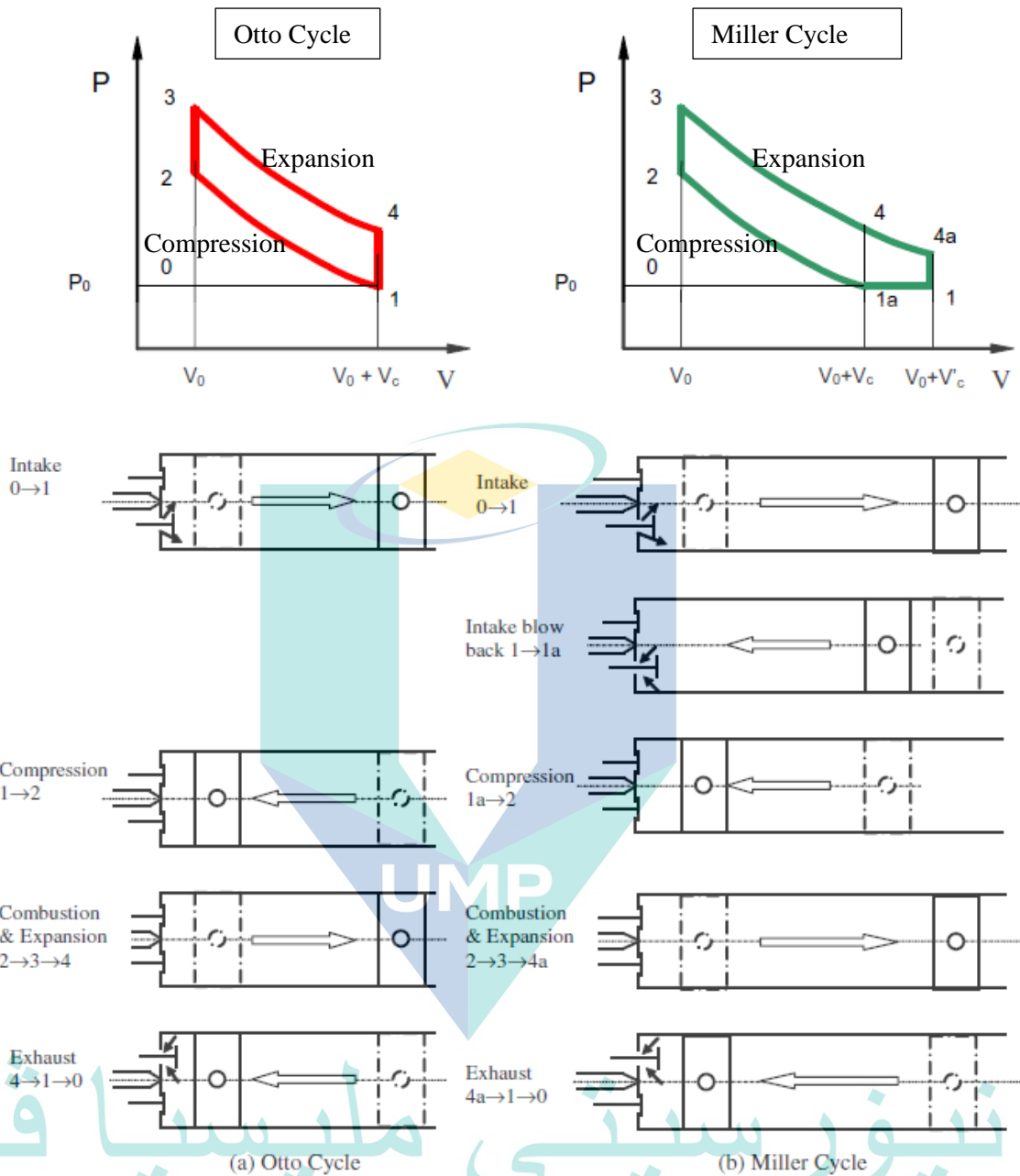


Figure 2.5 A comparison of the standard Otto cycle with the Miller cycle.

Source: Wang, Lin et al. (2008)

Figure 2.6 shows a p–V diagram comparison of the Otto cycle and the Miller cycle. The Miller cycle referred to as a “cold cycle”, thus the application of this attribute may reduce the temperature at the end of the compression process (at point 2 in the p–V diagram). Thus, it reduces the temperature at the end of the combustion process (point 3 in the p–V diagram). In the following decades, the concept of the Miller cycle was developed further with a focus on thermal efficiency (Braun, Klaas et al. 2018) and NOx

reduction (Kesgin 2005, Wang, Zeng et al. 2005) due to reduced combustion temperatures.

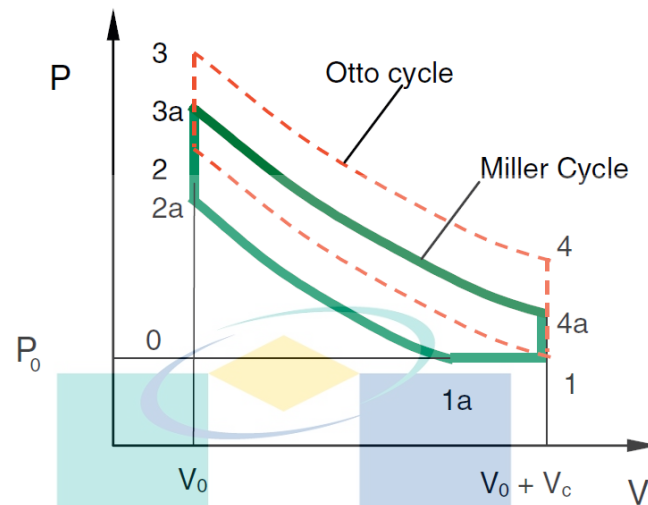


Figure 2.6 A p–V diagram comparison of the Otto cycle and the Miller cycle

Source: Wang, Lin et al. (2008)

Luo and Sun (2016) presented the Miller cycle with a turbocharged hydrogen engine. The Miller cycle not only shortens the compression, lengthens the expansion stroke, and improves the thermal efficiency but also significantly increases the power density using the turbocharging system. Miller cycle takes advantage of lower effective compression ratios compared to conventional Otto cycle engines. It leads to lower in-cylinder temperatures and reduced levels of NOx emissions (Martins and Lanzanova 2015).

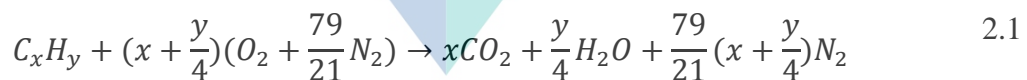
In a study to improve lean burned gas performance using the Miller cycle application, the most favourable effect is the NOx reduction in the case of EIVC and improve the engine efficiency without any reduction in power output due to supercharging and turbocharging utilization (Tavakoli, Jazayeri et al. 2016). In summary, Miller cycle can reduce pumping losses and NOx emissions, thus increase engine efficiency.

Wang, Zu et al. (2016) reported that the Miller cycle could improve fuel consumption only on the condition that the compression ratio and the IVC retardation angle were appropriately set. The improvement of fuel consumption performance by applying the Miller cycle is at the cost of power reduction (Wang, Zu et al. 2016).

2.2 The combustion process in an SI engine

Combustion is initiated by a spark produced between a set of electrodes as the piston approaches the top dead centre (TDC). The spark provides the necessary activation energy for the combustion reactions to begin. Combustion starts in the gap between the electrodes as a spherical nucleus of flame, often referred to as a 'flame kernel', which grows as the flame front propagates through the combustion chamber. The flame is extinguished upon arrival at the chamber walls, at which point approximately 90% of the cylinder contents have been burned (Heywood 1988). Further oxidation reactions continue on a smaller scale in the post-flame gases.

The efficiency and emissions of an internal combustion engine (ICE) are mainly driven by the combustion itself. The combustion process describes the exothermic conversion of chemically bonded energy into heat. In complete combustion, a hydrocarbon fuel C_xH_y reacts with oxygen O_2 to form carbon dioxide CO_2 and water vapour H_2O as describes in equation 2.1. Air, as the oxygen source, primarily contains nitrogen N_2 and is therefore found to a large extent in the exhaust gas. For combustion with excess air, exhaust gas also includes O_2 , whereas lack of O_2 results in unburnt hydrocarbons and carbon monoxide.



The most important factor in combustion is the overall time taken for the combustion process to occur. Assuming laminar flame propagation, the time taken to complete combustion would be an order of magnitude greater than that available in a typical IC engine. Thus, methods that improve flame propagation rates must be utilised. The primary method of reducing the time for combustion is by effective use of turbulence within the cylinder. Turbulence enhances combustion by 'wrinkling' the flame front, increasing the surface area of the flame to bring a greater quantity of fresh charge into the reaction zone (Stone 1992).

2.3 Motion inside the cylinder

In-cylinder charge motion and turbulence are mainly determined by the intake flow characteristics during the intake stroke (Ghauri 1999). The two motions tend to affect combustion to differing extents due to the behaviour of the flow as the piston approaches TDC. In the case of an axial swirl, the rising piston does not destroy the gas motion. In fact, the motion may be enhanced by the use of certain types of combustion chambers (pent-roof, for example), which induce an inward radially directed displacement (often referred to as squish).

The fact that the rotating charge is forced towards its axis causes its angular velocity to increase. In general, the swirl is not destroyed when combustion begins and may even persist well into the expansion stroke. Tumble differs fundamentally in that the motion suddenly degenerates into 'micro-turbulence' as the piston approaches TDC. This collapse of bulk flow is primarily due to the shape of the combustion chamber. The importance of this feature is that it ensures there is less chance of the flame kernel being swept away from its initial location.

Instead, the smaller scale of turbulence is more effective in wrinkling the flame front. Another feature of a tumble is that it is inherent to designs featuring two or more intake valves per cylinder. However, the required degree of in-cylinder motion can only be achieved by careful optimisation of the intake system, with the main aim being to keep the flow velocities high. Such an approach can be detrimental to high-speed performance, so inevitably, a compromise is required. The intensity and structure of the charge motion within the cylinder is predominantly a function of the intake port geometry (Stone 1992, Stone, Carden et al. 1993).

The coefficient of discharge is calculated to assess the efficiency of air flow (Sulaiman, Murad et al. 2010). The higher the coefficient value results in the better air flow into the engine (Zahidi, Hanipah et al. 2017). Thus, the coefficients give practical advice to engine designers and tuners on the sizing and location of ports and valves (Algieri 2011). The coefficient of discharge, C_D can be calculated by using equation 2.2.

$$C_D = \frac{\dot{m}_a}{\dot{m}_t} \quad 2.2$$

Where \dot{m}_a is the actual mass flow rate and \dot{m}_t is the theoretical mass flow rate. The actual mass flow rate can be calculated by using equation 2.3.

$$\dot{m}_a = Q \frac{P}{RT} \quad 2.3$$

Where Q is the volume flow rate, P is the local pressure, R is a gas constant of air and T is air temperature. While the theoretical mass flow rate can be calculated by using equation 2.4.

$$\dot{m}_t = \rho_s A_k V_s \quad 2.4$$

Where ρ_s is the air density, A_k is the valve seat area and V_s is flow velocity. The flow velocity can be calculated by using equation 2.5.

$$V_s = \sqrt{\frac{2\gamma}{\gamma-1} RT \left[1 - \left(\frac{P_2}{P_1} \right)^{\frac{\gamma-1}{\gamma}} \right]} \quad 2.5$$

Where P_1 is upstream pressure, P_2 is downstream pressure and γ is an index of isentropic expansion. As long as the flows remain in the subsonic region, no choked flow occurs in the design. The flow coefficient, C_f has same equation with C_D . But, it has different area calculation for \dot{m}_t in equation 2.4. For flow coefficient, the area is at the valve throat area.

2.4 Engine performance parameters

2.4.1 Engine parameters

The terms and definitions used in this section is a combination of information obtained from Heywood (Heywood 1988), Blair and Drouin (Blair and Drouin 1996) and Pulkrabek (Pulkrabek 1997) for internal combustion engines.

The definitions for the combustion chamber and cylinder geometry are shown in Figure 2.7. The diameter of the cylinder is the bore (B). The stroke (S) is defined as the distance travelled by the piston from (bottom dead center) BDC to (top dead center) TDC and the volume within the stroke is known as the swept volume (V_s). For a free-piston engine, the nominal stroke (S_{nom}) will be defined as the stroke length is not constant.

When the piston is at TDC, the remaining space between the top of the piston and the cylinder head is known as the clearance volume (V_c), which is contained within the clearance distance (c).

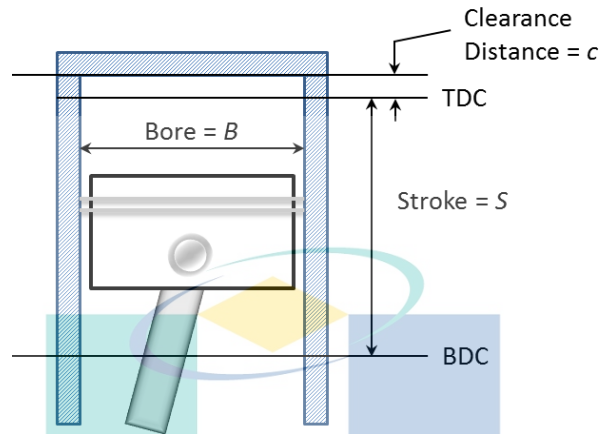


Figure 2.7 Cylinder geometry definitions for an engine with a flat top piston.
Source: Hanipah (2015)

Further parameters and definitions are given by the following equations:

- i. Swept volume, V_s :

$$V_s = \frac{(\pi B^2 S)}{4} \tag{2.6}$$

- ii. Geometric Compression Ratio, $(CR)_G$ is defined as:

$$(CR)_G = \frac{(V_s + V_c)}{V_c} \tag{2.7}$$

- iii. Woschni heat transfer:

The Woschni heat transfer sub-model can be used to calculate the amount of heat transfer to and from the cylinder charge. In this model, the charge is assumed to have a uniform heat flow coefficient and velocity on all surfaces of the cylinder.

$$h_g = 0.0128B^{-0.20}P^{0.80}T^{-0.53}v_c^{0.8}C_{enht} \tag{2.8}$$

The characteristic velocity is the sum of the mean piston speed and an additional combustion-related velocity that depends on the difference between the combustion and

motoring pressure. Further details on the characteristic velocity, as well as the variant of Woschni correlation can be obtained from (Heywood 1988).

iv. SI Wiebe Combustion

To model the combustion occurring in the cylinder, the SI Wiebe function was used to describe the rate of fuel mass burned, which has been observed in any premixed SI combustion obtained experimentally.

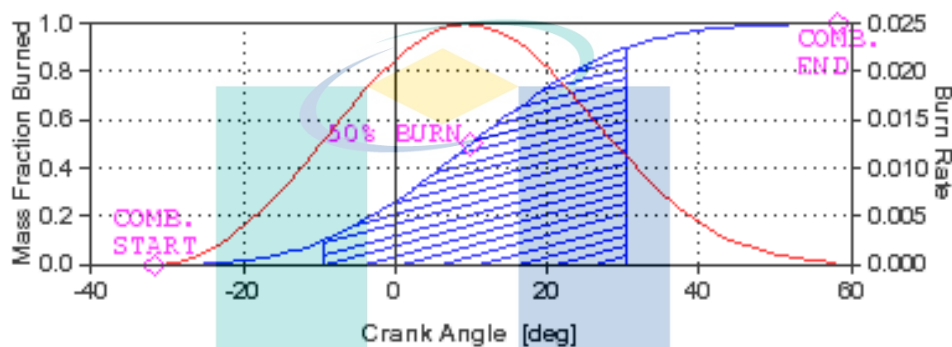


Figure 2.8 SI Wiebe combustion sub-model.

Source: Hanipah (2015)

The cumulative mass fraction burned $(MFB)_c$, is given as a function of crank angle by:

$$(MFB)_c = 1.0 - \exp\left(-K_{AWI} \left(\frac{\theta}{\theta_{dur}}\right)^{(W_{exp}+1)}\right) \quad 2.9$$

The impact of varying 50% burn point will shift the entire curve forward or backward while varying the 10%-90% duration will increase the total combustion duration. Also, varying the Wiebe exponent will change the burn rate profile.

v. CA50

The position where the accumulated heat release reaches 50% of the total released heat is called CA50 (Hakansson 2007). The burn rate, although primarily influenced by turbulence within the combustion chamber, is also dependent on a number of secondary factors. One of these is the reduction under lean mixture operation. Using a weaker mixture can give rise to a number of attendant benefits. In particular, it is widely

recognised that lean combustion is the most promising method of improving fuel economy (Inoue, Nagahiro et al. 1989).

The first law of thermodynamics states that for a given system, the energy is conserved. Treating the combustion chamber as our system and the released heat due to combustion (i.e. converted from chemically bonded energy to heat) as supplied heat to the system the model can be expressed as in equation 2.10:

$$dQ = dU + dW + dQ_{HT} + dQ_{leak} \quad 2.10$$

- dQ = heat release due to combustion
- dW = work performed by the system
- dQ_{HT} = heat transfer losses through cylinder walls
- dQ_{leak} = energy losses by leakage in small crevices
- dU = change in internal energy of the system

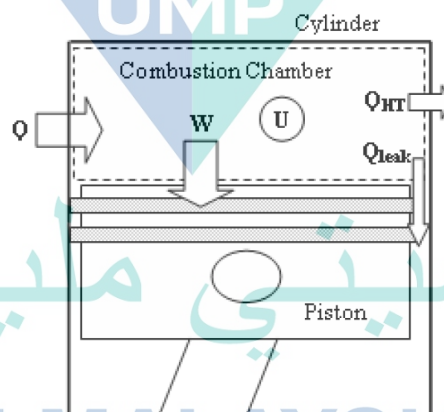


Figure 2.9 Heat release system.

Source: Hakansson (2007)

The advancement in CA50 values resulted in an increase in the ISFC values due to the injected fuel during the pre-injection causes charge stratification, resulting in locally rich fuel-air mixtures which advance the combustion. At the same time, retardation in combustion phasing improved the excess air ratio and ISFC (Samuel, Mithun et al. 2019). The CA50 correlated well with the changes in indicated torque

(Ayala, Gerty et al. 2006). Due to natural variation from each cycle in the engine, different spark advances rendered the same CA50 but each with different IMEP (Corti and Forte 2011). CA50 parameter is not immutable but depends strongly on the heat loss through cylinder walls (de O. Carvalho, de Melo et al. 2012).

2.4.2 Performance parameters

- i. Indicated work per cycle and power.

The work done per cycle can be calculated from the pressure vs. volume (p-V) curve from the integration of the area under the curve which can be represented by strips of elements with height p and wide dV over the entire engine cycle as shown in Figure 2.10.

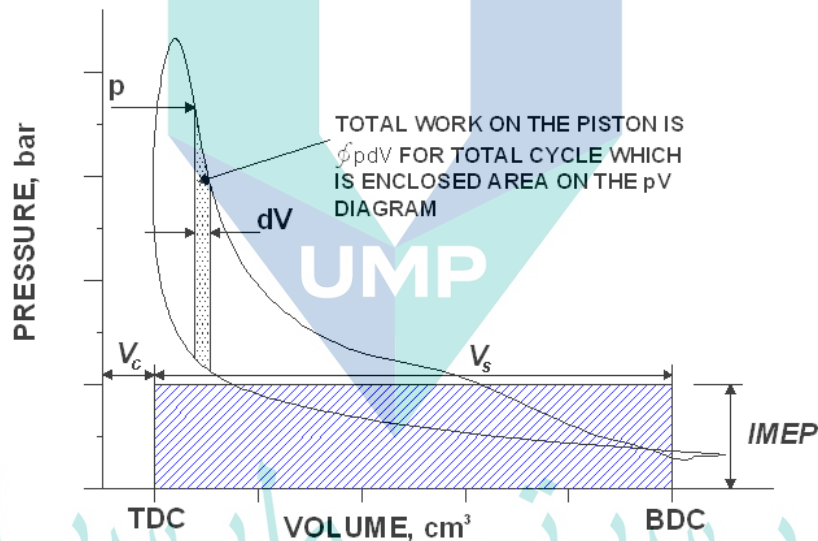


Figure 2.10 Work per cycle calculation and IMEP representation from p-V diagram.

Source: Hanipah (2008)

Power can be determined from the following equation:

$$P_i = \oint p dV \times N \quad 2.11$$

Where N is the engine speed in revolution per second. Alternatively, power can be determined from IMEP as follow:

$$P_i = IMEP \times V_s \times N \quad 2.12$$

ii. Mean effective pressure (MEP) and coefficient of variation (COV).

Mean effective pressure (MEP) is a normalized parameter, which is a useful relative measurement of an engine's performance. Unlike torque and power, MEP is independent of engine size. MEP is simply the work normalized by swept volume. Indicated mean effective pressure or IMEP, is a very important and fundamental engine performance variable which can be determined from the following (Brunt and Emtage 1996, Brunt, Rai et al. 1998):

- The measurement of digital cylinder pressure.
- The numerical integration of the cylinder pressure and volume.

IMEP is calculated by the numerical integration of the pressure vs. volume curve for a complete engine cycle. The representation of IMEP on the p-V diagram as summarized in Figure 2.10 and the following equation:

$$IMEP = \frac{\oint p dV}{V_s} \quad 2.13$$

However, there are several other methods which were evaluated that can be used to evaluate the IMEP numerically from the experimental data (Brunt and Emtage 1996) such as in the following equation which had been modified for time based instead of crank angle based:

$$IMEP = \frac{\Delta t}{V_s} \sum_{i=n1}^{n2} p(i) \frac{dV(i)}{dt} \quad 2.14$$

Cycle-to-cycle variation of the IMEP is expected for a spark-ignition engine. The variation is noticeable, especially if the engine operated under lean operation and at low speed (especially during idling).

The coefficient of variation (COV) can be quantified in the following ways:

1. Evaluate the average IMEP:

$$IMEP_{ave} = \frac{1}{n} \sum_{i=1}^n IMEP_i \quad 2.15$$

where n is the number of samples.

2. Evaluate the standard deviation of the IMEP:

$$\sigma_{IMEP} = \frac{1}{n} \sqrt{\sum_{i=1}^n \frac{(IMEP_{ave} - IMEP_i)^2}{n-1}} \quad 2.16$$

3. Finally, the COV can be calculated:

$$COV_{IMEP} = \frac{\sigma_{IMEP}}{IMEP_{ave}} \quad 2.17$$

For a conventional engine, the COV values must be lower than 10% (Heywood 1988).

- iii. Air-fuel ratio & fuel-air ratio, lambda and equivalence ratio.

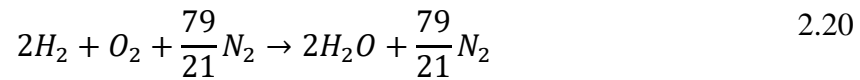
The air-fuel ratio (Ayala, F. A., et al.) and fuel-air ratio (Shojaeefard and Keshavarz) can be defined as follow:

$$AFR = \frac{m_a}{m_f} \quad 2.18$$

$$FAR = \frac{m_f}{m_a} \quad 2.19$$

where m_a is the mass of air and m_f is the mass of fuel.

Stoichiometric combustion can be defined as combustion in which all fuel is fully oxidized. The stoichiometric combustion equation of hydrogen in air is shown below:



Based on the molecular weight of the elements substituted into equation 2.18, the stoichiometric value of the AFR for hydrogen combustion can be obtained as follow:

$$AFR = \frac{32 + \frac{79}{21} \times 28}{2 \times 2} = 34.3 \quad 2.21$$

In addition, two normalized parameters will be introduced as follow:

The fuel-air equivalence ratio,

$$\phi = \frac{(AFR)_{actual}}{(AFR)_{stoich}} \quad 2.22$$

The relative air-fuel ratio, or popularly known as Lambda:

$$\lambda = \frac{(AFR)_{actual}}{(AFR)_{stoich}} \quad 2.23$$

At stoichiometric, $\phi = \lambda = 1$, for rich mixture, $\phi > 1$ and $\lambda < 1$, for lean mixture, $\phi < 1$ and $\lambda > 1$.

The indicators of internal combustion engine performance are important information to determine the engine performance level. Torque, power, brake mean effective pressure (BMEP), and brake specific fuel consumption (BSFC) are the parameters that have been used to represent the performance of engines. Further discussion on each parameter will be presented next.

iv. Torque.

The ability of the crankshaft engine to do work is represented by torque. The dynamometer has been used to measure the torque output of the IC engines. The torque reading from the dynamometer already included the overall losses of the engine. The forces done to the crankshaft by the combustion without any mechanical loss are being

recognized as the indicated torque. For the simulation process, the indicated torque could be calculated from the cylinder pressure.

Figure 2.11 shows the forces acting on a crankshaft engine. Torque is the force acting on the crankshaft (F_t) times radius of the crankshaft, in the equation:

$$T_i = r \cdot F_t \quad 2.24$$

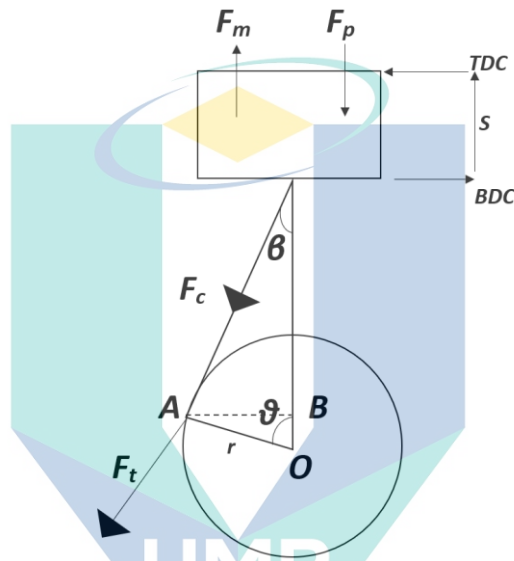


Figure 2.11 Forces acting on the crankshaft.

Where F_t is the component of the pressure, which is orthogonal to the crankshaft.

By trigonometric computation, F_t can be derived from pressure by:

$$F_t = p(\theta)A_p \frac{\sin(\theta + \beta)}{\cos \beta} \quad 2.25$$

The mechanical efficiency of the systems used in this experiment can be calculated by the difference of the measured and indicated torque by:

$$\eta_m = \frac{T_i - T_m}{T_i} \quad 2.26$$

Where:

T_i = indicated torque,

T_m = measured torque

v. Power

Power defined as work done by the engine that can be derived from torque by using the equation:

$$P = \frac{2\pi NT}{60} \quad 2.27$$

Where:

P = power output (W)

N = Engine speed (RPM)

T = Engine Torque

The power can be brake or indicated depending on the torque substituted in this equation.

vi. Brake Mean Effective Pressure (BMEP)

BMEP is a measure work output from an engine, and not of the pressure of an engine even-though Pascal arises as BMEP unit. BMEP is also a derivation from engine torque by the equation:

$$\bar{p}_b = \frac{2 \cdot \pi \cdot 2 \cdot T}{V_s} \quad 2.28$$

Where:

T = Engine torque (Kesner, Schleyer et al.)

V_s = Cylinder Swept Volume (m^3)

vii. Brake Specific Fuel Consumption (BSFC)

The main target of new engine technology is mainly based on fuel consumption and emission. Fuel consumption can be evaluated as BSFC, where BSFC is the fuel consumption of engine that used to produce one power output value. Deriving from BSFC definition, the relationship between fuel consumption and power are:

$$BSFC = \frac{FC \cdot 3600}{P} \quad 2.29$$

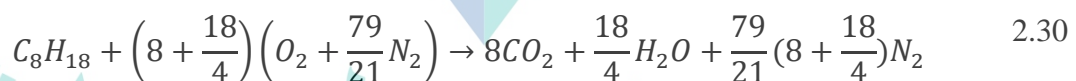
Where:

FC = fuel consumption (g/s)

P = Engine brake power output (kWh)

viii. Air-fuel ratio

AFR is the ratio of air and fuel entering the combustion chamber. The value of air-fuel ratio is an important indicator, especially to control the combustion in the engine. Each fuel has its specific air-fuel ratio for complete combustion known as stoichiometric AFR. AFR stoichiometric can be calculated using a chemical equation, for example, the AFR_{stoich} calculation for gasoline is:



Where equation 2.30 is derived from equation 2.1, substituting the value of gasoline combustion equation with its chemical formula C_8H_{18} .

$$AFR_{stoich} = \frac{\left(8 + \frac{18}{4}\right) \left(15.999 \times 2 + \frac{79}{21} \times 14.0067 \times 2\right)}{12.0107 \times 8 + 1.00784 \times 18} \approx \pm 14.7 \quad 2.31$$

The calculation of the mass of total air over the mass of gasoline in the combustion process is shown in equation 2.31, which produces the number of stoichiometric AFR. The atomic mass of those elements are as follows:

Carbon: 12.0107u

Hydrogen: 1.00784u

Oxygen: 15.999u

Nitrogen: 14.0067u

ix. Volumetric efficiency

The amount of air that enters the combustion chamber is depended on the efficiency of the whole intake systems. In order to get inside the combustion chamber, the air has to go through some parts. Air filters, intake runner, intake port and intake valve are the main parts that build a complete intake system. Total loss comes from intake systems can be observed by calculating the volumetric efficiency of the engine. Volumetric efficiency defined as the comparison of actual air mass that enters the chamber to the total displacement volume of a specific engine.

$$\eta_v = \frac{2(\dot{m}_a + \dot{m}_f)}{\rho_o V_d N} \quad 2.32$$

Where:

η_v = Volumetric Efficiency

\dot{m}_a = Actual air mass that enters the combustion chamber (g)

\dot{m}_f = Actual fuel mass (g)

V_d = Displacement volume (m³)

ρ_o = Air intake density (kg/m³)

In the equation, \dot{m}_f is the mass of fuel inducted, which is for a direct injection system, $\dot{m}_f = 0$. Volumetric efficiency is one of the important parameters to the engine performance in which the high volumetric efficiency value of the engine is expected. There are alternatives that have been proposed to increase the volumetric efficiency of

the engine. Intake air boosting through supercharging or turbocharging and variable valve timing (VVT) are the most popular that have been implemented in modern IC engines.

2.4.3 Emissions

The four main pollutants emitted from the exhaust of a four-stroke internal combustion engine are carbon dioxide (CO_2), carbon monoxide (CO), unburned hydrocarbons (HC) and oxides of nitrogen (NO_x). Although these exhaust emissions are unwanted, they are useful since mixture dilution with exhaust gas tends to slow combustion to a greater degree than the use of air as the diluent (Ghauri 1999). Furthermore, lean-burn operation is the concept of stoichiometric combustion with high levels of residual gas fraction (RGF). In particular, exhaust gas re-circulation (EGR) allows dramatic reductions in NO_x emissions coupled with improvements in fuel economy.

1. Carbon Dioxide

CO_2 can be reduced through the improvement in Brake Specific Fuel Consumption (BSFC) of the engine. The other three are subjected to extensive controllable, careful design of the engine and after-treatment of the exhaust gases. Although CO_2 is not toxic and is not currently legislated against. It is one of the greenhouse gases which is likely to be controlled in future legislation. Carbon dioxide in Earth's atmosphere is a trace gas, having a global average concentration of 415 parts per million by volume (or 630 parts per million by mass) as of the end of year 2020 (Pashley & Alex 2016). The extraction and burning of fossil fuels, using carbon that has been sequestered for many millions of years in the lithosphere, has caused the atmospheric concentration of CO_2 to increase by about 50% since the beginning of the age of industrialization up to year 2020 (Friedlingstein, P. et al. 2019).

2. Carbon Monoxide

The combustion of hydrocarbons is accompanied by the formation of carbon monoxide CO, which is favoured by high temperature and pressure. It is oxidised to CO_2 relatively late in the combustion process and represents about 45% of the fuel heat released (Merker, Eckert et al. 2012). The presence of carbon monoxide is normally due to incomplete combustion. This is particularly so under rich conditions when there is insufficient oxygen to completely oxidise the fuel. However, even with lean mixtures,

CO cannot completely be removed due to the dissociation of the chemical species at the high temperatures within the chamber. During the expansion stroke, cylinder temperature drops and effectively 'freezes' the reverse dissociation reactions, thus preventing the oxidation of CO to CO₂. Carbon monoxide levels are also dependent on the degree of air/fuel homogeneity. Inconsistent mixing of air and fuel may lead to local regions containing a rich mixture causing incomplete combustion (Ghauri 1999). Effective use of in-cylinder motion should help to reduce this effect (Dost and Getzlaff 2018).

3. Unburned Hydrocarbon

Hydrocarbons are one of the two main pollutants (together with oxides of nitrogen) emitted from engine exhausts and extensive work has been carried out to investigate the mechanisms that may account for their presence. They are found in the exhaust of SI engines due to a portion of the inducted fuel escaping combustion and exiting the cylinder partially or completely not oxidised (Thompson and Wallace 1994). The generally accepted explanation is that part of the fuel becomes trapped in such a way that the flame cannot reach it. Regions not reached by the flame are called 'crevices', which is a narrow region connected to the main combustion chamber that the mixture can enter or escape, but the flame cannot propagate into since it is extinguished by the cold wall. The gas density in the crevices is several times higher than that in the chamber, as the cold cylinder wall cools it down rapidly (Neher 2017). Crevices include such areas as the piston ring pack, the head gasket, spark plug thread and valve seats. In addition, absorption and subsequent desorption may occur from the oil film on the cylinder wall and any accumulated deposits in the combustion chamber (Thompson and Wallace 1994). HC consist of numerous species, which some may react in the atmosphere with NO₂ to form smog in the presence of sunlight (Kim and Bae 1999, Ferguson and Kirkpatrick 2015).

4. Oxides of Nitrogen

According to Heywood (1988), NO forms in both the flame front and the post flame gases. Oxides of nitrogen (NO_x) are formed during combustion by the oxidation of nitrogen under the high-temperature conditions in the cylinder. The major component is nitric oxide (NO), although there are much smaller amounts of nitrogen dioxide (NO₂). However, as the flame front is extremely thin, the residence time is extremely short, so it

can be assumed that NO is formed behind the flame front. The rate of formation of NO increases exponentially with temperature. In particular, the gases from the early stages of combustion, close to the spark plug, will continue to rise in temperature as the pressure rises.

5. Air-Fuel-Ratio on emission products

Stoichiometric combustion takes place at $\lambda=1.0$ while $\lambda>1.0$ and $\lambda<1.0$ defines the combustion of lean and rich mixtures, respectively. The relative air-fuel ratio strongly influences both combustion temperature and the laminar burning velocity, thus affecting engine performance and emissions significantly (Neher 2017). One of the best methods of reducing the levels of harmful emissions (including CO₂) is by use of a mixture leaner than stoichiometric. Such an engine would offer benefits in fuel economy as the load can be controlled by changes in AFR, leading to a reduction in pumping losses, as well as lower emissions (particularly NO_x), as shown in Figure 2.12. Further benefits are the increase in cycle efficiencies brought about by the possibility to use higher compression ratios and the higher ratio of specific heats for leaner mixtures (Ghuri 1999).

UMP

اونيورسيتي ملايسيا قهغ

UNIVERSITI MALAYSIA PAHANG

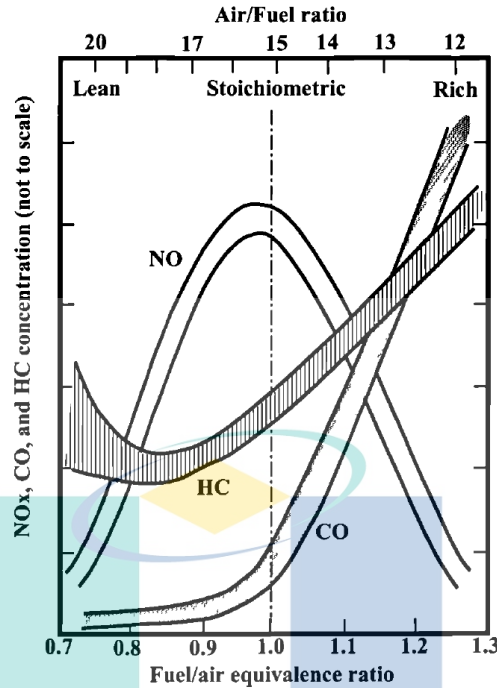


Figure 2.12 Variation in pollutant concentration with air-fuel-ratio
Source: Heywood (1988)

Equation 2.1 represents a very simplified approach to describe the combustion process. The exhaust gas contains far more components than calculated from ideal combustion caused by an insufficient amount of O_2 molecules or reactions that take place slowly to achieve chemical equilibrium. As a result, the exhaust gas contains pollutants such as carbon monoxide (CO), nitrogen oxide (NO_x), unburnt hydrocarbons (HC) and particulates. NO_x , HC and CO emissions highly depend on the relative air-fuel ratio λ , as shown in Figure 2.13.

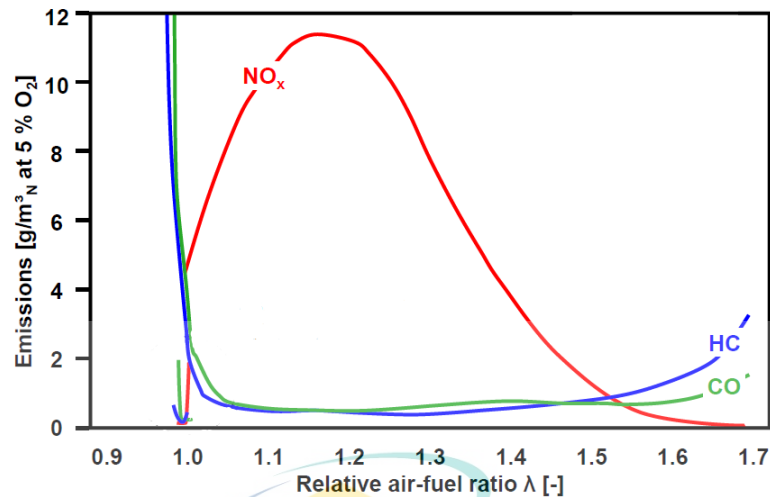


Figure 2.13 NO_x, HC and CO emissions over air-fuel ratio

Source: Auer (2010)

Although pollutants form a small part of the exhaust gas, they pose a threat to human health and the environment (Merker, Eckert et al. 2012). There are various ways in which pollutant reductions can be achieved. Some of it can be either improving engine fuel consumption or using alternative fuels of a lower ratio between CO₂ and lower heating value (LHV) (Merker, Eckert et al. 2012).

2.5 Poppet valve system

There are two distinct gaseous exchange processes required in a 4-stroke cycle, namely the intake and exhaust strokes. These are normally controlled by poppet valves located in the cylinder head. Traditionally, both intake and exhaust valves are controlled by a pear-shaped cam that runs on a camshaft. This connection sets both valves to a fixed timing of opening and closing intervals. A general arrangement of this valve control is shown in Figure 2.14, which consists of a belt, a cam sprocket, a camshaft, a set of intake and exhaust valves, tappets and valve springs.

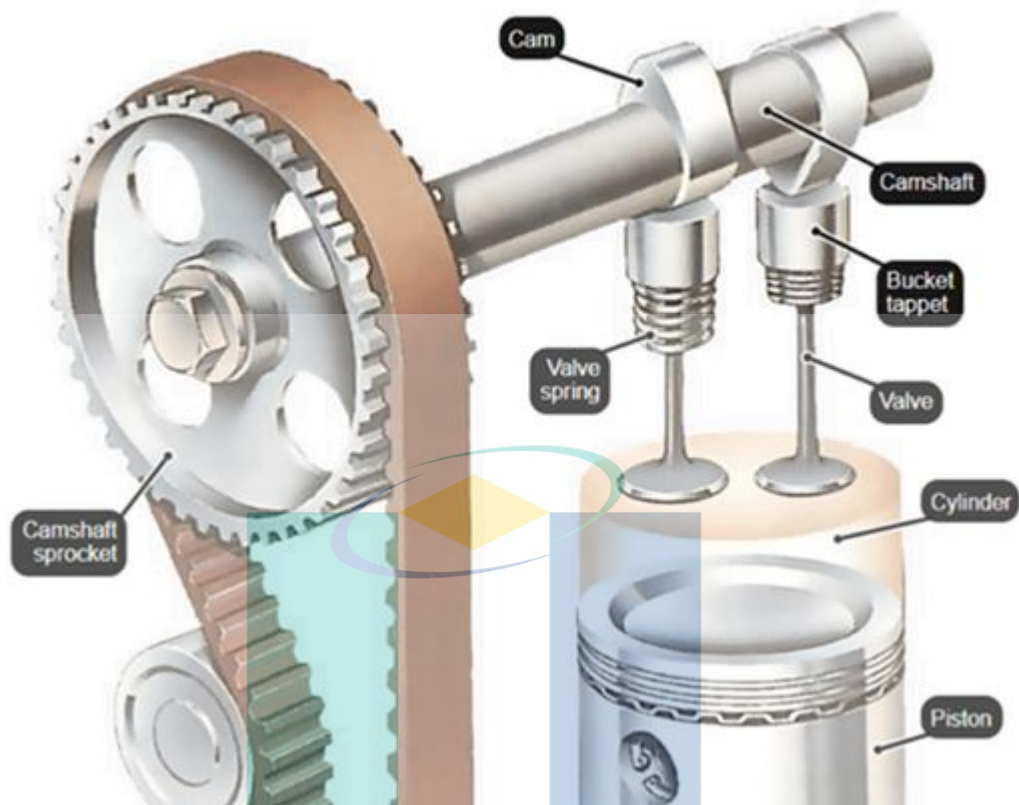


Figure 2.14 Conventional valve cam timing system

Source: Siddiqui (2017)

The valves are operated by either one or two camshafts which may be driven by a belt, a chain or gears from the crankshaft. Due to these mechanical constraints, the timing for the opening and closing of the valves and their lift are normally fixed by design, which were decided based on engine performance requirements over its full operating range.

The intake and exhaust valves only open once for every two rotations of the engine crankshaft; during the intake stroke and exhaust stroke, respectively. Furthermore, each valve opens and closes gradually at a fixed profile following the cam lobe profile in the whole speed of the engine. In order to obtain higher power outputs or fewer emissions at different engine speeds and loads, the valve lift profile must be changed accordingly. These changes include varying valve timing by advancing or delaying the valve or changing their total lift.

In an ideal four-stroke cycle the intake stroke would begin with the inlet valve opening at TDC and end at BDC in preparation for compression of the fresh charge.

Similarly, the exhaust stroke would begin and end at BDC and TDC, respectively, as shown in Figure 2.15. This type of operation is only suitable for very low engine speeds and is never used in practice since full-load performance becomes severely reduced at all speeds. The indicated power of an internal combustion engine at a given speed is proportional to the mass flow rate of air. Thus, inducting the maximum air mass at WOT, and retaining that mass within the cylinder, is one of the primary aims of the gas exchange process (Heywood 1988).

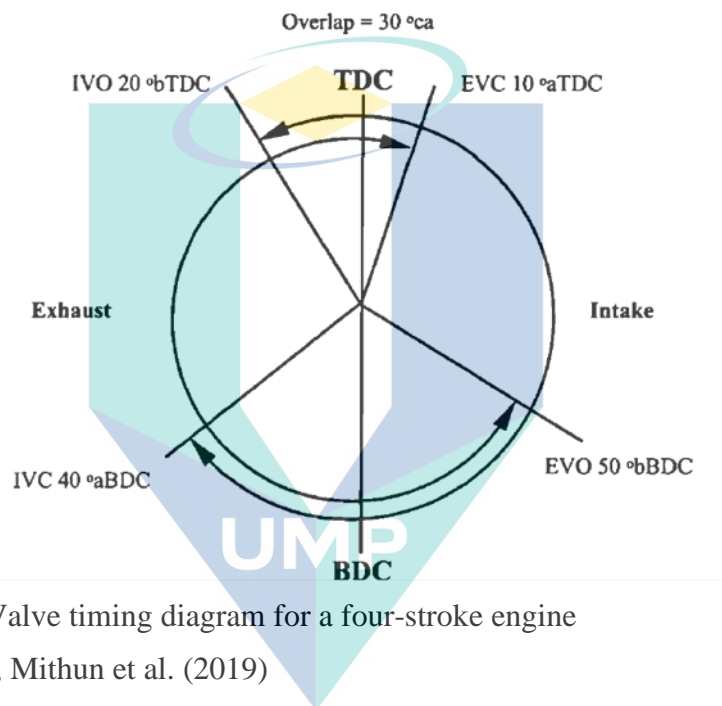


Figure 2.15 Valve timing diagram for a four-stroke engine
 Source: Samuel, Mithun et al. (2019)

The exhaust valve normally opens before BDC on the expansion stroke in order to ensure a good blowdown of the cylinder contents to reduce pumping work, especially at higher speed. The penalty is a loss in expansion work that could have been extracted had the valve remained shut. This loss can be demonstrated with reference to the p-V diagram in Figure 2.16. The shaded area represents additional work that could have been extracted from the combustion gases had the expansion been allowed to continue to the bottom of the piston stroke.

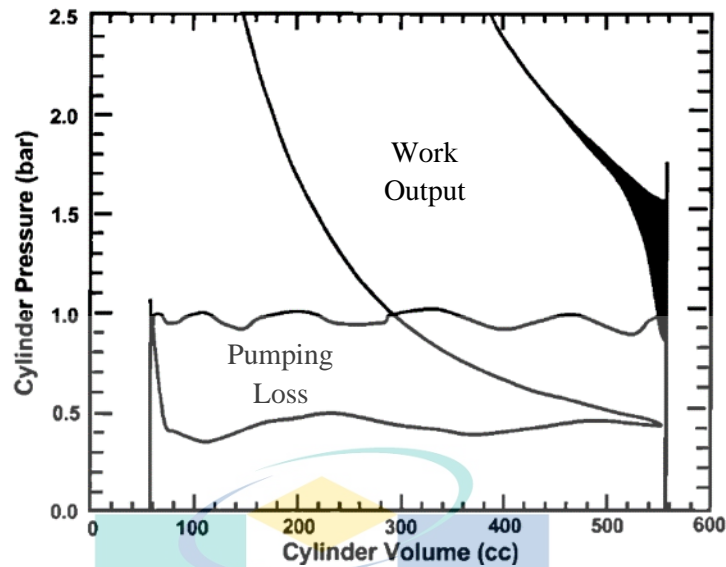


Figure 2.16 p-V diagram for gas exchange processes

Source: Li, Liu et al. (2018)

The early opening of the exhaust valve has an impact on emissions, in particular the level of unburned hydrocarbons. By allowing further time for post-combustion reactions to take place, particularly at low speeds and light loads when combustion is slowest, the number of unburned hydrocarbons released into the exhaust can be reduced. Conditions during the later stages of the expansion stroke are especially important if crevice effects are significant since post-combustion oxidation is the only mechanism available within the cylinder (Ghauri 1999).

2.6 Variable valve timing

Engine breathing is controlled by valve timing, while the timing of air intake and exhaust is controlled by the shape and phase angle of cams. In order to optimise the breathing, the engine requires different valve timing at a different speed. When engine speed increases, the duration of intake and exhaust stroke decreases, limiting the amount of fresh air that enters the combustion chamber, and the exhaust has less time to leave the combustion chamber. Therefore, the best solution is to open the inlet valves earlier and close the exhaust valves later. In other words, the overlapping between the intake period and the exhaust period should be increased as speed increases (Middleton, Olesky et al. 2015).

The indicated power of an internal combustion engine at a given speed is proportional to the mass flow rate of air (Ghauri 1999). Thus inducting the maximum air

mass at WOT, and retaining that mass within the cylinder, is one of the primary aims of the gas exchange process (Heywood 1988). For this reason, the actual valve opening and closing characteristics become a compromise between idle stability, low-speed torque and WOT power.

Varying the cam timing resulted in more engine torque and power delivery over a wide range of engine speed and load. Table 2.1 shows how each driving condition of a vehicle determined by the camshaft position and matched with variable valve timing target and performance outcome (Halderman and Mitchell 2014).

Table 2.1 Variable valve timings targets and impacts

Driving condition	Camshaft position	Target	Outcome
Idle	No change	Minimize valve overlap	Stabilize Idle Speed
Light engine load	Retard valve timing	Decrease valve overlap	Stable engine output
Medium engine load	Advance valve timing	Increase valve overlap	Better fuel economy with lower emissions
Low to medium RPM with heavy load	Advance valve timing	Advance intake valve closing	Improve low to midrange torque
High RPM with heavy load	Retard valve timing	Retard intake valve closing	Improve engine output

Source: Halderman and Mitchell (2014)

G. B. Parvate-Patil (2003) presented an assessment of eight variable valve timing philosophies investigated using numerical modelling. Those philosophies are:

- Late intake valve closing (LIVC): the closing of the intake valve is delayed towards the end of the compression stroke.
- Early intake valve closing (EIVC): the closing event of the intake valve is advanced earlier in the compression stroke.
- Late intake valve opening (LIVO): the opening event of the intake valve is delayed towards the beginning of intake stroke.
- Early intake valve opening (EIVO): the opening event of the intake valve is advanced into towards the last part of exhaust stroke.
- Late exhaust valve closing (LEVC): the closing of the exhaust valve is delayed towards the end of the intake stroke.

- Early exhaust valve closing (EEVC): the closing event of the exhaust valve is advanced earlier in the intake stroke.
- Late exhaust valve opening (LEVO): the opening event of the exhaust valve is delayed towards the beginning of exhaust stroke.
- Early exhaust valve opening (EEVO): the opening event of the exhaust valve is advanced into towards the last part of power stroke.

Figure 2.17 shows how these philosophies were varied in the study with respect to conventional IC engine valve profiles. The same definitions are used throughout the thesis for this research.

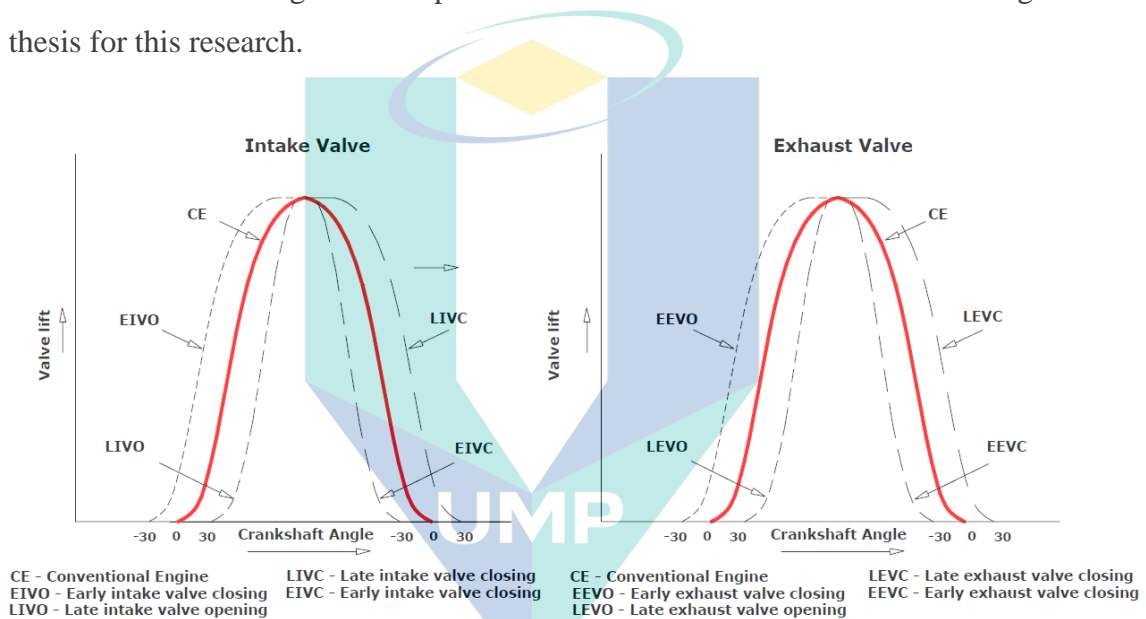


Figure 2.17 Variable valve timing philosophies.

Source: Parvate-Patil, Hong et al. (2003)

اونيور سیتی ملیسیا فہق

2.6.1 Valve overlap

UNIVERSITI MALAYSIA PAHANG

During the gas exchange process in a four-stroke cycle, there is an overlap period when both the exhaust and inlet valves are open simultaneously. This is known as valve overlap, which helps in reducing the amount of exhaust gas from the previous cycle through the opening of the intake valve while the exhaust valve is closing. The intake air flow pushes the remaining exhaust gas in the cylinder and reducing the final residual gas fraction (RGF) to a minimum. The exhaust residuals, although desirable for emissions control under certain operating conditions, will rarely be at an optimum level.

Figure 2.18 shows the influence of valve overlap at full load and idle operations in a four-valve engine (Ghauri 1999). The phase shifting of the overlap angle affects the specific power rating of the engine at WOT and difference in IMEP at idle.

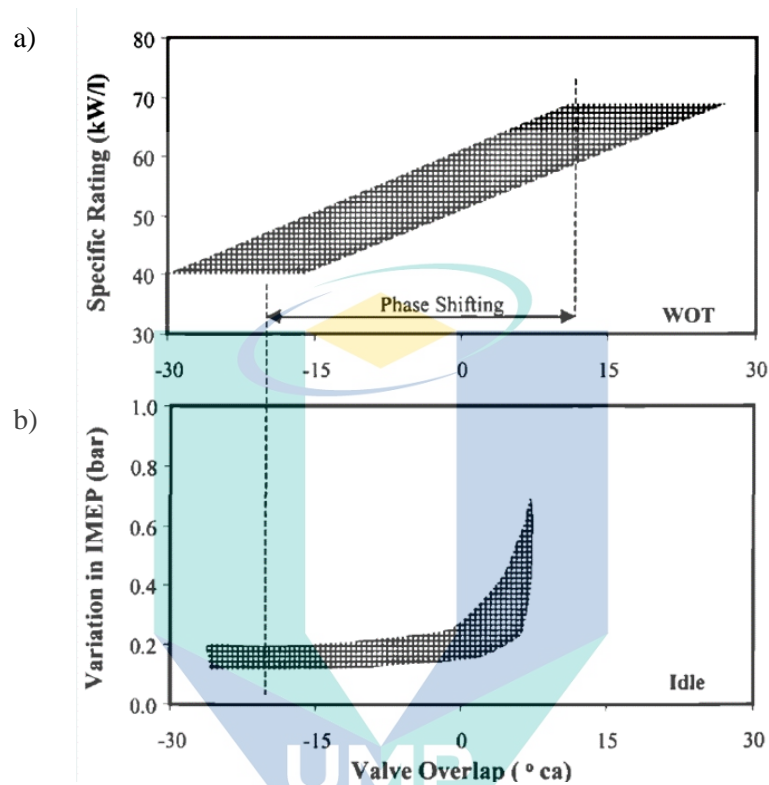


Figure 2.18 Influence of valve overlap at (a) full-load and (b) idle.
Source: Ghauri (1999)

Exhaust valve closing (EVC) normally occurs after TDC to take advantage of exhaust tuning effects at a higher speed. However, the exhaust gas is drawn back into the cylinder at lower engine speed, which affects the performance detrimentally. The inlet valve is closed later after BDC to increase volumetric efficiency at higher engine speed. However, at lower engine speed, the maximum torque is compromised since a part of the fresh charge is pushed back into the intake port as the piston entering its compression stroke. Consequently, the effective compression ratio is reduced.

2.6.2 Variable valve actuation

Variable valve actuation (VVA) represents the range of VVT technologies. VVA offers the potential to alleviate some or all of the drawbacks associated with the conventional valve trains. By effectively varying the valves' opening and closing characteristics, it should be possible in theory to achieve the optimum running condition

for the engine under any loads or speeds. This optimum can be defined in terms of performance, emissions or fuel economy, although in practice, these goals may be distinct under certain conditions. Figure 2.19 shows the possibilities to influence engine characteristics by means of VVA. The effect of valve timing improves pumping work, flow turbulence and charge composition during the cycle. Improved pumping work results in greater efficiency. Improved turbulence results in a better mixture preparation, which leads to a better combustion. Improved charge composition means a better air-fuel ratio, which leads to a better combustion. Combining all these effects, efficiency, exhaust emissions, idle stability, power and torque are augmented.

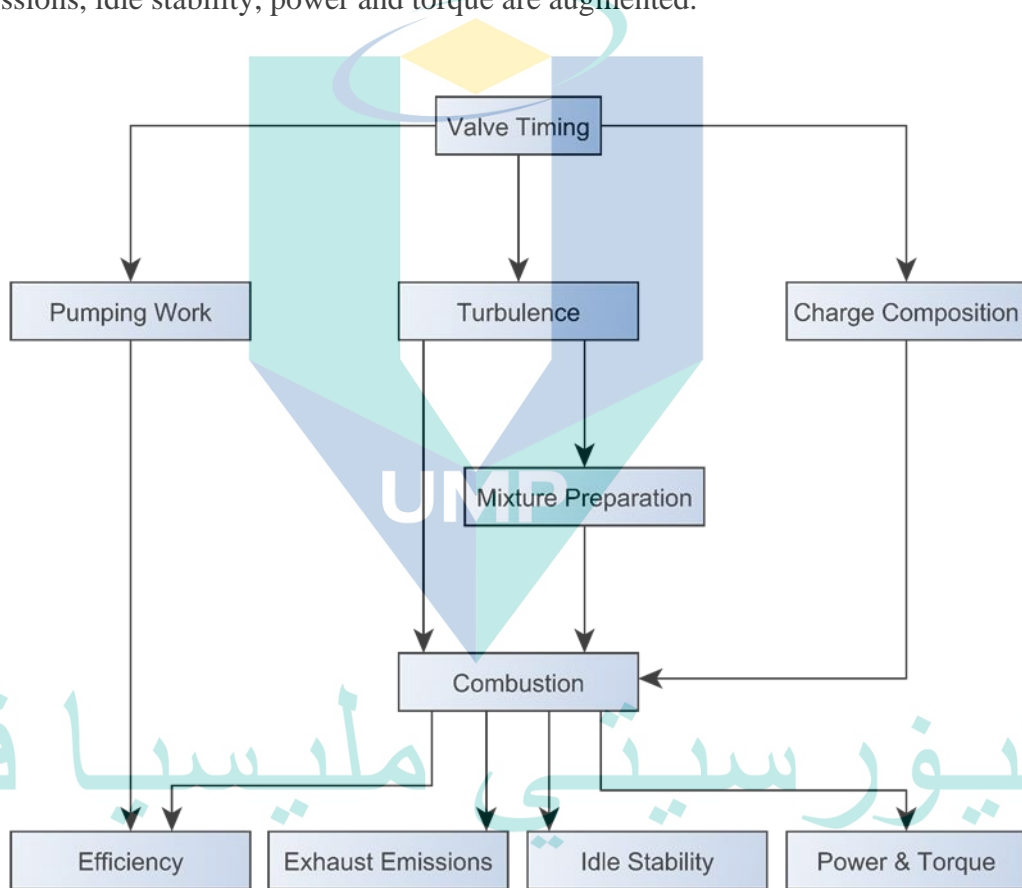


Figure 2.19 Possibilities to influence engine characteristics by means of VVA

Source: Ghauri (1999)

2.6.2.1 Current VVA technology

Following the introduction of multi-valve technology in the IC engine, several key manufacturers focus on variable valve timing to enhance engine output. In these past decades, several VVA technologies have been introduced by car manufacturers, namely Honda i-VTEC, Toyota Valvematic and VVT-i, BMW Valvetronic and VANOS as well

as Koenigsegg Freevalve. The key characteristics of these systems is summarised in Table 2.2.

Table 2.2 Summary and comparison of the current variable valve control technologies in the market

Variable Valve Technology	Valve Timing	Valve Lift	Valve Duration
Honda VTEC	Yes. Limited to 2 camshaft profiles.	Yes. Limited to 2 camshaft profiles.	Yes. Limited to 2 camshaft profiles.
Toyota VVT	Yes. Limited to certain angle.	No.	No.
BMW Vanos	Yes. Limited to certain angle.	No.	No.
BMW Valvetronic	No.	Yes. Fully variable valve lift.	No.
Koenigsegg Freevalve	Yes. Fully variable valve timing.	Yes. Not fully variable. Lift actuation is fixed.	Yes. Fully variable valve duration.

Honda VTEC

VTEC is the acronym for variable valve timing and lift electronic control, an evolution of Honda's VTEC engine system, which was introduced in 2001. This engine equipped with cam profile switching that varies valve timing, duration and lift simultaneously depending on engine speeds. During low engine speeds, the valves will open smaller lift to achieve maximum fuel efficiency, whereas they will open wider at higher engine speeds to achieve higher performance. In other words, there are two cam profiles operate independently of each other, one designed for low-RPM operation and fuel efficiency, the second one, which is the taller cam, designed for performance. The ECU decides when to select which profile based on several engine parameters to combine the best features of each camshaft by actuating the locking pin that runs through the rocker arms.

Toyota VVT

Variable valve timing technology also known as VVT, was developed in 1991 by the Japanese automobile manufacturer, Toyota. Introducing VVT to a combustion engine allows more precise control of the engine output and can greatly increase fuel economy. With a VVT system, it is possible to have the timing altered to match the engine speed,

torque requirements, and valve overlap. Another great advantage of VVT is its ability to take some of the load off the crankshaft by opening the valve before the end of the combustion stroke. This made Exhaust Gas Recirculation (EGR) valves outdated, where EGR system reroutes a small amount of Nitrous Oxides back into the intake manifold (Chaichan 2018). The VVT system controls the timing to leave inert gas in the chamber for the next combustion cycle, thus, controlling the combustion temperature and the production of nitrous oxides.

BMW Valvetronic

The BMW Valvetronic system was the first continuously variable valve lift mechanism, which went into production in the BMW 316ti in 2001. Compared with a conventional engine, Valvetronic adds an electric motor, an eccentric shaft and at each intake valve, an intermediate rocker arm. The system works by adjusting the valve lift with a lever positioned between the camshaft and the intake valves. It adds an intermediate rocker arm between the camshaft and the roller finger follower that actuates the valve. The pivot location of the intermediate rocker arm then is varied with an eccentric shaft controlled by an electric motor through a worm gear set. Rotating the eccentric shaft to extend the pivot location of the intermediate rocker arm results in an increase in valve lift. In order to ensure the tangency among cam follower, crankshaft and eccentric shaft at high engine speed levels, a spring generates a pre-load force between the cam follower and eccentric shaft. Generally, the valve lifting distance varies between a minimum of 0.2 mm and a maximum of 9.0 mm. At the same time, the engine speed of Valvetronic systems is limited to 6500 RPM by the inertia.

The main target of this system was to reduce fuel consumption. Since air flow, and thus engine output, is controlled by valve lift with the Valvetronic system, the conventional throttle valve is disabled, which reduces pumping losses. VVA throttle-less load control can be achieved by different intake valve actuation strategies like combining variable valve lift, duration and timing (Bernard, Ferrari et al. 2009). This claim can also be supported by similar research done (Kreuter, Heuser et al. 2003, Hannibal, Flierl et al. 2004, Patel, Ladommatos et al. 2010, Clenci, Bizziac et al. 2013).

Thus, the solution used by BMW with its Valvetronic-Vanos mechanism is outstanding. In general, BMW claims that Valvetronic can provide a 10% reduction in

fuel consumption and emission (Unger, Schwarz et al. 2008). Even though it was the first system to allow a new range of valve train possibilities, Valvetronic has some important disadvantages. The maximum power is not increased since the additional components result in additional friction and inertia, even though Valvetronic reduces fuel consumption at part load. Besides, the Valvetronic system also adds a significant height above the cylinder head, which limits its applicability to smaller vehicles.

BMW VANOS

Variable Nockenwellensteuerung', a system developed by a German car manufacturer, BMW, is a cam phasing technique to adjust the valve timing. The ability of this technology is to change valve timing. A helical gear is used in this system to connect the standard camshaft to a hydraulic piston. A controller (ECU) signals the solenoid to introduce high-pressure oil flow to either side of the hydraulic piston, causing the piston to move axially. Due to the helical gear, any linear motion of the hydraulic piston causes rotation of camshaft, which advances or delays the valve timing. However, the system does not allow for any change to the valve lift.

Koenigsegg Freevalve

Koenigsegg Freevalve, one of camless piston engines that has poppet valves operated by means of pneumatic actuators instead of conventional cams. It uses compressed air to control the valve events. Freevalve technology allows full control of the combustion cycle. No other variable valve actuation system offers this level of control and reliability. Both intake and exhaust valves can be opened and closed at any desired crankshaft angle since the valve actuation is not dependent on the actuation of the other valves (Gould, Richeson et al. 1991). It means both valves can remain open longer or even open and close at an interval completely free from what other cylinders are doing in the engine. This flexibility enables an engine to deliver lower fuel consumption and emission numbers, while still delivering increased torque and horsepower. To put it another way, better control means flexible power and complete combustion, which would, in turn result in reduced emissions. However, the high cost of implementation and high frequency of operation for electrical actuators are the largest deterrents to the system.

2.6.3 Applications of VVT

Varying the engine valve event duration, timing and lift are well-known methods of increasing engine performance, lowering the exhaust emission and therefore have been the object of a considerable number of researches since 1880. Many studies have shown that a 15% improvement of engine efficiency can be achieved and a potential of up to 20% improvement has been estimated when optimizing the engine valve timing at all engine loads and speeds (Dresner and Barkan 1989). Advancing or retarding the opening and closing of valves can reap large improvements in torque (Jankovic and Magner 2002), emissions and fuel consumption (Moriya, Watanabe et al. 1996).

Moreover, several studies have been reported to support the ideas of the impacts when variable timing cam is applied. The mechanism and design of variable valve timing influence the combustion and performance (Saied, Ahmad et al. 2008). The following examples show the application and advantages of variable valve control.

2.6.3.1 Variable Compression Ratio using the Atkinson Cycle concept

It is possible to have a variable compression ratio by timing the intake valve to close later after the piston has started moving in upward direction. Some of the air is forced back into the intake manifold, reducing the volume of air that was drawn during BDC. Since the formula of compression ratio is,

$$CR = \frac{Volume_{Total}}{Volume_{clearance}} = \frac{V_1 + V_2}{V_2} \quad 2.33$$

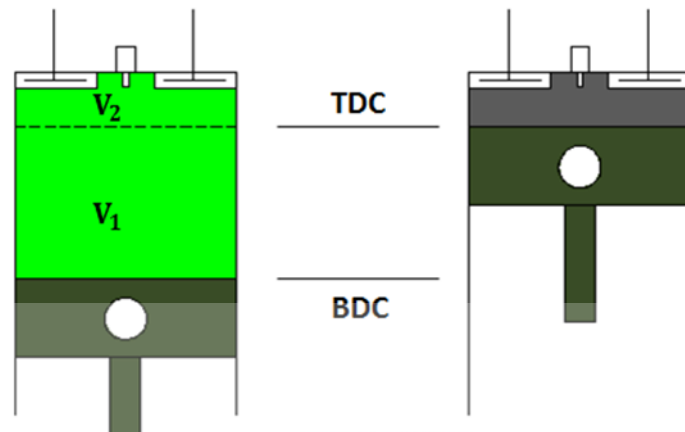


Figure 2.20 Combustion chamber volume at TDC and BDC

In recent years some automobile manufacturers have established Atkinson cycle-based engines via a variable valve train in their hybrid vehicles such as Toyota (Muta, Yamazaki et al. 2004), Ford (Karden, Ploumen et al. 2007), Mazda (Pertl, Trattner et al. 2012), Mercedes (Voelcker 2009). During conditions in which the engine is not required to produce maximum power, it can operate using a more efficient Atkinson cycle simply by changing its valve timing. Whereas, when more power is required, the engine seamlessly will switch back to Otto cycle. The effect of having variable compression ratio, we could have the best of both worlds in terms of efficiency and outright output, where a lower compression ratio aids fuel economy, while a higher compression ratio boosts power. The Atkinson cycle, realized via the crank train, is a very effective single measure to enhance efficiency and can be combined very well with ongoing development trends (Pertl, Trattner et al. 2012).

2.6.3.2 Variable stroke cycle engine

Conventional 2-stroke crankcase scavenging type engines have some problems in emissions and the lubrication system. In order to solve these problems, 2-stroke engine with poppet valves is widely in development. Basically, 2-stroke engines have the following advantages over 4-stroke engine, which are greater torque and power, smoother and less torque fluctuation (Lou, Deng et al. 2013).

The developing 2-stroke poppet valve engines have almost similar components with the conventional 4-stroke engine. What makes this interesting is, it is possible to change between the 4-stroke cycle and the 2-stroke cycle in this engine with the same

valve arrangement and combustion chamber configuration by inserting two camshaft profiles in the program of the stepper motor control system.

2.6.3.3 Throttle-less engine

This strategy is identical to the BMW Valvetronic. With throttle bodies, one has close to atmospheric pressure on the filter side, and a vacuum on the intake manifold side. With a throttle-less engine, one will have near atmospheric pressure directly outside the intake valves, and thus the engine does not have as much resistance to pulling in air, making it more efficient.

This strategy also increases the response of the engine. With throttle bodies, once it is floored, one has to wait for the air to travel from the throttle body to the intake valve. By using the intake valves to regulate airflow, and already having nearly atmospheric pressure right outside the cylinder, the air intake is instantly inducted.

2.6.3.4 Cylinder Deactivation

When an internal combustion engine is operating at part load, each of its cylinders is only producing a proportion of its maximum work output. It would be possible to achieve the same engine output with a smaller number of cylinders, each working at higher output.

Cylinder deactivation removes some cylinders of an engine from the operating cycle and results in the remaining cylinders operating at a higher load. The increased load on the working cylinders reduces the amount of throttling that is required, with a corresponding drop in pumping losses and hence improved part-load fuel economy.

Cylinders are not deactivated individually because the unequal cylinder firing intervals would cause unstable running. Hence it is conventional to deactivate groups of cylinders. For example, with a V8 engine, four cylinders would be deactivated so that the engine would operate as a four-cylinder engine with equal firing intervals.

2.7 Design of Experiment

Design of Experiments (DOE) techniques enables designers to determine simultaneously the individual and interactive effects of many factors that could affect the

output results in any design. DOE also provides a full insight of interaction between design elements; therefore, it helps turn any standard design into a robust one. Simply put, DOE helps to pin point the sensitive parts and sensitive areas in designs that cause problems in Yield. Designers are then able to fix these problems and produce robust and higher yield designs prior to going into production.

In recent years, the numerical simulation and optimization have been widely used to improve the engine performance under wide operating parameters owing to the advantage of the shorter time cost compared with experimental methods (Xu, Jia et al. 2019). Formal methods for the design of experiments date back to the early years of the 20th century when researchers in the subject came to realise that some of the new methods being developed, such as analysis of variance, were intimately related to the problem of experimental design.

Three basic techniques fundamental to designing an experiment are replication, local control (blocking), and randomization (Gupta and Parsad 2005). A popular measure of the experimental error is the Coefficient of Variation (CV).

Design of experiments is a series of tests in which purposeful changes are made to the input variables of a system or process and the effects on response variables are measured. The design of experiments is applicable to both physical processes and computer simulation models. Experimental design is an effective tool for maximizing the amount of information gained from a study while minimizing the amount of data to be collected (Telford and K 2007).

The conventional experiment design usually proceeds so that changes are made one variable at time. The first variable is changed, and its effect is measured and the same takes place for the second variable and so on. This is an inefficient and time-consuming approach. It cannot also find probable interactions between the variables. Result analysis is straightforward, but care must be taken in interpreting the results and multivariable modelling is impossible. Systematic design is usually based on so-called matrix designs that change several variables simultaneously according to the program decided beforehand. Changing is done systematically and the design includes either all possible combinations of the variables or at least the most important ones (Leiviskä 2013).

Experimental design and optimization methodology are important in modern research and development efforts. In combination, these two strategies can help in optimizing experimental procedures in a reduced number of studies as well as providing essential information for appropriate decisions of the future (Hanrahan and Lu 2006). There are too few examples that demonstrate the effectiveness of the designs studied, and too many that seem bent on criticizing decisions in published examples (Ryan and Morgan 2007). The use of genetic algorithms (GAs) is enjoying ever-increasing popularity among engineers and designers as a way of optimizing their products and processes. One of the major advantages of such techniques is that they allow true multi-objective optimization. Based on the Darwinian idea of “survival of the fittest”, the genetic algorithm (GA) has been utilized to explore the entire design space and find the best solutions for engineering optimization. For practical engines, the objectives needed to be optimized are usually more than one, and the trade-off relationship (such as NOx and soot emissions) always exist (Xu, Jia et al. 2019).

2.7.1 Factorial and Fractional Designs

Factorial experimental designs investigate the effects of many different factors by varying them simultaneously instead of changing only one factor at a time. Factorial designs allow estimation of the sensitivity to each factor and also to the combined effect of two or more factors (Telford and K 2007).

In an experimental setting which there are several factors studied together and each factor has several levels, the treatments comprise of all the possible combinations of several levels of all the factors. Such experiments where several factors with several levels are tried and the treatments are the treatment combinations of all the levels of all the factors are known as factorial experiments (Gupta and Parsad 2005).

Factorial experimentation is a method in which the effects due to each factor and to combinations of factors are estimated. Factorial designs are geometrically constructed and vary all the factors simultaneously and orthogonally. Factorial designs collect data at the vertices of a cube in p -dimensions (p is the number of factors being studied). If data are collected from all of the vertices, the design is a full factorial at two levels, requiring 2^p runs. Since the total number of combinations increases exponentially with the number of factors studied, fractions of the full factorial design can be constructed. As the number

of factors increases, the fractions become smaller and smaller ($1/2$, $1/4$, $1/8$, $1/16$, ...). Fractional factorial designs collect data from a specific subset of all possible vertices and require 2^{p-q} runs, with 2^{-q} being the fractional size of the design. If there are only three factors in the experiment, the geometry of the experimental design for a full factorial experiment requires eight runs, and a one-half fractional factorial experiment (an inscribed tetrahedron) requires four runs (Telford and K 2007).

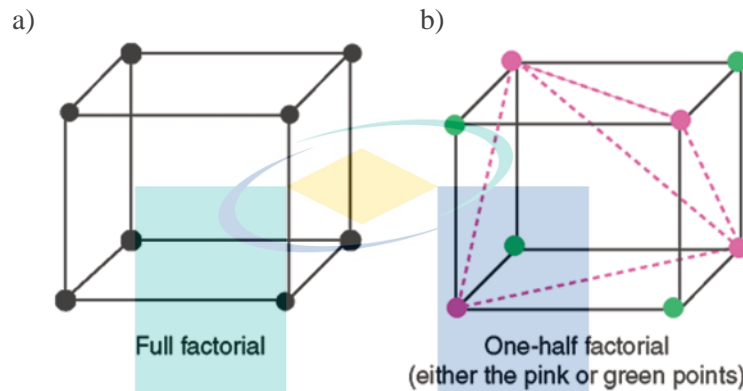


Figure 2.21 Full factorial (a) and one-half factorial (b) in three dimensions.

Factorial experiments can be laid out in a completely randomized design (CRD), randomized complete block (RCB) design, Latin square design (LSD) or any other design. A full factorial experiment is only suitable when a relatively small number of variables at a few levels are involved. For example, a three-variable experiment at two levels requires eight trials, whereas one with four variables at five levels requires 625. With such a potentially large number of trials, it is understandable why the experimenter may consider adopting the 'change one variable at a time' strategy. However, factorial experiments, particularly at two or three levels, can be used to form the building blocks for many other experimental designs. Generally, full factorial and Latin hypercube designs are representative DoE sampling types. Full factorial indicates that all possible combinations of factors are included, so it is necessary to define the minimum and maximum values and the number of levels for each factor. Latin hypercube sampling means that a Latin hypercube partial factorial design was used. A partial factorial design can determine the relationship between the dependent (response) and independent (factor) variables from fewer experiments than would be required for a full factorial design (Park and Song 2017).

The Central Composite Rotatable Design (CCRD) is an effective alternative to factorial designs (Venkatesan, Harris et al. 2014). The number of tests required for the

CCRD are 2^k standard factorial points with its origin at the centre, 2^k points fixed axially at distance β from the centre to generate the quadratic terms, replicate tests at the centre, where k refers to the number of variables to be tested (Obeng, Morrell et al. 2005). The statistical optimization technique using full factorial design of experiments is generally applied to determine the boundary conditions, which allows the maximum output of the desired products. Using a proper design matrix one can obtain a regression equation, which highlights the effect of individual parameters and their relative importance in given operation/process (Öztürk and Kavak 2004). The interactional effects of two or more variables can also be known, this is not possible in a classical experiment (Singh, Besra et al. 2002).

2.8 Summary

In this chapter, a thorough literature review on the relevant topics has been conducted to gain sufficient information before proposing ideas and strategies to run the investigation. The area of study in this chapter covered the internal combustion engine in general, then delve specifically into valve timing and engine performance. In summary, exhaust valve timings alteration primarily helps to reduce exhaust emissions, whereas varying the intake valve timings helps the engine produce more power and torque. There are several potential benefits of VVT, which are beyond the scope of this thesis such as; improved engine braking, residual exhaust control, and cylinder deactivation. Few strategies of variable valve timing have been identified with different impact variation to engine performance. The current technologies of valve timing systems also compiled to study the differences and to determine a novel investigation in the variable valve timing field.

CHAPTER 3

METHODOLOGY

The quality of the result of any work, project or research hugely determined by the effectiveness of how the work is being conducted. The methodology is a way to find out the result of a given problem on a specific matter. The right methodology will produce a convincing outcome in terms of quality and worthiness. If research does not work systematically on the problem, there would be less possibility to find out the final result. In this chapter, the method of carrying out this research until producing the result is explained in detail. The flowchart will show all the steps taken in order to acquire the final result.

3.1 Overview of Research

The flowchart diagram is mapped out as shown as in Figure 3.1, containing comprehensive information of the procedures taken step by step in order to obtain inclusive data and results as provided in CHAPTER 4. The flowchart delivers a quick information about each stack of the flow starting from the beginning through the end.

A thorough study on variable valve timing strategies and approaches used by the various researcher in their previous work from a wide variety of sources was done to gain an excellent understanding of the topic. Ideas, understanding, facts and figures were gathered to establish a solid fundamental on the research topic. Diagrams and statistics were compiled and studied to create an idea on conducting this investigation, thus be able to define the objectives and scope of this research.

Cam profile measurements were conducted using a setup with a dial gauge to determine the baseline valve lift profile in order to simulate the engine camshaft profile in 1-dimensional simulation tool. Port flow assessment was conducted in order to obtain

the valve flow coefficient data, which is necessary and to replicate the flow behaviour at the intake and exhaust valves during the 4-stroke cycle. The engine specifications, inclusive of geometry, performance data and other significant parameters were gathered and compiled, hence sufficed the necessity needed to develop and replicate the real 65cc engine in the 1-dimensional tool.

The simulation of the baseline model was run, and the performance was discussed in the analysis section. The baseline model was validated by comparing the specifications of the engine performance of peak power provided by the engine manufacturer and performance data obtained from the simulation. After the validation succeeds, a design of experiment was conducted on the baseline model to investigate the intake and exhaust behaviour on engine performance. Involved factors and levels were identified to form a design of experiment. A full factorial experiment with six factors and three levels was conducted on the baseline model with the application of 12 FVT strategies.

Further analysis of the performance results was carried out to investigate the intake and exhaust philosophies for variable valve timing. Using a combination of a few valve timing strategies, best valve lift profiles from the design of experiment were acquired and identified as the FVT profiles. The FVT profiles were applied in the baseline model in a 1-dimensional tool to boost engine performance. The engine performance results of the FVT application were analysed and compared with baseline model performance to verify the performance improvement.

اونيورسيتي ملايسيا قهغ

UNIVERSITI MALAYSIA PAHANG

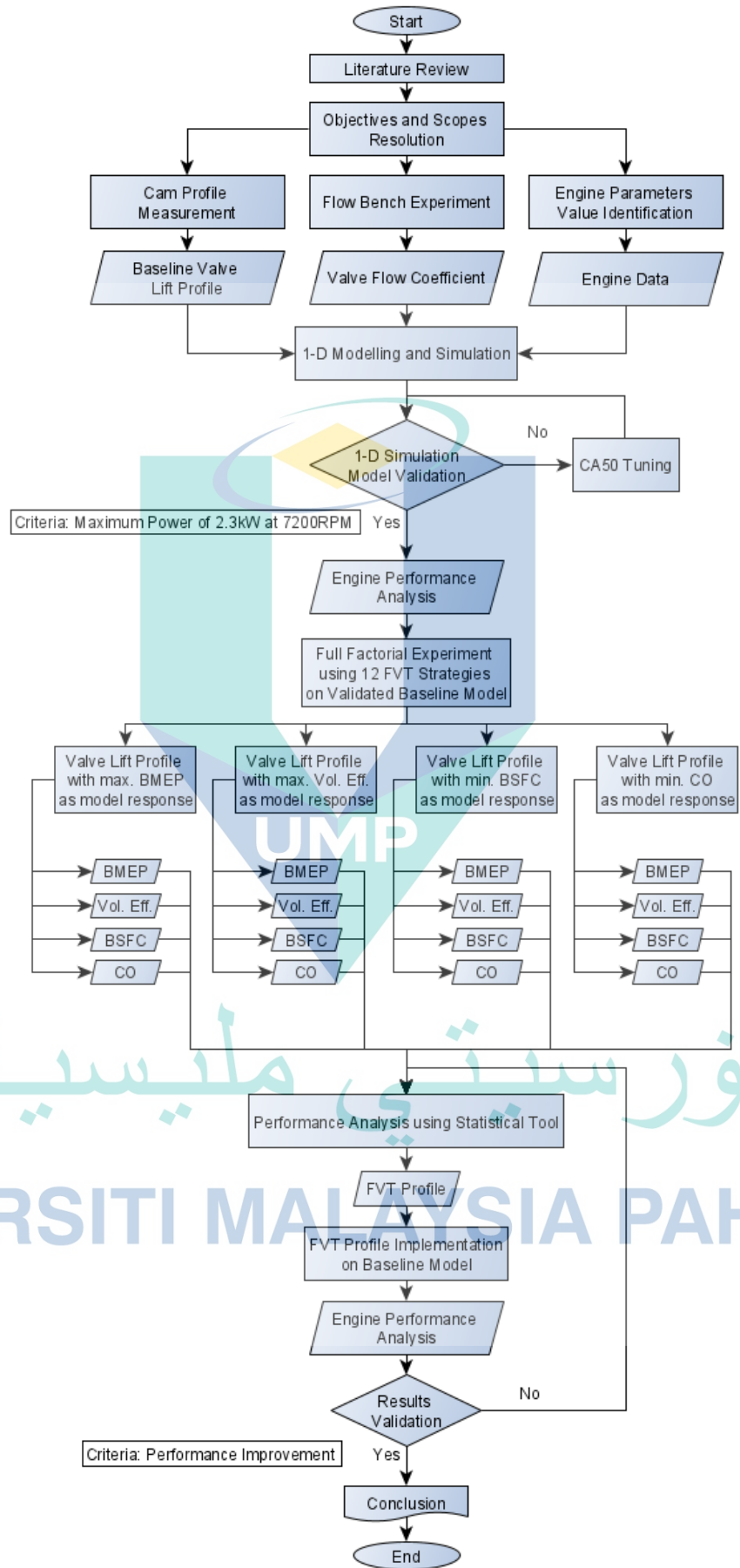


Figure 3.1 Methodology Flowchart

3.2 One-dimensional Simulation Tool

The base tool used in this project is GT-POWER Engine Simulation Software, owned by Gamma Technologies, the supplier of engine and vehicle simulation company. GT-POWER Software was chosen to realize this project because of its reliability to handle the simulation of the internal combustion engine in terms of modelling in pre-processing, the accuracy of in predicting the behaviour of complex engine-related phenomena and quick data extraction in post-processing. It provides the ability for users to generate and combine multiple data in its post-processing software, GT-POST. Furthermore, most of the previous work on variable valve timing and internal combustion engine simulation study were achieved using GT-POWER software. MATLAB is also used in plotting the valve lift profile and results from simulation and experiment.

3.3 Baseline Engine Specifications

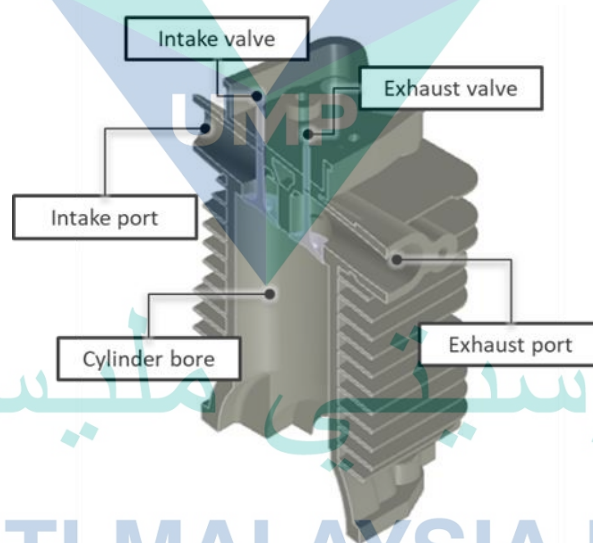


Figure 3.2 Engine Components Layout

The investigation was conducted by using the specification of a 65cc four-stroke gasoline engine from Stihl product manufactured by Andreas Stihl AG & Company KG, Germany. The engine is widely used in handheld power equipment such as trimmers, blowers and chainsaws. The detailed engine specifications was obtained from previous work (Hanipah 2015) and can be viewed as in Table 3.1.

Table 3.1 Baseline Engine Specifications

Parameter	Value
Capacity	65cc
Bore	50mm
Stroke	33mm
Geometric Compression Ratio	9.5:1
Valve Lift	2.74mm
Intake Valve Diameter	20mm
Exhaust Valve Diameter	18mm
Maximum Power	2.3kW @7200RPM

3.4 One-dimensional Modelling

The engine modelling based on Stihl 4MIX 65cc engine was constructed in 1-dimensional simulation software using the respected engine specifications. The structure of the engine, which set as a baseline model in this project, is as shown in Figure 3.3. The injection rate of the engine model was set to be a constant parameter which assumed stoichiometric in all conditions. The calculated clearance volume of the cylinder is 6.8cm^3 .

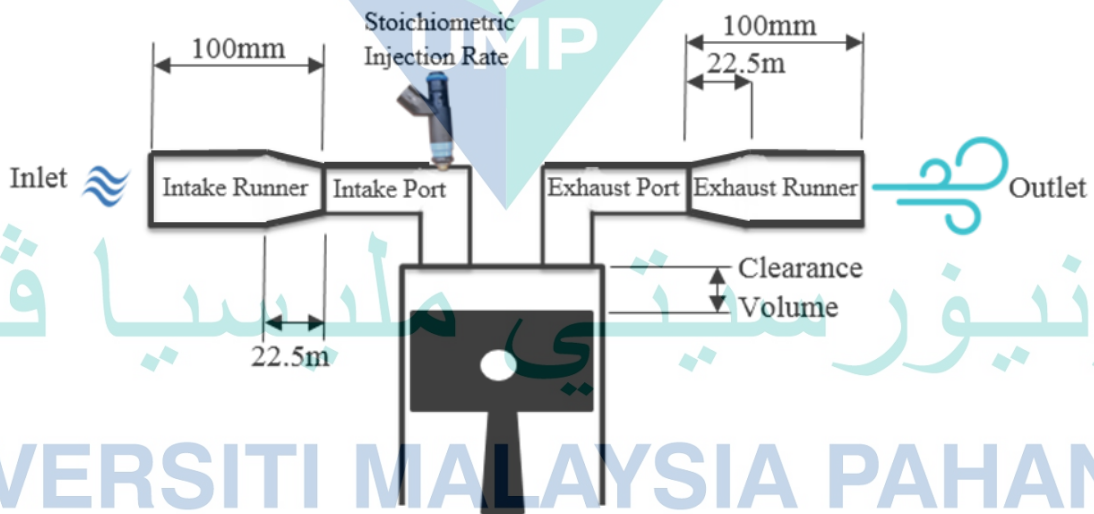


Figure 3.3 Engine Structure of Baseline Model

The structural parts of the engine with their respective parameter value were transferred and rebuilt as a model as shown in Figure 3.4.

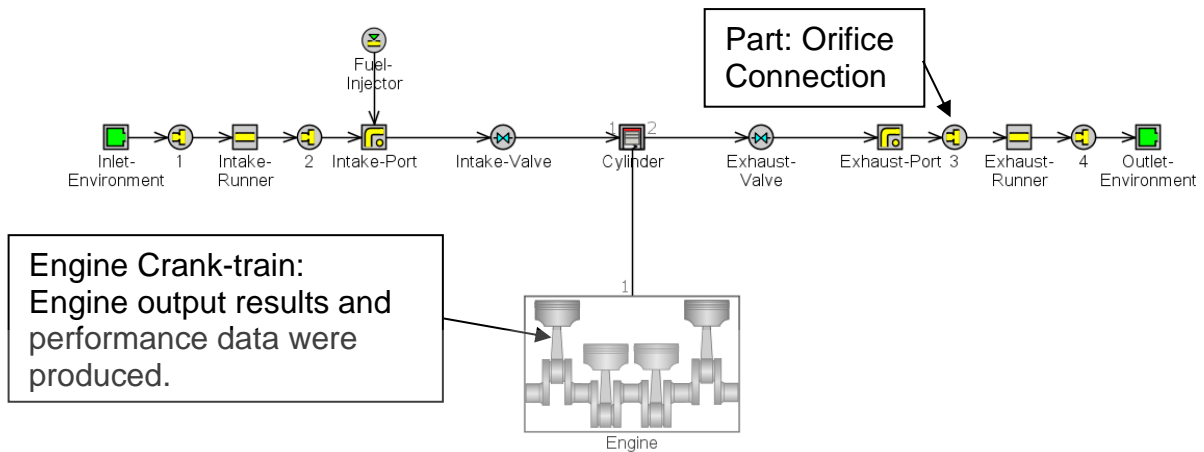


Figure 3.4 One-dimensional Schematic of Baseline Model

The baseline was created according to the specifications of the baseline engine, Stihl 4MIX 65cc. The details of every structural part of the baseline model constructed were displayed in Table 3.2.

Table 3.2 Part Specifications of 1-D Baseline Model

Parts	Details
Intake Runner	Round Intake Runner Pipe Diameter: 20mm Length: 100mm Discretization Length: 22.5mm
Intake Port	Round Intake Port Pipe Inlet Diameter: 20mm Outlet Diameter: 18.5mm Discretization Length: 27.5mm
Fuel Injector	Stoichiometric Injection Rate Air to Fuel Ratio: 14.7 Located exactly in middle of intake port
Cylinder	Combustion Model: SI Wiebe Heat Transfer Model: Woschni GT
Cranktrain	4-stroke cycle, 65cc
Exhaust Port	Round Exhaust Port Pipe Inlet Diameter: 16.5mm Outlet Diameter: 18mm Length: 90mm Discretization Length: 27.5mm
Exhaust Runner	Round Exhaust Runner Pipe Diameter: 18mm Length: 100mm Discretization Length: 22.5mm
End Environment (Inlet and Outlet)	1 Bar atm.

3.5 Valve Lift Profile of Baseline Model

The valve lift profile of the engine was obtained from the actual measurement of the Stihl 4MIX 65cc engine. The lift profile for the intake and exhaust valve with respect to Crank Angle Degree (CAD) was plotted in MATLAB, as shown in Figure 3.5 with a measured maximum valve lift of 27.4mm. This profile was set to be a baseline valve lift profile used in valve timings investigation later. The valve lift events of this profile were summarized in Table 3.3.

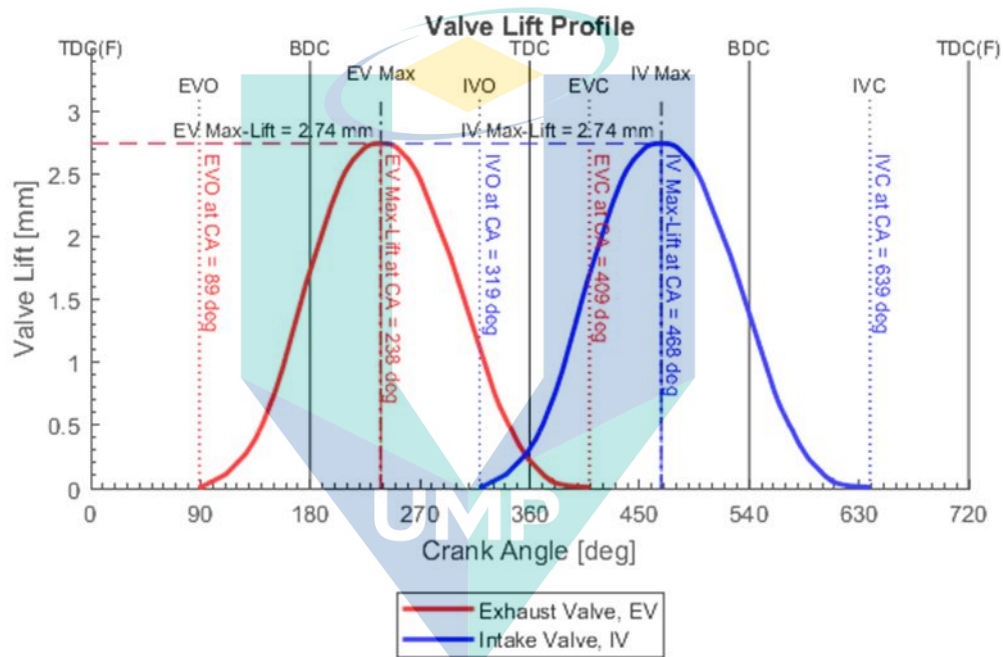


Figure 3.5 Valve Lift Profile of Baseline Model

Table 3.3 Valve Lift Profile Parameters of Baseline Model

Parameter		Unit	Baseline
Engine Speed		RPM	Entire Speed
Intake Valve	Opening	at CA°	319
	Closing	at CA°	639
	Maximum Lift	mm	2.74
Exhaust Valve	Duration	CA°	320
	Opening	at CA°	89
	Closing	at CA°	409
	Maximum Lift	mm	2.74
	Duration	CA°	320
Valve Overlap		mm	90

3.6 Valve Flow Coefficient

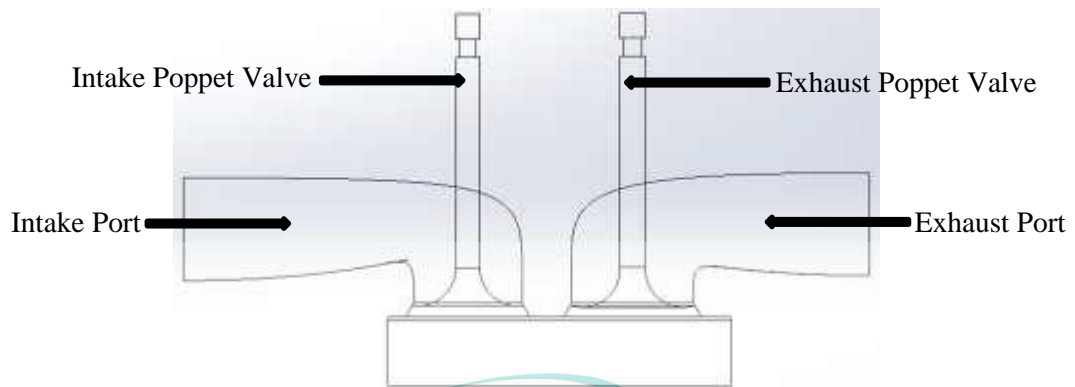


Figure 3.6 Engine Head Part for Flow Assessment

The flow coefficient is a relative measure of efficiency at allowing fluid flow. It describes the relationship between the pressure drop across an orifice, valve or other assembly and the corresponding flow rate. Using the principle of conservation of energy, Daniel Bernoulli found that as a liquid flow through an orifice, the square of the fluid velocity is directly proportional to the pressure differential across the orifice and inversely proportional to the specific gravity of the fluid. The greater the pressure differential, the higher the velocity. The greater the density, the lower the velocity. The flow coefficient of intake and exhaust valve is as shown as in Table 5.1 and Table 5.2, respectively. The data was obtained from the experimental procedure on the flow behaviour of the identical engine (Zahidi, Hanipah et al. 2017) used in this investigation as a baseline model. This data is necessary for constructing the baseline 1-dimensional simulation model.

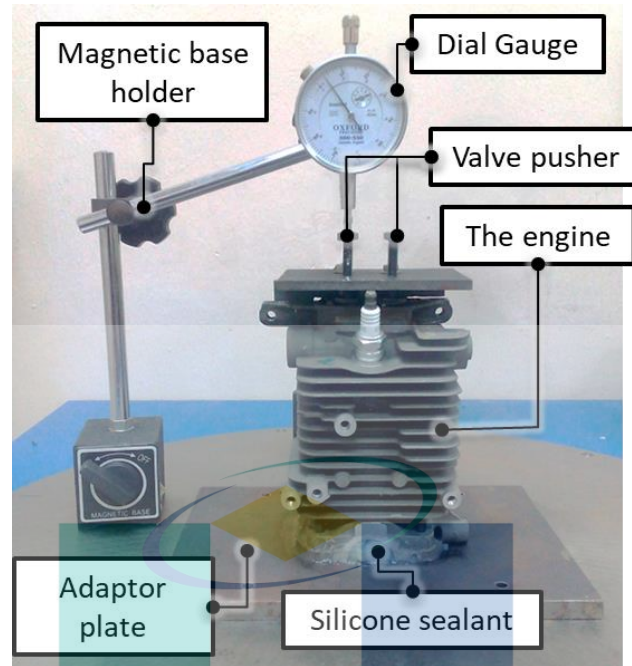


Figure 3.7 Engine head setup for flow coefficient experiments.

3.7 Flexible Valve Timing Strategies

There are six identified valve events that take place in an internal combustion engine, namely:

1. Intake Valve Opening (IVO)
2. Intake Valve Closing (IVC)
3. Intake Valve Maximum Lift (IVMAX)
4. Exhaust Valve Opening (EVO)
5. Exhaust Valve Closing (EVC)
6. Exhaust Valve Maximum Lift (EVMAX)

Based from a literature review on previous works regarding the research and study of variable valve timings in the internal combustion engine, 12 strategies were proposed to be applied in this investigation to inspect how they affect the engine in terms of performances, efficiencies, fuel consumption and emissions. The application of these 12

strategies is meant to affect one another as they were applied simultaneously at a time by means of the factorial design of experiment. The strategies namely:

1. Late Intake Valve Closing (LIVC)
2. Early Intake Valve Closing (EIVC)
3. Late Intake Valve Opening (LIVO)
4. Early Intake Valve Opening (EIVO)
5. Low Lift Intake Valve Profile (Low-IVMAX)
6. High Lift Intake Valve Profile (High-IVMAX)
7. Late Exhaust Valve Closing (LEVC)
8. Early Exhaust Valve Closing (EEVC)
9. Late Exhaust Valve Opening (LEVO)
10. Early Exhaust Valve Opening (EIVO)
11. Low Lift Exhaust Valve Profile (Low-EVMAX)
12. High Lift Exhaust Valve Profile (High-EVMAX)

The valve duration of the intake valve will be affected by the tuning of IVO and IVC position, while the valve duration of exhaust valve will be affected by the tuning of EVO and EVC position. Valve overlap will be affected by the tuning of IVO and EVC position.

Following the objectives and problem statement mention earlier in the previous section, these 12 strategies have been identified to have the potential in boosting the engine performance. Based on the literature survey done earlier, every strategy carries an independent advantage in enhancing engine performance. With the combination of these

in the FVT system, a true potential of engine performance can be unleashed and fill the research gap.

The flexible valve timing strategies used in this investigation are represented in Figure 3.8 in the form of Valve Lift (mm) with respect to Crank Angle Degree (CAD).

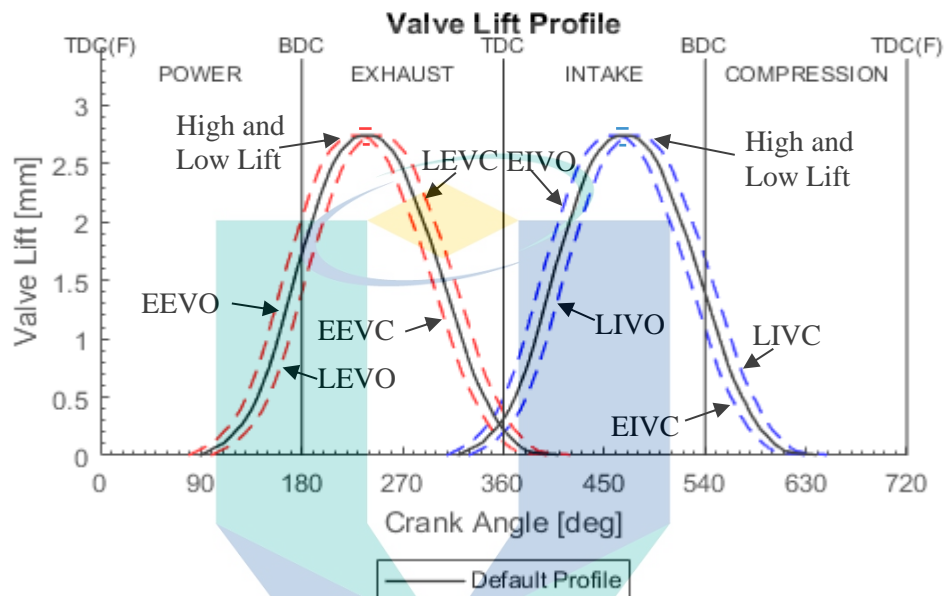


Figure 3.8 Flexible Valve Timing Strategies

3.8 Design of Experiment

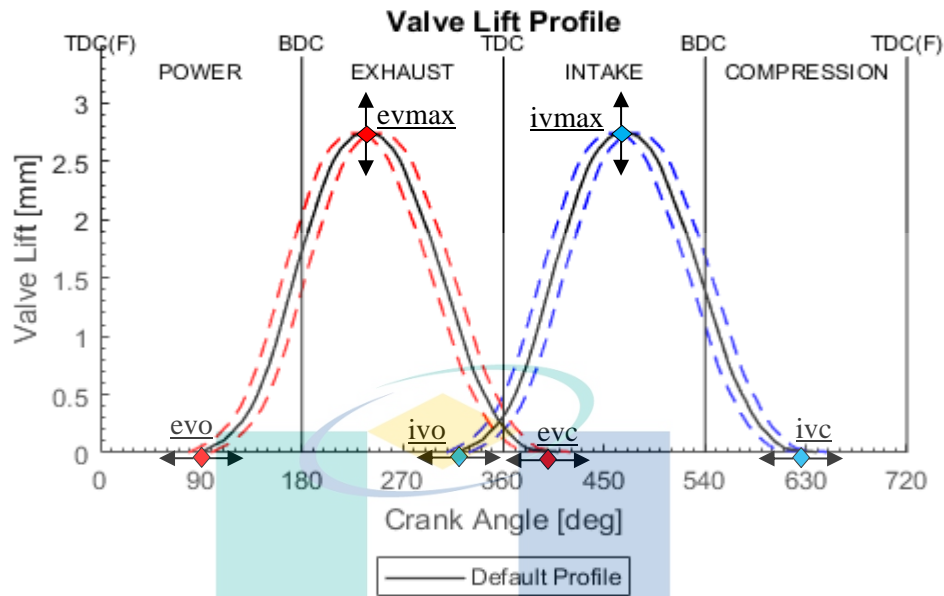


Figure 3.9 DOE Strategy of 3 Level Full Factorial Experiment

The variation of valve opening and closing point, maximum lift of intake and exhaust valve lift was conducted using a full factorial experiment. There are six variables involved in this experiment, which are ivo, ivc, ivmax, evo, evc, and evmax. The variables were identified as the six factors in the DOE setup with a variation of three levels.

The equation for experiment numbers in full factorial experiment design was obtained using equation 3.1.

$$N = L^f \quad 3.1$$

Where:

L = the number of levels

f = the number of factors

Thus,

$$N = 3^6$$

$$N = 729$$

With each experiment run at one-speed level at a time, ten full factorial experiments were conducted to accomplish the study of flexible valve timing strategies through whole engine speed regions. An amount of 7,290 cases of experiments were executed in this study.

The angle of modification used for valve event timing is 20 CAD in increment from the minimum point, and height modification used for valve lift is 0.17mm in increment from the minimum point. Thus, multiplier difference for angle used to tune the opening and closing point (valve part) in this experiment is 0.0625 (6.25%) as it will affect amount of 20 CAD of increment or reduction.

Angle multiplier will affect the duration of the valve thus, affects the closing point (ivc and evc) of the valve. A similar multiplier value is used to tune the maximum valve lift and it affect the amount of 0.17mm lift increment and reduction. Table 3.4 delivers the overview of this DoE full factorial strategy in matrix form in the assessment towards developing the FVT system.

Table 3.4 Design of Experiment Matrix

Parameter	Unit	Factor	Minimum (-1)	Baseline (0)	Maximum (+1)	No. of Levels	
Intake Valve	Opening	at CA°	ivo	299	319	339	3
	Closing	at CA°	ivc	619	639	659	3
	Max. Lift	mm	ivmax	2.57	2.74	2.91	3
Exhaust Valve	Opening	at CA°	evo	69	89	109	3
	Closing	at CA°	evc	389	409	429	3
	Max. Lift	mm	evmax	2.57	2.74	2.91	3

CHAPTER 4

RESULTS AND DISCUSSION

4.1 Baseline port flow performance

The result from the flow bench experiment is volume flow rate data of intake and exhaust port. The experimental result is calculated with the theoretical equation of coefficient. The result from the coefficient calculation is compared against the small block Chevrolet (SB Chevy) engine coefficient.

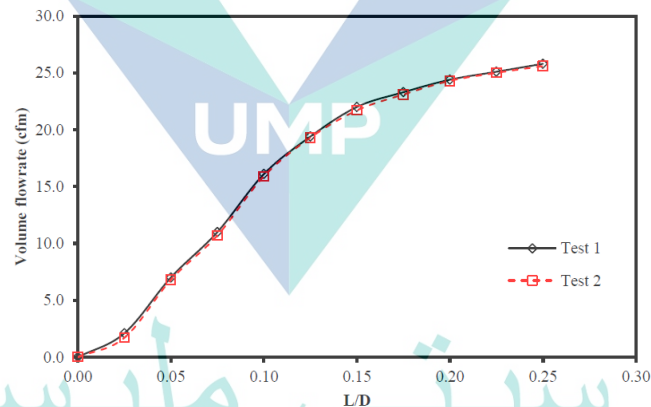


Figure 4.1 Volume Flow Rate of Intake Port

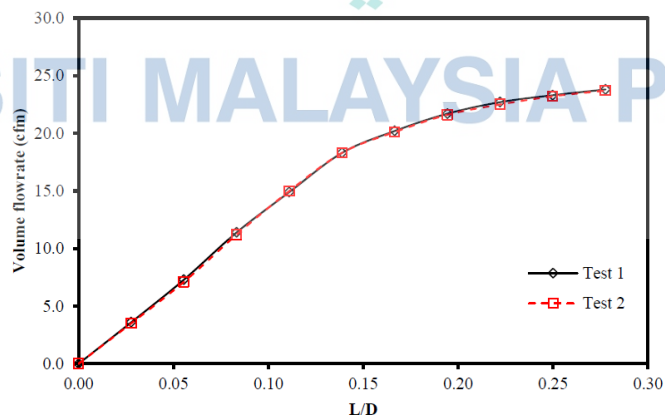


Figure 4.2 Volume Flow Rate of Exhaust Port

Figure 4.1 and Figure 4.2 show the result of the air volume flow rate through the intake and exhaust port respectively. The results from test 1 and test 2 show a slightly different value of the volume flow rate. The volume flow rate is 0 cubic feet per minute, CFM at 0 L/D ratio at intake and exhaust port. Then it increases gradually to 25.8 CFM at 0.25 L/D ratio and to 23.8 CFM at 0.278 L/D ratio, respectively.

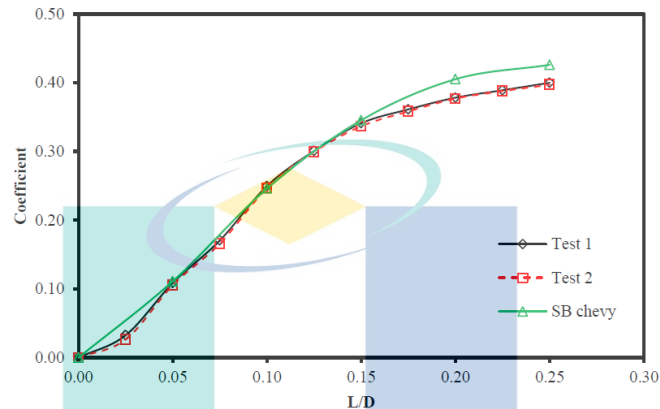


Figure 4.3 Flow Coefficient of Intake Port

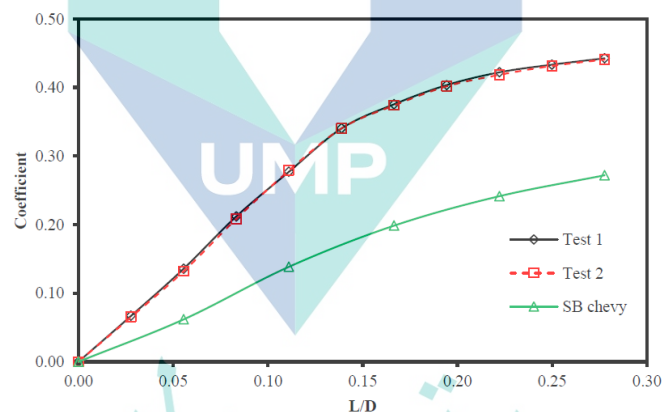


Figure 4.4 Flow Coefficient of Exhaust Port

Figure 4.3 and Figure 4.4 show the flow coefficient of intake and exhaust port poppet valve engine respectively, and in comparison, with SB Chevy. The figure shows the intake port flow coefficient did not have much different from SB Chevy. The coefficient is 0 at 0 L/D ratio and augmented gradually to 0.4 at 0.25 L/D for the engine. While SB Chevy coefficient is 0 at 0 L/D and increases gradually to 0.42 at 0.25 L/D ratio. Meanwhile, the exhaust port flow coefficient has a high coefficient value compare to SB Chevy. Both heads start with 0 coefficients at 0 L/D ratio. But at peak 0.278 L/D ratio, the poppet valve has a 0.44 coefficient and SB Chevy has 0.27 coefficient value.

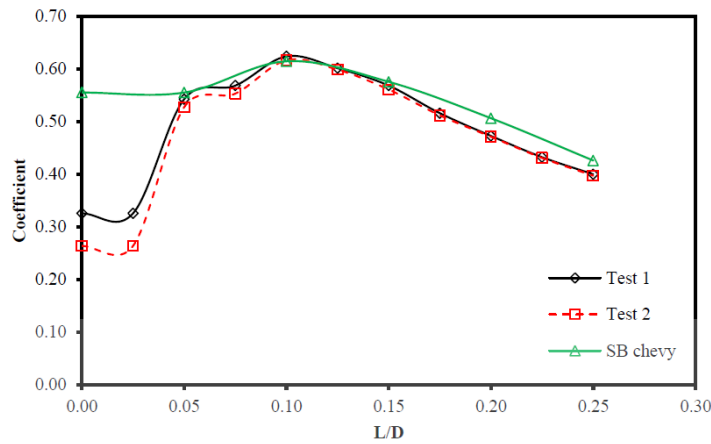


Figure 4.5 Discharge Coefficient of Intake Port

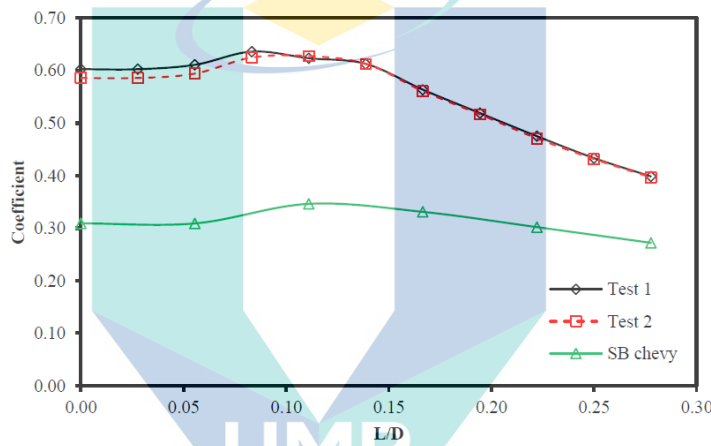


Figure 4.6 Discharge Coefficient of Exhaust Port

Figure 4.5 and Figure 4.6 displays the discharge coefficient of intake and exhaust port poppet valve engine respectively, and in comparison with SB Chevy. The result shows SB Chevy has a higher discharge coefficient of intake port from 0 until 0.05 L/D ratio. At 0 L/D ratio, SB Chevy has a 0.55 coefficient and the poppet valve engine is 0.32 and 0.26 coefficient for test 1 and test 2, respectively. Then the coefficients for both engine head have similar values at 0.05, 0.1 and 0.15 L/D ratio with 0.54, 0.61 and 0.57 coefficient, respectively. The highest coefficient value is at 0.1 L/D ratio. Then, the coefficient values decrease gradually until 0.25 L/D ratio with 0.4 for the poppet valve and 0.42 for SB Chevy. The results show the intake port coefficient of the poppet valve engine is almost the same value as SB Chevy. The result shows that the poppet valve intake port is comparable with SB Chevy.

The poppet valve has remarkably higher discharge coefficients of the exhaust port compare to SB Chevy. The poppet valve engine has 90% higher coefficients between 0 until 0.05 L/D ratio. Then the percentage of coefficient difference is reducing gradually

until 46% at 0.279 L/D ratio. The result shows the coefficient of the two-stroke poppet valve engine exhaust port has better coefficients compare to SB Chevy. The higher coefficient shows the exhaust gas can release faster at a limited time in engine cycle duration.

The port flow experimental investigation of the two-stroke poppet valve has highlighted that the flow and discharge coefficient of the intake port has almost similar values with SB Chevy. Except at zero L/D ratio of intake CD, the SB Chevy has 89% higher value than the two-stroke poppet valve. The flow and discharge coefficient of the exhaust port for the two-stroke poppet valve has higher values than SB Chevy.

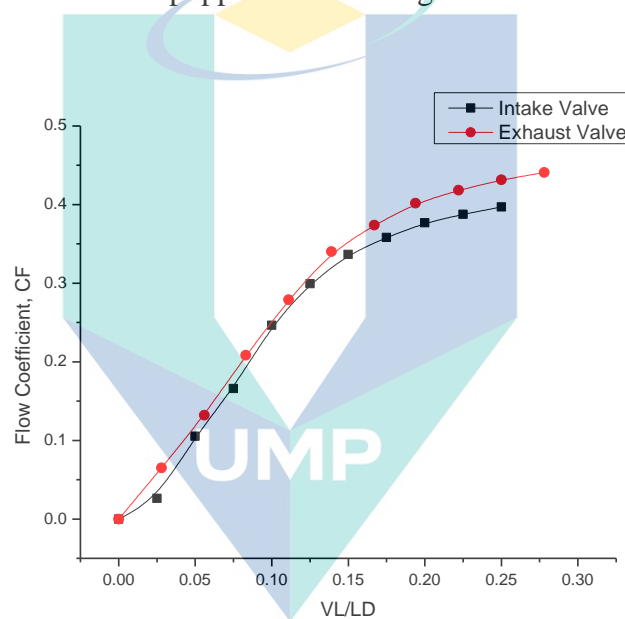


Figure 4.7 Valve Flow Coefficient of Intake and Exhaust Valve of Baseline Model

Figure 4.7 shows the flow coefficient graph of intake and exhaust valve graphically replotted. Table 5.1 and Table 5.2 (in Appendix A) respectively display the flow coefficient of intake and exhaust valve calculated from the port flow assessment data. The flow coefficient data is essential in developing the 1-dimensional engine model using 1-dimensional tool.

4.2 Baseline model performance

In order to initiate all the flexible valve timing strategies, a baseline model was built in 1-D simulation software and the validation of the baseline model was conducted

to ensure the strategies are applied into a validated simulation model, which will deliver actual results.

Figure 4.8 shows the fitted power curve represented from the simulation of 65cc four-stroke Stihl 4MIX engine, as also presented by Hanipah M. R. B (Hanipah 2015). The peak power for the original 65cc Stihl 4MIX is 2.3kW at 7200rpm as acquired from manufacturer data which can be set as a reference to validate the baseline simulation model shows good correlation to the fitted power curve from 4000RPM and above with the percentage of error of less than 20% and almost in agreement with the manufacturer data. The method of developing a validated baseline model based on the peak power specification is by optimising the combustion profile, CA50, which using the SI Wiebe combustion model curve. The position where the accumulated heat release reaches 50% of the total released heat is called CA50, which is the parameter that is optimised to obtain a validated baseline model in the simulation.

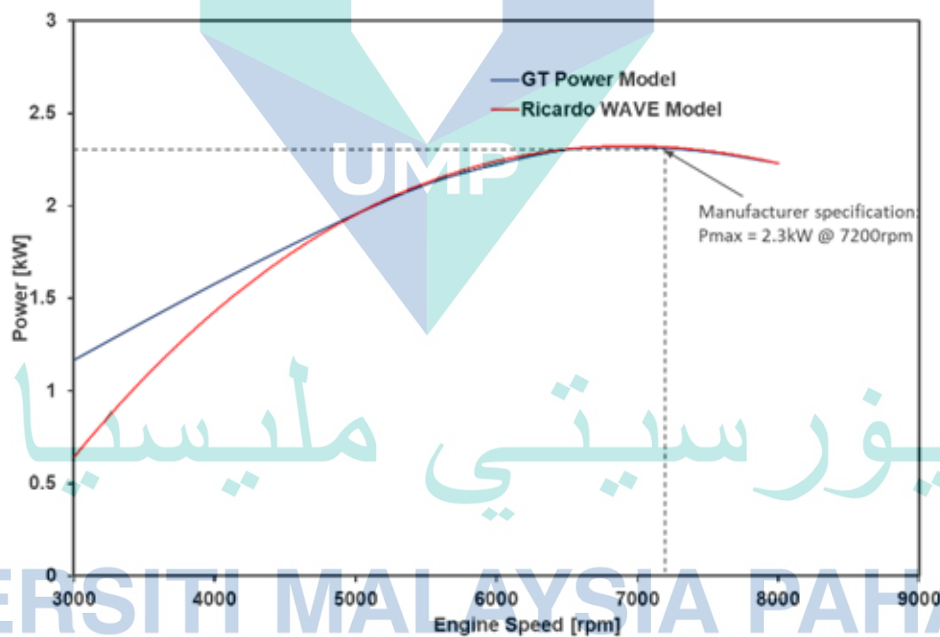


Figure 4.8 Power Curve Validation from Tool Simulation

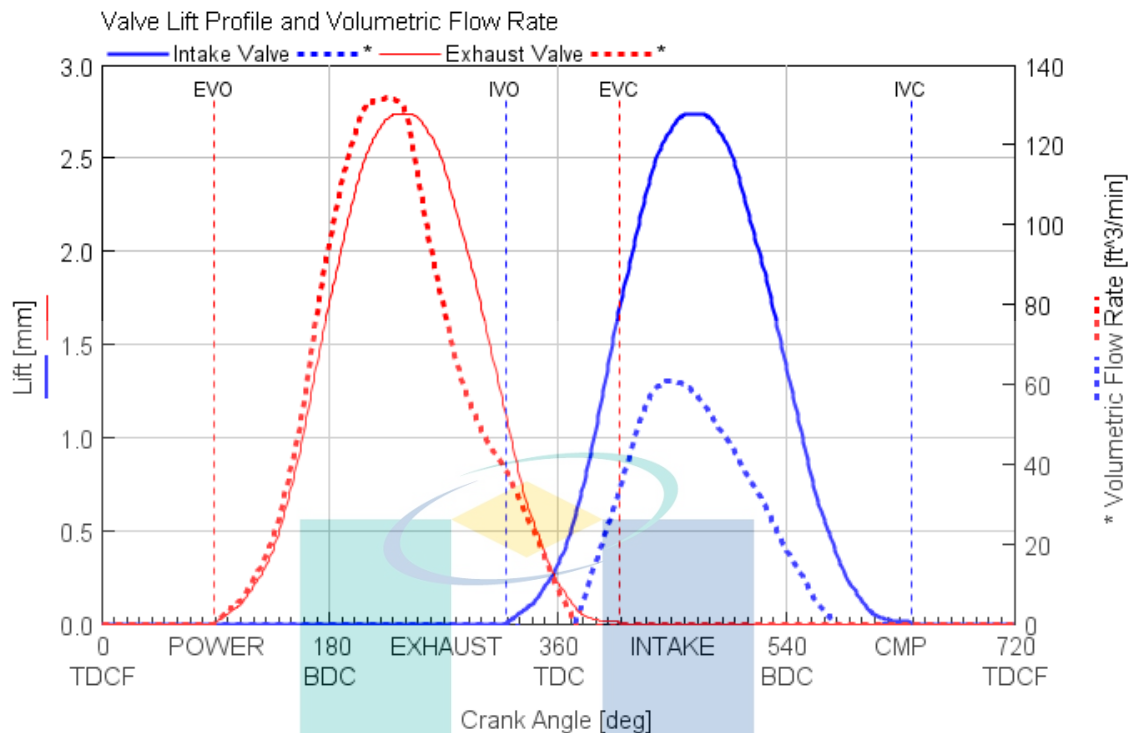


Figure 4.9 Valve Lift Profile and Volumetric Flow Rate

Figure 4.9 shows the valve lift and volumetric flow rate against CAD at 7200RPM. The flow behaviour shows that the volumetric flow rate at the exhaust valve is greater than at intake valve by 50% although the lift, duration and event timing of intake and exhaust valves are the same. Due to combustion, which produce high pressure in the chamber, this phenomenon occurred. During the valve overlap, there is no overlapping of volumetric flow observed even though the intake valve was opened earlier. The intake flow starts right after exhaust flow expelled. This behaviour is observed at high-end RPM.

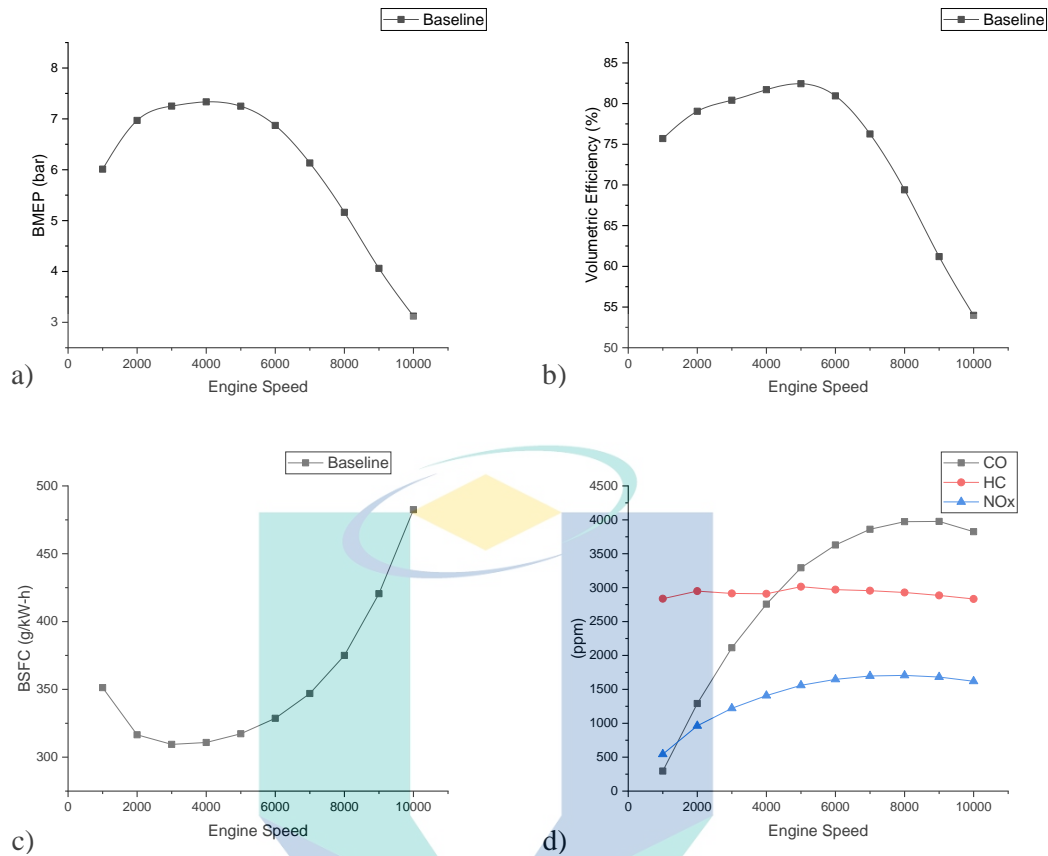


Figure 4.10 BMEP, Volumetric Efficiency, BSFC and Emissions of Baseline model

Figure 4.10 shows the performance result of baseline model performance run in a simulation tool. The peak power produced is 2.3kW at 7200RPM, as shown in Figure 4.8. The peak torque and BMEP are produced at 4000RPM with 3.78Nm and 7.31bar, respectively. The volumetric efficiency demonstrated an excellent increment trend from 1000RPM up to 7500RPM with a maximum value of 82% at 5000RPM and average of 80%. The efficiency trend then deteriorates remarkably down to 53% at 10,000RPM.

The BSFC result of the baseline model indicates that the trend is decreasing as speed increase from 1000RPM to 3000RPM, where the lowest fuel consumption is observed with 309 g/kW-h. The trend then changes to increment of BSFC up until high-end RPM with a maximum value of 482 g/kW-h.

The emissions result of the baseline model displays three gas emissions produced from the run, which is CO, HC and NOx. The increment trend of the CO curve shows an obvious bend compared to HC and NOx, which are less inclined. The CO emission increase as speed increase with maximum CO produced is 4002 ppm at 8500RPM. The presence of carbon monoxide is normally due to incomplete combustion (Merker, Eckert

et al. 2012). NO_x curve shows an increment of the amount of gas as speed increases with maximum value 1707 ppm at 7500RPM. However, the rise of NO_x emissions is lower than CO. NO_x emissions are formed during combustion by the oxidation of nitrogen under the high-temperature conditions in the cylinder. As speed increases, temperature increases.

HC emissions display a flat trend across the entire engine speed with an average of 2925 ppm. Peak HC was observed at 5000RPM with an undistinguished difference. Peak HC emissions occur under cold conditions that hinder their oxidation and, in the case of liquid fuels, their evaporation process (Ferguson and Kirkpatrick 2015).

4.3 FVT model optimization

The flexible valve timing model was structured with six variables, as outlined in section 3.8. These variables represent the intake and exhaust timings and lifts, which have conventionally fixed for each internal combustion engine design. This section presents the results obtained from the optimization using DOE conducted on the baseline model.

There are four output performance parameters selected as the objectives for this investigation, namely BMEP, volumetric efficiency, BSFC and CO in order to investigate the effects on performances, fuel consumption and emissions. Mean effective pressure (MEP) is a normalized parameter, which is a useful relative measure of an engine's performance. Unlike torque and power, MEP is independent of engine size. Volumetric efficiency is a measurement of efficiency related to volume swept, which determines the breathing performance of an engine. Volumetric efficiency defined as the comparison of actual air mass that enters the chamber to the total displacement volume of a specific engine. Turbocharger, supercharger and VVT have been used to improve volumetric efficiency in ICE. BSFC is selected to observe the effects of this investigation on fuel consumption. CO emissions have been selected to evaluate the effects of this investigation on emissions. Based on Figure 4.10, compared to HC and NO_x, CO has a larger curve gradient.

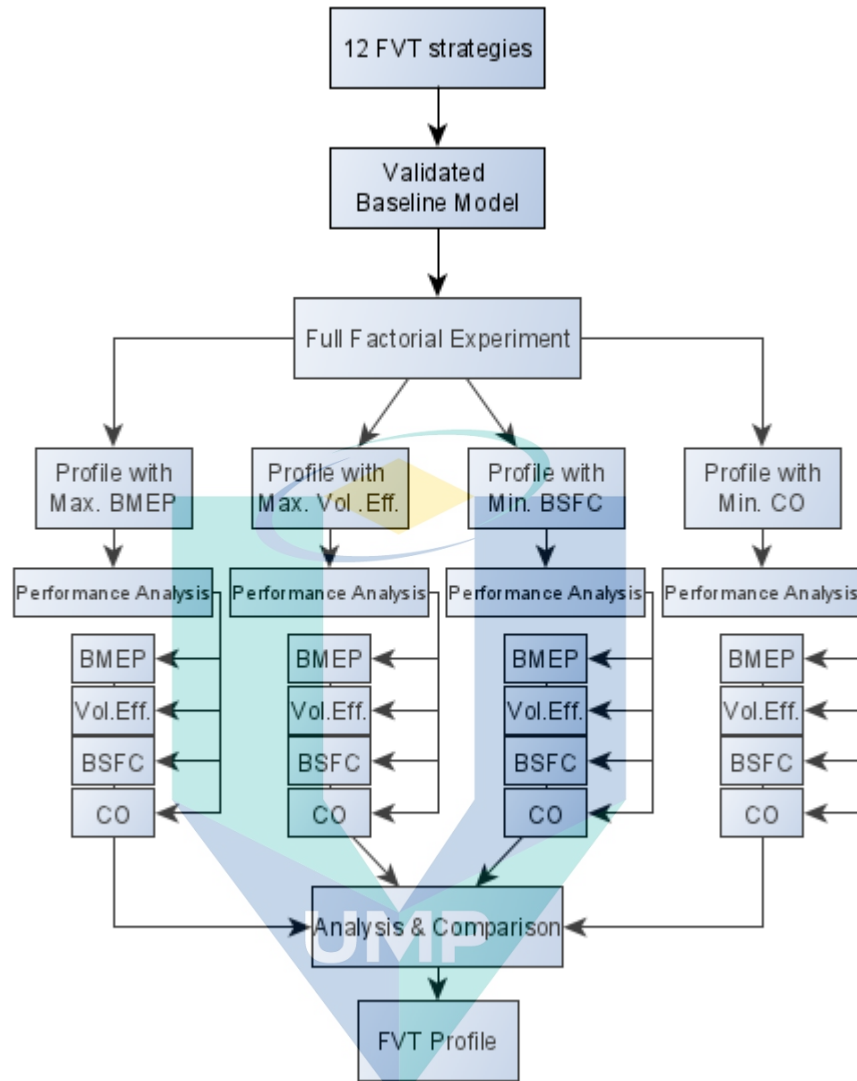


Figure 4.11 FVT Model Optimization Flowchart

Figure 4.11 shows the flowchart in determining the best valve lift profile for FVT. Four model responses target were aimed, which are maximum BMEP, maximum volumetric efficiency, minimum BSFC and minimum CO. At every speed level, these model responses target were achieved by four different valve lift profiles. In rare cases, one profile achieved two key performances target, such as valve lift profile with case number 234 and 321, which can be viewed in the next section. Case 234 proved to achieve maximum BMEP and minimum BSFC at high-end RPM while case 321 achieved maximum BMEP and maximum volumetric efficiency at 4000RPM to 5000RPM. However, valve lift profile case 234 has contributed to a sudden increasing trend of CO emission at high-end RPM as shown in Figure 4.12 and Figure 4.14.

The overall performance from four model responses target, carrying different valve lift profiles in each speed level, were compared and underwent statistical analysis to determine the best valve lift profile for FVT for performance boosting without jeopardizing other aspects such as fuel consumption and emissions.

4.3.1 Maximum BMEP as model response

Table 4.1 shows the performance result of valve lift profile cases that achieved maximum BMEP from the factorial experiment. The other three performances were also compiled together to compare the performances result between model responses later. With maximum BMEP as a model response target, maximum BMEP was produced in the whole engine speed. The maximum BMEP produced is 7.79 bar at 4000RPM, maximum volumetric efficiency produced is 84.63% at 4000RPM, minimum BSFC produced is 300.107 g/kW-h at 3000RPM and minimum CO produced is 91.5 ppm at 1000RPM.

Table 4.1 Summary of performances result for maximum BMEP as the model response.

Engine speed [RPM]	Case Number	BMEP [bar]	Vol. Eff. [%]	BSFC [g/kW-h]	CO [ppm]
1000	262	6.78772	81.3030	334.197	91.5010
2000	24	7.58282	82.9982	305.391	526.236
3000	78	7.77963	83.6790	300.107	1014.39
4000	321	7.78670	84.6306	303.245	1435.55
5000	321	7.58158	84.4596	310.820	1793.04
6000	153	7.13948	82.1344	320.977	3518.62
7000	234	6.64636	80.1013	336.255	3887.54
8000	234	5.99592	76.5774	356.334	4117.79
9000	234	5.16641	71.6452	386.911	4341.16
10000	234	4.21715	65.1241	430.845	4412.57

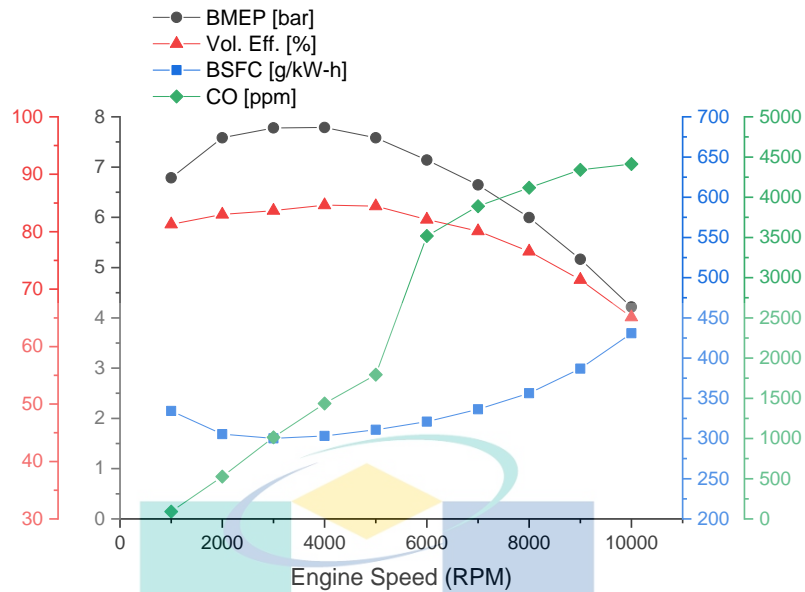


Figure 4.12 Summary of performances result for maximum BMEP as the model response.

The performance trend can be viewed in Figure 4.9. BMEP curve indicates a slight rise until 4000 RPM then decline gradually. The volumetric efficiency curve shows a similar trend but with a very minimum rise below 4000RPM. BSFC curve displays a slight decline until at 4000RPM then begin to rise steadily. CO curve shows a steady increasing trend until at 5000RPM then reveals a sudden dramatic increase in trend.

4.3.2 Maximum volumetric efficiency as model response

Table 4.2 shows the performance result of valve lift profile cases that achieved maximum volumetric efficiency from the factorial experiment. The other three performances were also compiled together to compare the performance result between model responses later. With maximum volumetric efficiency as the model response target, maximum volumetric efficiency was produced in the whole engine speed. The maximum BMEP produced is 7.79 bar at 4000RPM, maximum volumetric efficiency produced is 84.63% at 4000RPM, minimum BSFC produced is 302.06 g/kW-h at 3000RPM and minimum CO produced is 91.12 ppm at 1000RPM.

Table 4.2 Summary of performance result for volumetric efficiency as the model response.

Engine speed [RPM]	Case Number	BMEP [bar]	Vol. Eff. [%]	BSFC [g/kW-h]	CO [ppm]
1000	264	6.77867	81.3620	334.884	91.1252
2000	264	7.58014	83.2233	306.328	545.050
3000	265	7.73570	83.7478	302.059	1032.13
4000	321	7.78670	84.6306	303.245	1435.55
5000	321	7.58158	84.4596	310.820	1793.04
6000	402	7.09809	82.7211	325.157	2093.90
7000	243	6.55910	80.4545	342.235	2276.20
8000	243	5.82552	76.6053	366.896	2426.13
9000	243	4.9975	72.0406	402.201	2618.75
10000	243	4.04998	65.6703	452.411	2690.54

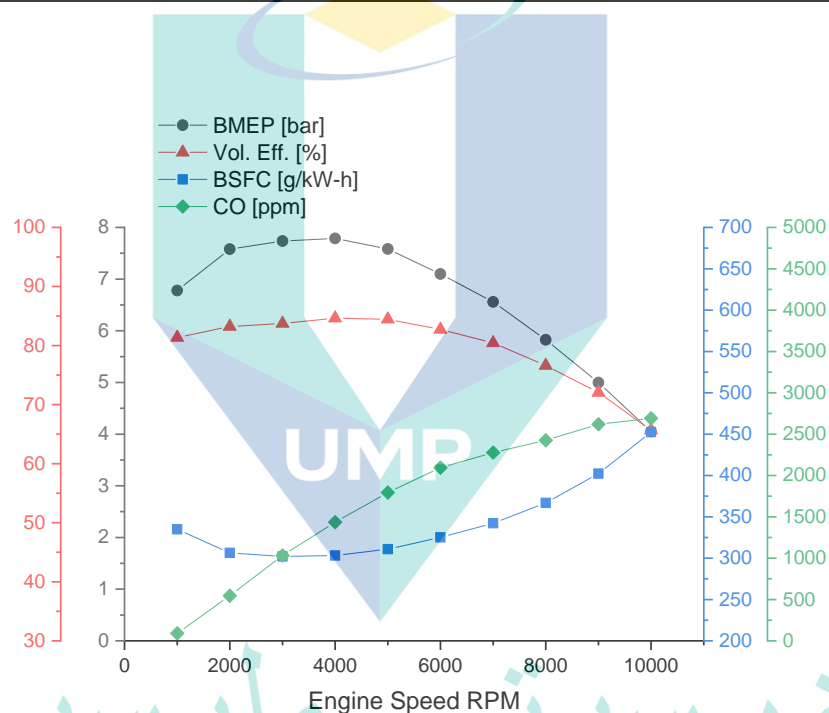


Figure 4.13 Summary of performance result for volumetric efficiency as the model response.

The performance trend can be viewed in Figure 4.13. BMEP curve indicates a slight rise until 4000 RPM then declines gradually. The volumetric efficiency curve shows a similar trend but with a very minimum rise below 4000RPM. BSFC curve displays a slight decline until at 4000RPM then begin to rise steadily. CO curve shows a steady increasing trend until 5000RPM then increase slightly with a smaller gradient.

4.3.3 Minimum BSFC as model response

Table 4.3 shows the performance result of valve lift profile cases that achieved minimum BSFC from the factorial experiment. The other three performances were also compiled together to compare the performance result between model responses later. With minimum BSFC as the model response target, minimum BSFC was produced in the whole engine speed. The maximum BMEP produced is 7.77 bar at 3000RPM, maximum volumetric efficiency produced is 83.95% at 4000RPM, minimum BSFC produced is 300.11 g/kW-h at 3000RPM and minimum CO produced is 82.44 ppm at 1000RPM.

Table 4.3 Summary of performance result for minimum BSFC as the model response.

Engine speed [RPM]	Case Number	BMEP [bar]	Vol. Eff. [%]	BSFC [g/kW-h]	CO [ppm]
1000	25	6.70269	80.0711	333.307	82.4425
2000	77	7.55194	82.6242	305.258	523.497
3000	78	7.77963	83.6790	300.107	1014.39
4000	78	7.74410	83.9546	302.477	1409.55
5000	78	7.48383	83.0747	309.716	1745.85
6000	153	7.13948	82.1344	320.977	3518.62
7000	153	6.55291	78.8247	335.616	3818.09
8000	234	5.99592	76.5774	356.334	4117.79
9000	234	5.16641	71.6452	386.911	4341.16
10000	234	4.21715	65.1241	430.845	4412.57

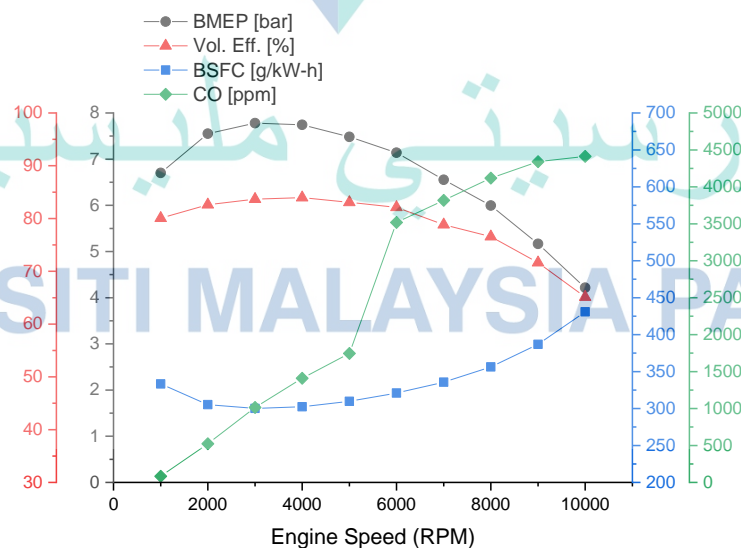


Figure 4.14 Summary of performance result for minimum BSFC as the model response.

The performance trend can be viewed in Figure 4.14. BMEP curve indicates a slight rise until 3000 RPM then declines gradually. The volumetric efficiency curve shows a similar trend but with a very minimum rise below 4000RPM. BSFC curve displays a slight decline until at 3000RPM then begin to rise steadily. The CO curve shows a steady increasing trend until 5000RPM then reveals a sudden dramatic change when a steep increasing in trend is observed.

4.3.4 Minimum CO emission as model response

Table 4.4 shows the performance result of valve lift profile cases that achieved minimum CO from the factorial experiment. The other three performances were also compiled together to compare the performance result between model responses later. With minimum CO as the model response target, minimum CO was produced in the whole engine speed. The maximum BMEP produced is 6.94 bar at 4000RPM, maximum volumetric efficiency produced is 78.46% at 5000RPM, minimum BSFC produced is 309.62 g/kW-h at 4000RPM and minimum CO produced is 49.69 ppm at 1000RPM.

Table 4.4 Summary of performance result for CO emission as the model response.

Engine speed [RPM]	Case Number	BMEP [bar]	Vol. Eff. [%]	BSFC [g/kW-h]	CO [ppm]
1000	729	5.03872	62.2850	344.877	49.6901
2000	702	6.01152	68.0091	315.642	409.030
3000	729	6.27609	70.2210	312.170	889.246
4000	208	6.94302	77.0485	309.618	1297.58
5000	46	6.91129	78.4562	316.721	1535.07
6000	19	5.86449	71.0525	338.028	1693.28
7000	19	4.72518	62.9432	371.644	1773.72
8000	19	3.51549	53.9356	428.033	1729.38
9000	19	2.42071	45.5958	525.474	1592.35
10000	19	1.46109	37.9824	725.209	1433.99

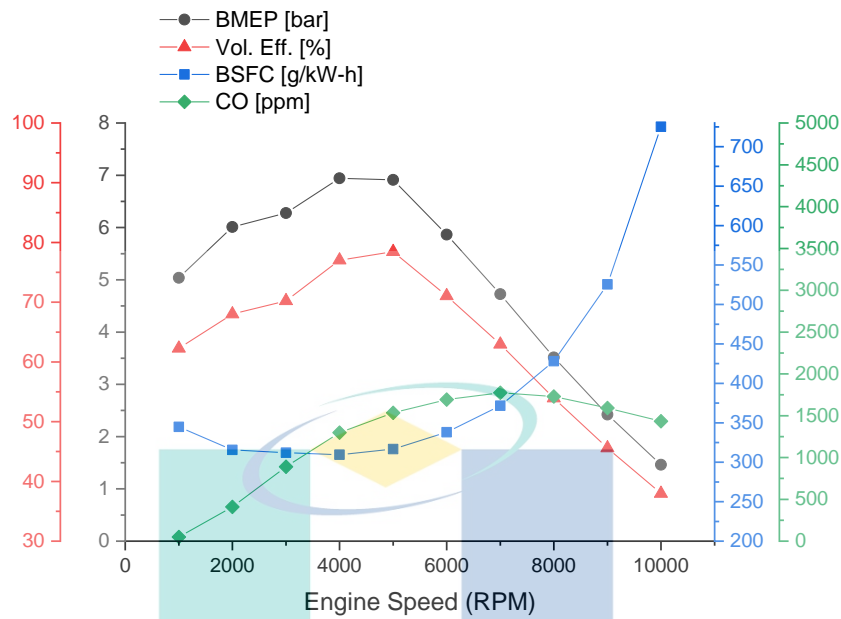


Figure 4.15 Summary of performance result for minimum CO emission as the model response.

The performance trend can be viewed in Figure 4.15. BMEP curve indicates a volatile rise until 5000 RPM then decline significantly. The volumetric efficiency curve shows a similar trend with the BMEP curve. BSFC curve displays a slight decline until at 4000RPM then begin to rise dramatically. CO curve shows a steady increasing trend until at 7000RPM then start to fall slightly.

4.3.5 Model response performances comparison

In this section, the performances of each model responses in terms of BMEP, volumetric efficiency, BSFC and CO were compared to provide an overview of the performance curve for further analysis.

BMEP

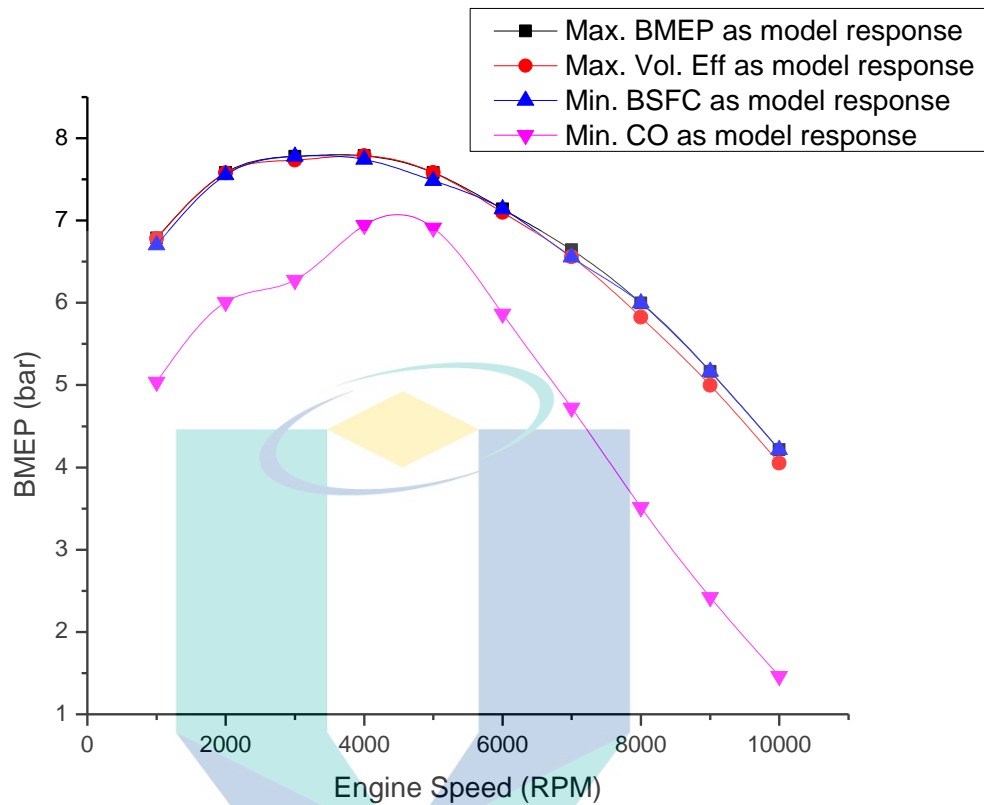


Figure 4.16 BMEP performance curve comparison

Figure 4.16 illustrates the BMEP curves of all model responses discussed earlier in the previous section. The BMEP curve from minimum CO as model response indicates a large margin difference from other model responses curves. The performance is reduced in the entire engine speed. The rest of the model response shows almost the same trend and value of BMEP performance. Thus, minimum CO as model response considered jeopardized the engine performance.

Volumetric Efficiency

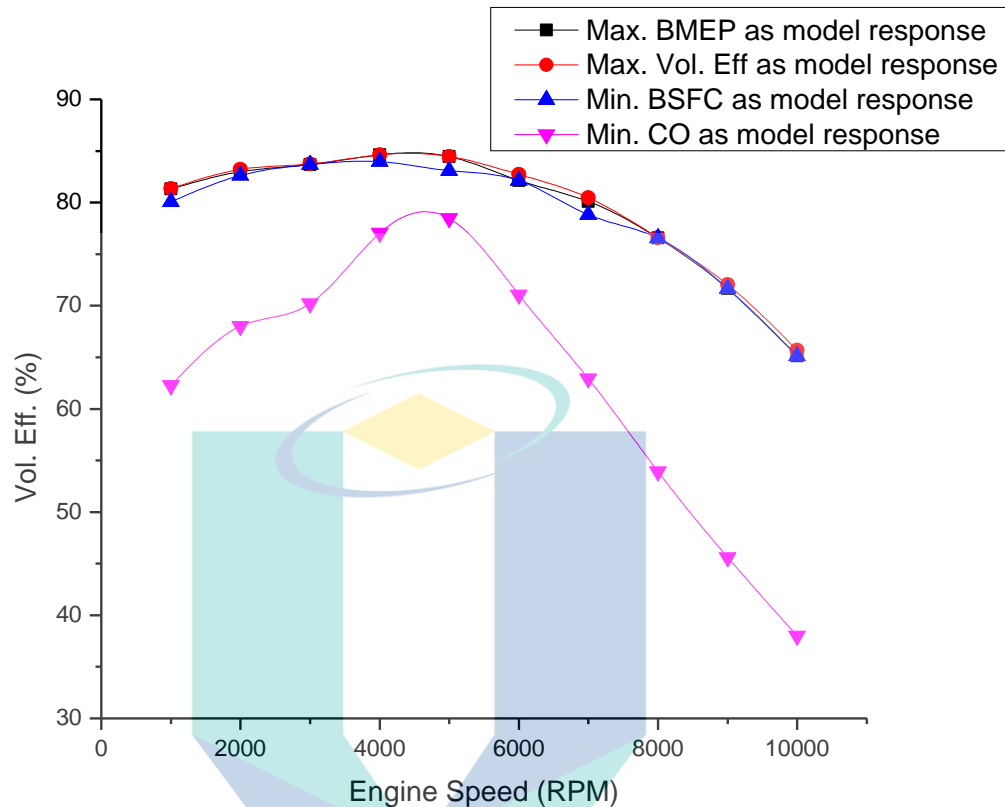


Figure 4.17 Volumetric efficiency performance curve comparison

Figure 4.17 illustrates the volumetric efficiency curves of all model responses discussed earlier in the previous section. The curve from minimum CO as model response indicates a large margin difference from other model responses curves. The volumetric efficiency is reduced in the entire engine speed. The rest of the model responses shows almost the same trend and value of BMEP performance. Thus, minimum CO as model response considered jeopardized the engine performance.

BSFC

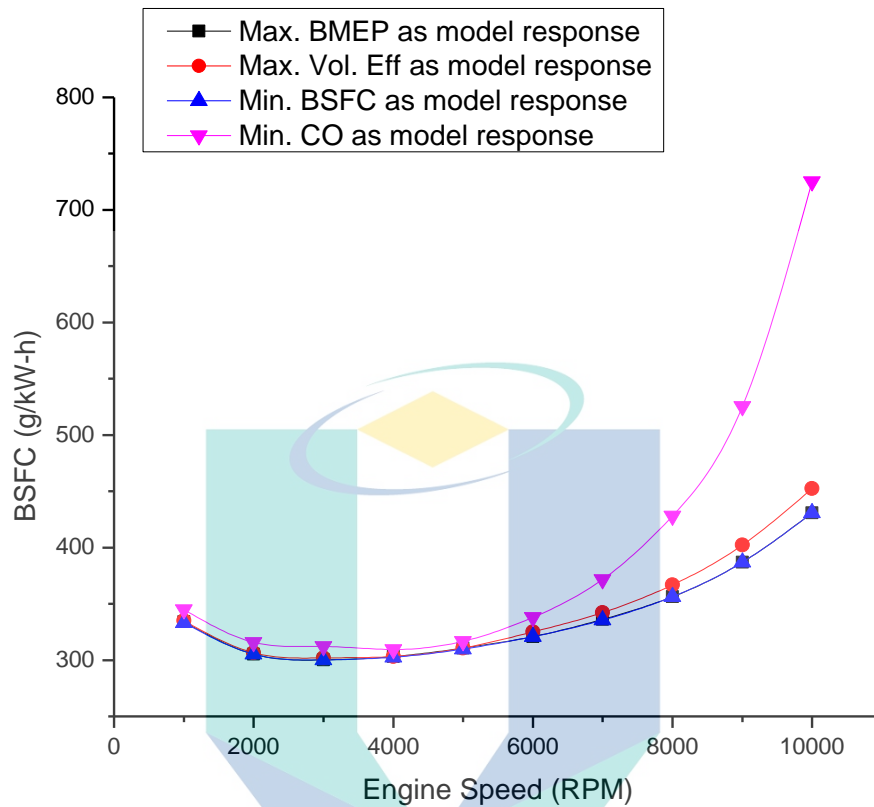


Figure 4.18 BSFC performance curve comparison

Figure 4.18 illustrates the BSFC curves of all model responses discussed earlier in the previous section. The curve from minimum CO as model response starts to reveal an increasing margin difference from other model response curves. The value of BSFC produced is dramatically skyrocketed up to 729 g/kW-h at 10 000RPM. The rest of the model responses shows almost the same trend and value of BSFC performance. Thus, minimum CO as model response considered jeopardized the fuel consumption rate at high speed.

CO emission

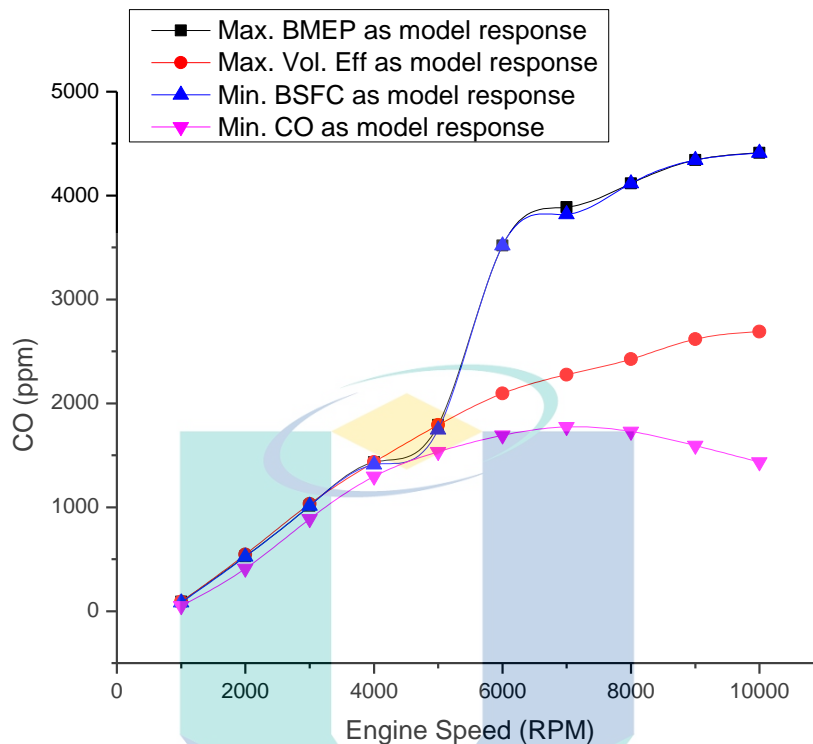


Figure 4.19 CO performance curve comparison

Figure 4.19 illustrates the CO curves of all model responses discussed earlier in the previous section. The CO curve of maximum BMEP and minimum BSFC as model response display the same trend where there is a sudden increase of CO emissions at 6000RPM. This is considered as jeopardizing the emissions rate of the engine.

The CO curve of maximum volumetric efficiency as the model response shows a slight and steady increment in the entire run. The CO curve of minimum CO as model response indicates a gradual increase until 7000RPM, then declines slightly in a small degree. While minimum CO as the model response has jeopardized most of the discussed engine performances, even though the CO produced is at the lowest level.

4.3.6 Response surface correlation for engine performance

In this section, two figures of three-dimensional (3D) surface plot are used to illustrate the response surface of BSFC and CO against BMEP and volumetric efficiency from the DOE simulation. These variables were chosen to represent the correlation between BMEP and volumetric efficiency in affecting BSFC and CO level.

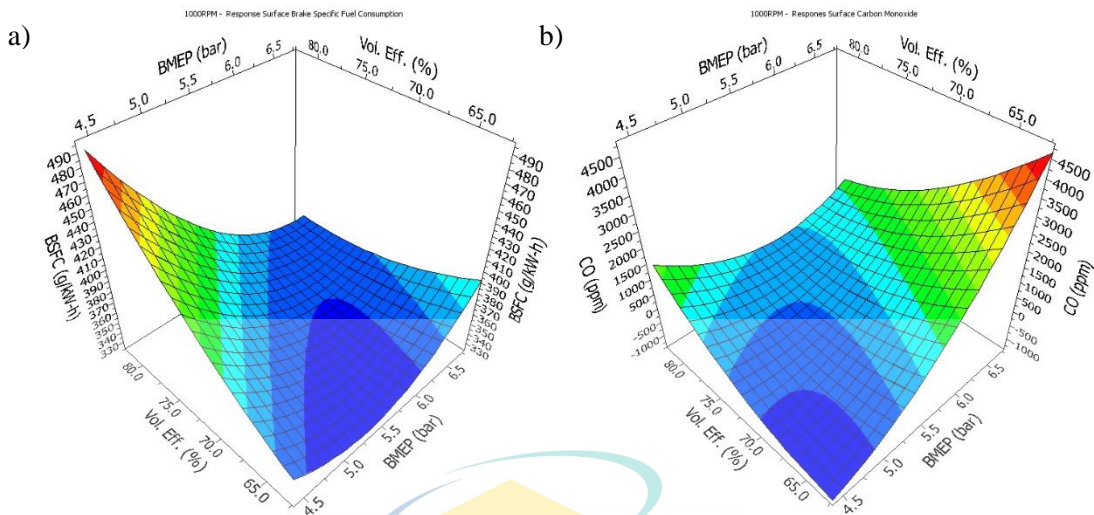


Figure 4.20 Response Surface of BSFC (a) and CO (b) against BMEP and Volumetric Efficiency at 1000 RPM

Based on Figure 4.20, the BSFC is less affected by the simultaneous increment of BMEP and volumetric efficiency. The BSFC is at the lower region on the surface. While CO has shown a slight contour difference with increasing BMEP and volumetric efficiency. BSFC and CO produced are at the lower level on the contour.

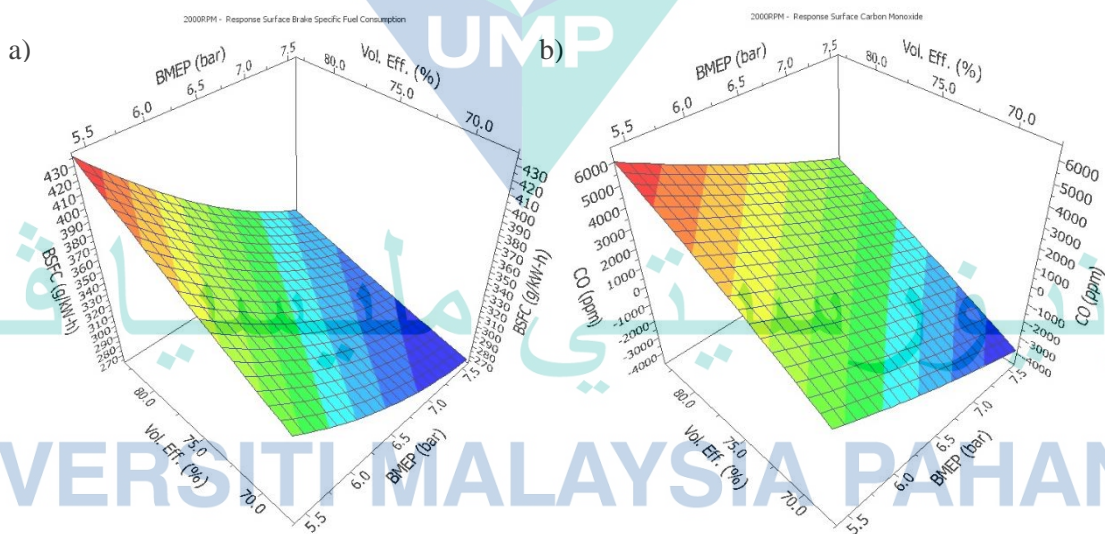


Figure 4.21 Response Surface of BSFC (a) and CO (b) against BMEP and Volumetric Efficiency at 2000 RPM

Based on Figure 4.21, the BSFC indicates a slight reduction as BMEP and volumetric efficiency increases simultaneously at 2000RPM. While CO level has shown no contour difference with increasing BMEP and volumetric efficiency. Both BSFC and CO produced are at a moderate level in the contour.

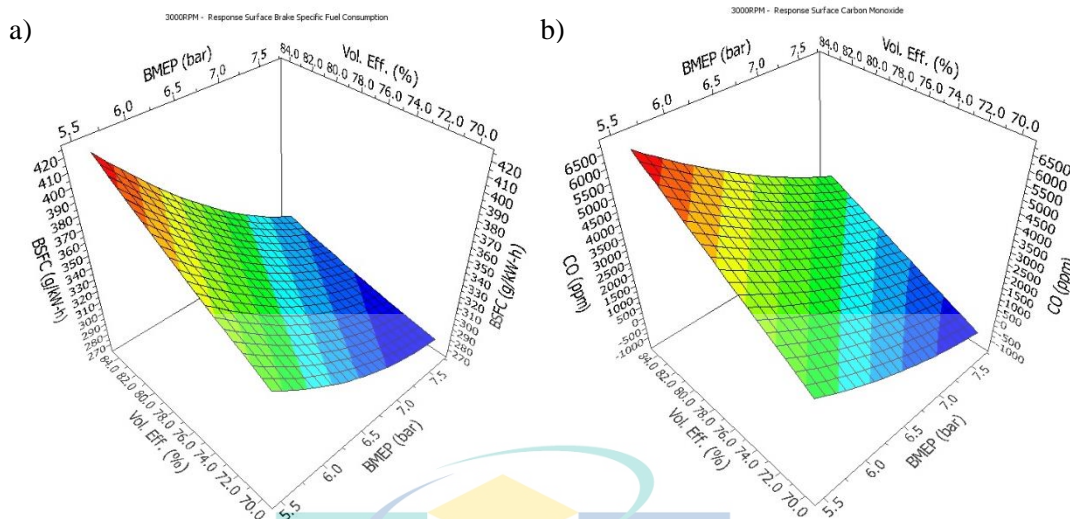


Figure 4.22 Response Surface of BSFC (a) and CO (b) against BMEP and Volumetric Efficiency at 3000 RPM

Based on Figure 4.22, the BSFC indicates a slight reduction as BMEP and volumetric efficiency increases simultaneously at 3000RPM. The BSFC produced is at the lower region on the surface. While CO level has not shown an obvious sign of contour difference. CO produced is at a moderate region on the surface contour.

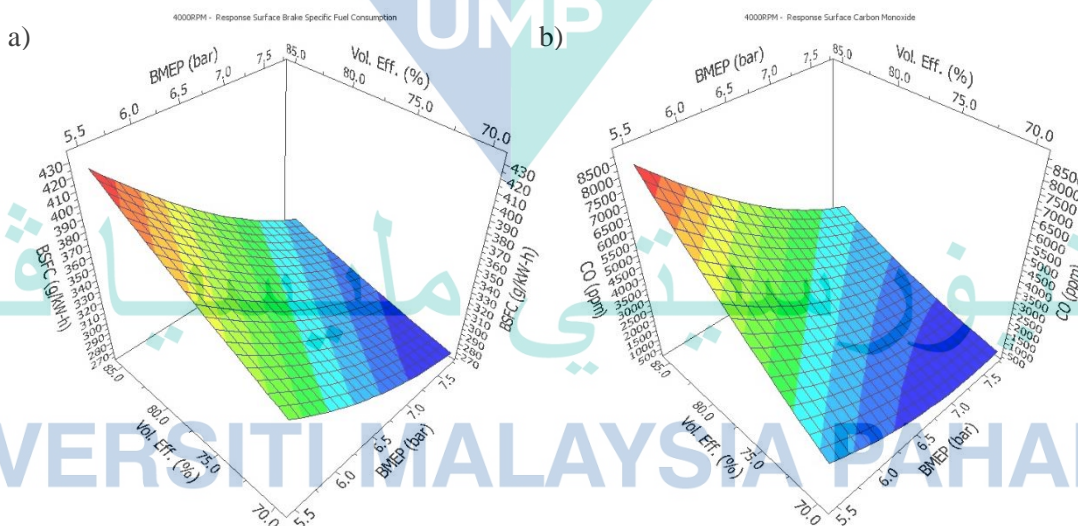


Figure 4.23 Response Surface of BSFC (a) and CO (b) against BMEP and Volumetric Efficiency at 4000 RPM

Based on Figure 4.23, the BSFC indicates a minimal contour reduction as BMEP and volumetric efficiency increases simultaneously at 4000RPM. While CO level has shown no contour change with increasing BMEP and volumetric efficiency. The BSFC and CO produced at this speed are at lower level in the contour surface.

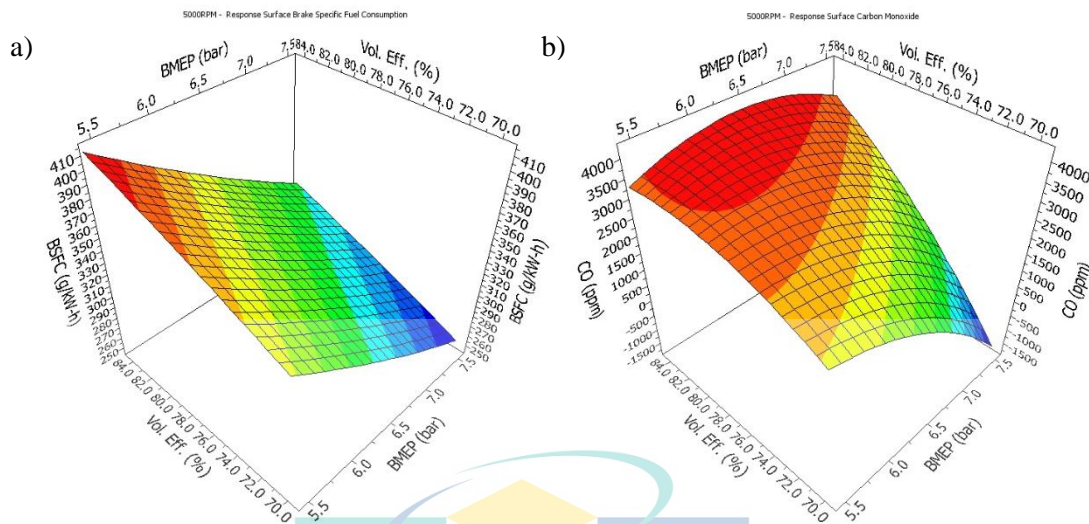


Figure 4.24 Response Surface of BSFC (a) and CO (b) against BMEP and Volumetric Efficiency at 5000 RPM

Based on Figure 4.24, the BSFC indicates minimal contour change as BMEP and volumetric efficiency increases simultaneously at 5000RPM. While CO level has shown a slight increment with increasing BMEP and volumetric efficiency. The BSFC produced at this speed is at a lower level in the contour surface, while the CO level has reached the red region on the contour surface.

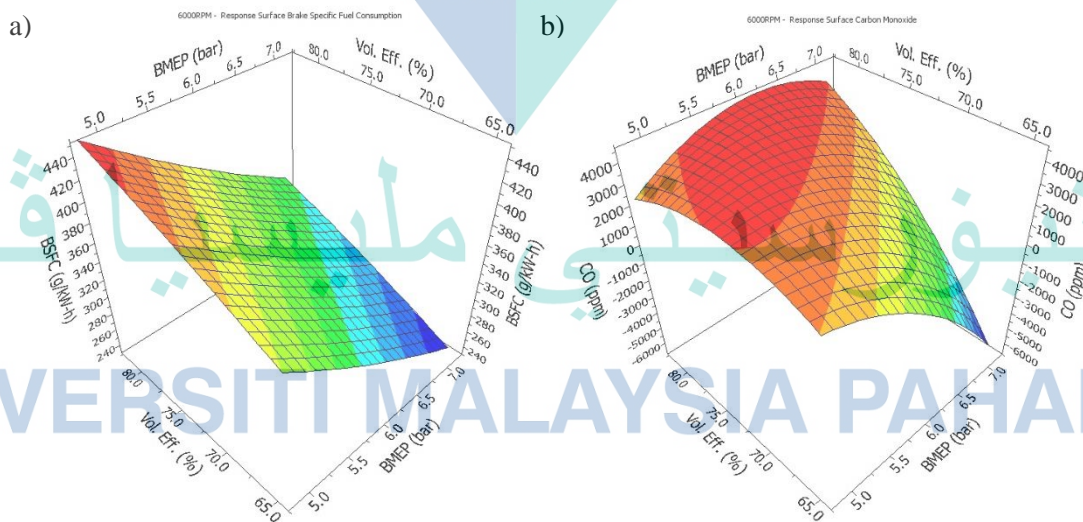


Figure 4.25 Response Surface of BSFC (a) and CO (b) against BMEP and Volumetric Efficiency at 6000 RPM

Based on Figure 4.25, the BSFC indicates minimal contour change as BMEP and volumetric efficiency increases simultaneously at 6000RPM. While CO level has shown a slight increment with increasing BMEP and volumetric efficiency. The BSFC produced

at this speed is at a lower level in the contour surface, while the CO level has reached the red region on the contour surface.

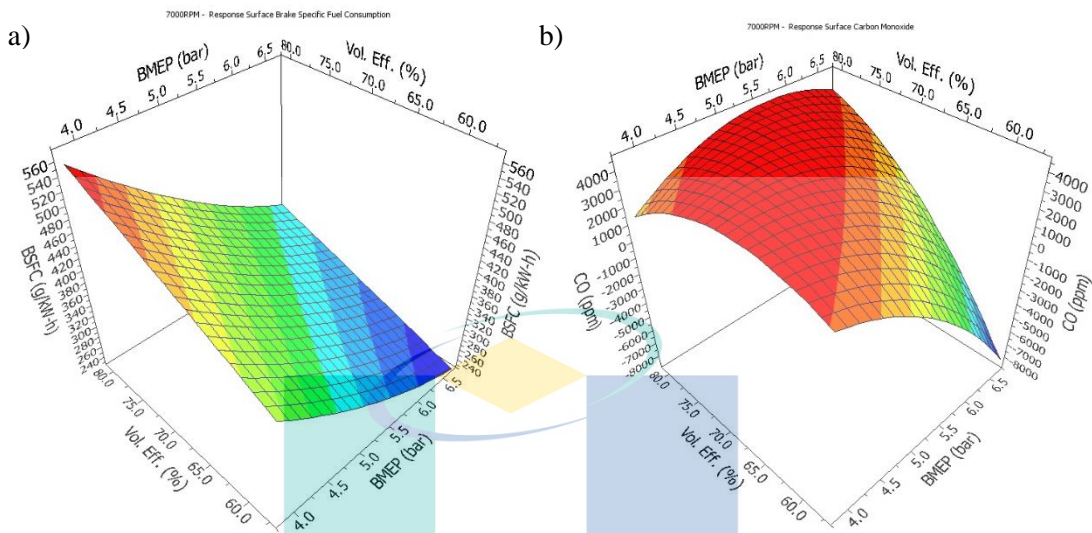


Figure 4.26 Response Surface of BSFC (a) and CO (b) against BMEP and Volumetric Efficiency at 7000 RPM

Based on Figure 4.26, the BSFC indicates minimal contour change as BMEP and volumetric efficiency increases simultaneously at 7000RPM. While CO level has shown no contour change with increasing BMEP and volumetric efficiency. The BSFC produced at this speed is at a lower level in the contour surface, while the CO level has reached the highest red region on the contour surface.

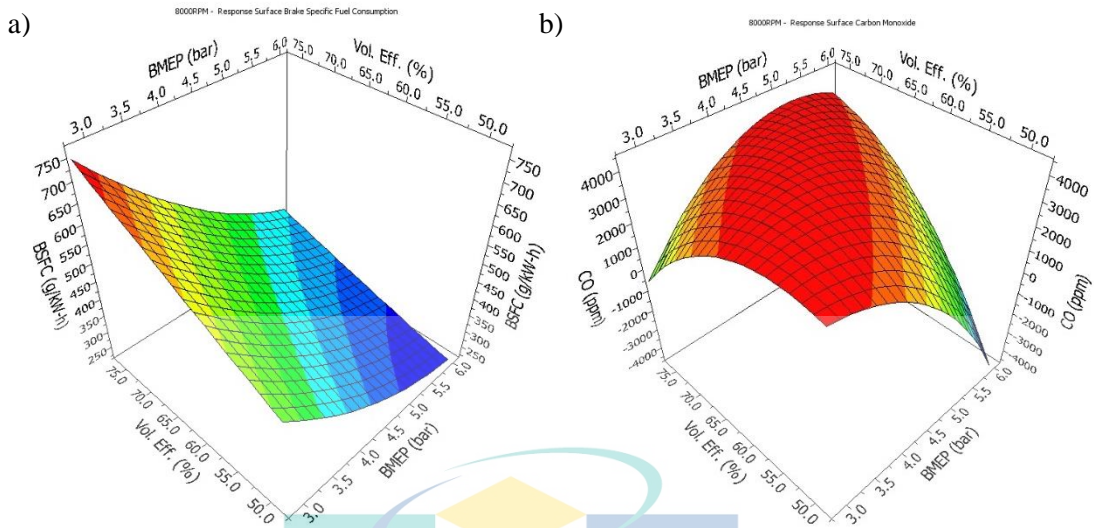


Figure 4.27 Response Surface of BSFC (a) and CO (b) against BMEP and Volumetric Efficiency at 8000 RPM

Based on Figure 4.27, the BSFC indicates minimal contour change as BMEP and volumetric efficiency increases simultaneously at 8000RPM. While, CO level has shown no contour change with increasing BMEP and volumetric efficiency. The BSFC produced at this speed is at lower level in the contour surface, while, the CO level has reached the peak of the red region on the contour surface.

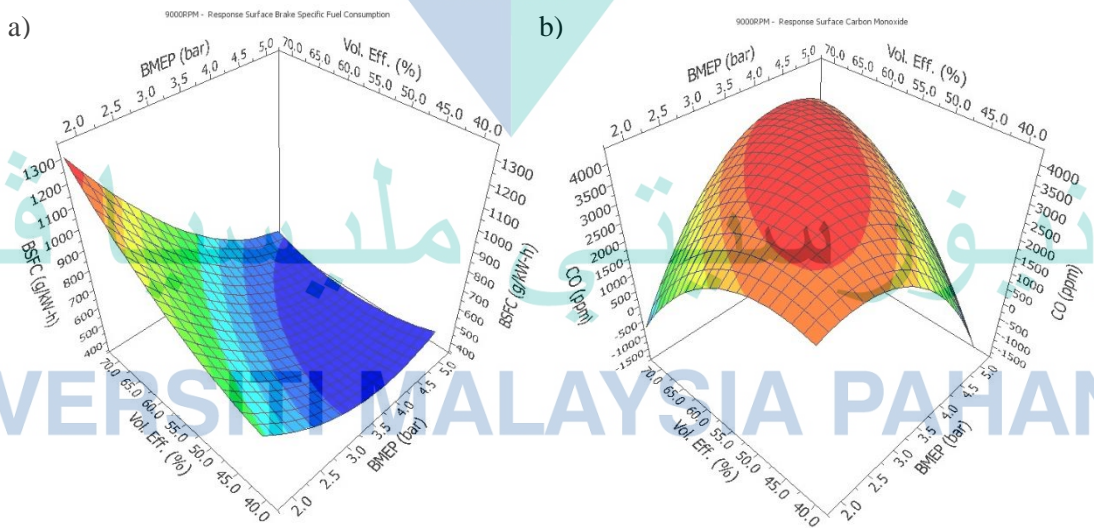


Figure 4.28 Response Surface of BSFC (a) and CO (b) against BMEP and Volumetric Efficiency at 9000 RPM

Based on Figure 4.28, the BSFC indicates minimal contour change as BMEP and volumetric efficiency increases simultaneously at 9000RPM. While CO level has shown a slight increment of contour level with increasing BMEP and volumetric efficiency. The

BSFC produced at this speed is at a lower level in the contour surface, while the CO level has reached the peak of the red region on the contour surface.

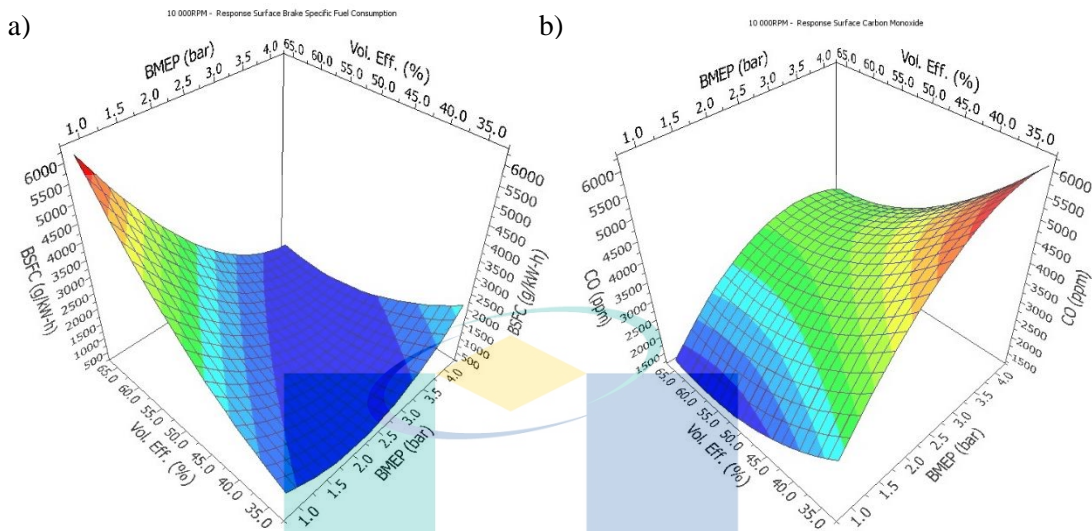


Figure 4.29 Response Surface of BSFC (a) and CO (b) against BMEP and Volumetric Efficiency at 10 000 RPM

Based on Figure 4.29, the BSFC indicates insignificant contour change as BMEP and volumetric efficiency increases simultaneously at 10,000RPM. While CO level has shown a slight rise of contour level with increasing BMEP and volumetric efficiency. The BSFC produced at this speed is at a lower level in the contour surface, while the CO level is moderate.

4.3.7 Valve events sensitivity against engine response (Volumetric Efficiency)

In statistics, the main effect is the effect of an independent variable on a dependent variable averaged across the levels of any other independent variables. Main effect is evaluated by where one variable is being changed at a time. Whereas, an interaction effect may arise when considering the relationship among three or more variables, and describes a situation in which the effect of one causal variable on an outcome depends on the state of a second causal variable (Cox 1984, Dodge and Commenges 2006). In this section, the main effects and interaction effects of the independent variables used in the factorial experiments are discussed.

Summary of valve events sensitivity

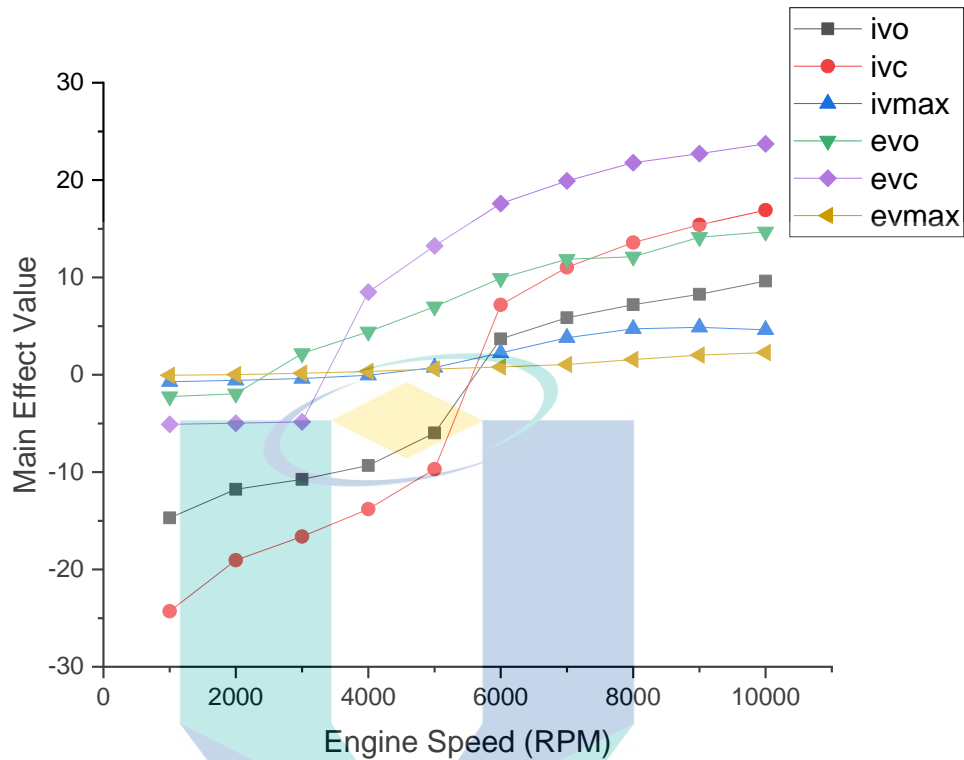


Figure 4.30 Main Effect Value of Valve Events against Engine Speed

Figure 4.30 summarizes the main effect value of valve events against speed. At speed below 5000 RPM, IVC shows the largest effect on engine response (volumetric efficiency) followed by IVO, EVC, EVO, IVMAX and EVMAX. Above 5000 RPM, the largest effect is produced by EVC, followed by IVC, EVO, IVO, IVMAX and EVMAX. The intake and exhaust valve closing timings (IVC and EVC) are more influential on combustion, as demonstrated from previous work (Samuel, Mithun et al. 2019).

Figure 4.31 summarizes four significant interaction effects of valve events against speed. In overall, the interaction between EVO and EVC affects the engine response the most, especially at high-speed level. The second biggest impact is influenced by the interaction between IVO and IVC, then followed by interaction between IVO and EVC, which defined the valve timing overlap. The least impact was produced by the interaction between IVO and EVO.

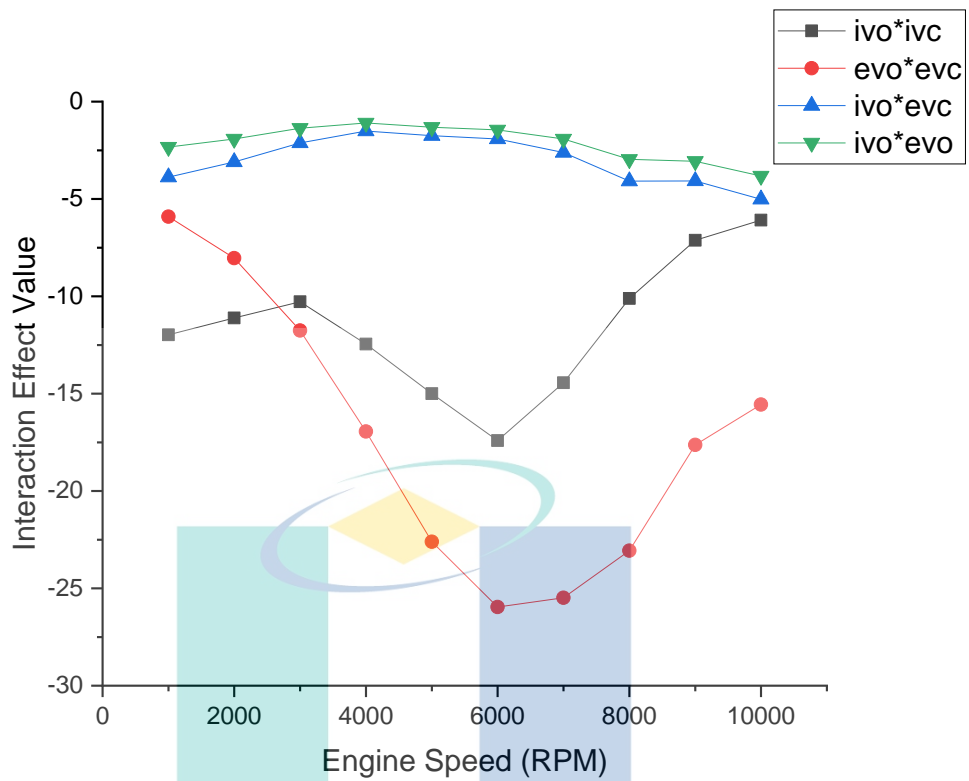


Figure 4.31 Interaction Effect Value of Four Significant Interaction against Engine Speed

4.3.8 Summary of ANOVA

Table 4.5 shows the ANOVA summary of the factorial experiment using volumetric efficiency as the model response. According to the P-value, the ANOVA table indicated that all the models of the experiment are significant as they have P-values of less than 0.05. A high R^2 coefficient ensures a satisfactory agreement between the calculated and observed data (Noordin, Venkatesh et al. 2004). The table indicates that all the experiments have good R^2 value. A high R^2 value of close to 1 is desirable, which means an excellent indicator of goodness of fit of the data. Furthermore, a reasonable agreement with adjusted R^2 is necessary (Nithyanandan, Wu et al. 2014). R^2 value indicates the total variability of responses after considering the significant factors and the value accounts for the number of predictors in the model.

Table 4.5 ANOVA Table for Engine Performance (Volumetric Efficiency)

Experiment	F-value	p-value	R^2	Adjusted R^2	Max % Error	SD Residual
1000 RPM	3.6804E05	< 0.0001	0.9999	0.9999	0.2055	0.045

2000 RPM	64285.5719	< 0.0001	0.9996	0.9996	0.4945	0.0855
3000 RPM	13188.8227	< 0.0001	0.998	0.998	0.7241	0.1678
4000 RPM	5215.2605	< 0.0001	0.995	0.9949	0.8599	0.2435
5000 RPM	3144.3196	< 0.0001	0.9918	0.9915	0.9507	0.2742
6000 RPM	6026.0154	< 0.0001	0.9957	0.9955	1.0263	0.2396
7000 RPM	7252.3942	< 0.0001	0.9964	0.9963	1.3442	0.2902
8000 RPM	5851.7223	< 0.0001	0.9956	0.9954	2.7495	0.3877
9000 RPM	6129.81	< 0.0001	0.9958	0.9956	3.6395	0.4133
10 000 RPM	5212.5439	< 0.0001	0.995	0.9949	4.8651	0.472

The difference between the actual and predicted values is called residuals (Montgomery and Woodall 2008). The general impression from actual and predicted data display is that the error value is approximately acceptable and there are no large deviations between them. Also, the regression models for all responses were determined to be statistically less than 95% confidence level. There are evidences of a good agreement between the experimental results of engine performance responses with the predicted values using the developed regression equation.

4.4 FVT profiles for various engine speed

In this section, the best valve lift profile that produces highest volumetric efficiency as performance result in the full factorial experiment of every speed level previously were chosen to be the FVT profiles to be applied on the baseline model. Five valve lift profiles have been identified as the FVT to be the optimum profiles for the engine performance boosting throughout ten levels of engine speed from 1000 RPM to 10 000 RPM. These FVT profiles are changing according to engine speed.

FVT profile from 1000 RPM to 2000 RPM

Figure 4.32 illustrates the valve lift profile of FVT against the crank angle degree at 1000 RPM and 2000 RPM. The FVT strategies applied at 1000 RPM and 2000 RPM are EIVC, Low-IVMAX, LEVO, EEVO and High-IVMAX. The intake valve duration is reduced by 20 CAD and exhaust valve duration is reduced by 40 CAD. The amount of valve overlap decreases by 20 CAD. For a smooth and emission-free engine start, EEVC is recommended (Muzakkir and Hirani 2015). EIVC with reduced valve lift are preferred strategies at the engine start, during the warm-up period and part load conditions (Muzakkir and Hirani 2015). LEVO is beneficial, which can increase expansion work (Cairns, Zhao et al. 2013). HC emissions have generally degraded as a result of reduced mixture motion caused by the EIVC (Pierik and Burkhard 2000). EIVC also is a proven

method to reduce the compression-to-expansion ratio of an engine (Chandras, McCarthy Jr et al. 2018). Furthermore, reduced IVMAX can significantly increase the swirl ratio by enhancing swirl flow velocity (Wang, Liu et al. 2015).

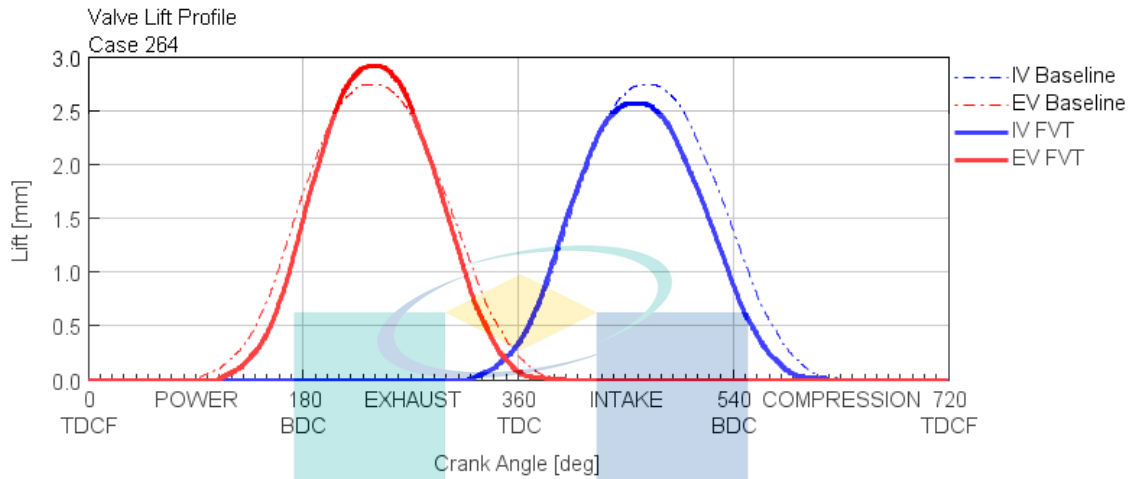


Figure 4.32 FVT Valve Lift Profile Curve from 1000 RPM to 2000 RPM

FVT profile at 3000 RPM

Figure 4.33 illustrates the valve lift profile of FVT against the crank angle degree at 3000 RPM. The FVT strategies applied at 3000 RPM are EIVC, Low-IVMAX, LEVO and Low-IVMAX. The intake valve duration is reduced by 20 CAD and exhaust valve duration is reduced by 20 CAD. The amount of valve overlap remains unchanged.

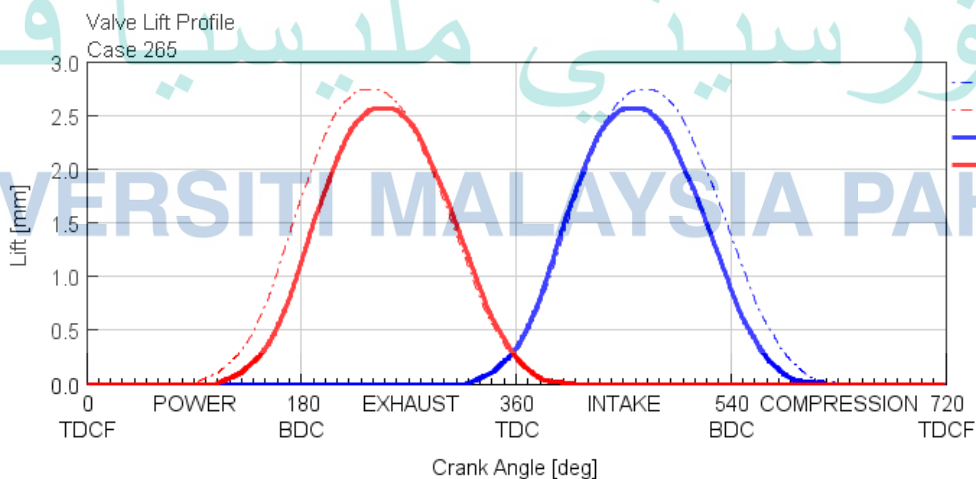


Figure 4.33 FVT Valve Lift Profile Curve at 3000 RPM

FVT profile from 4000 RPM to 5000 RPM

Figure 4.34 illustrates the valve lift profile of FVT against the crank angle degree at 4000 RPM and 5000 RPM. The FVT strategies applied at 4000 RPM and 5000 RPM are EIVC, High-IVMAX, LEVO and High-IVMAX. The intake valve duration is reduced by 20 CAD and exhaust valve duration is reduced by 20 CAD. The amount of valve overlap remains unchanged.

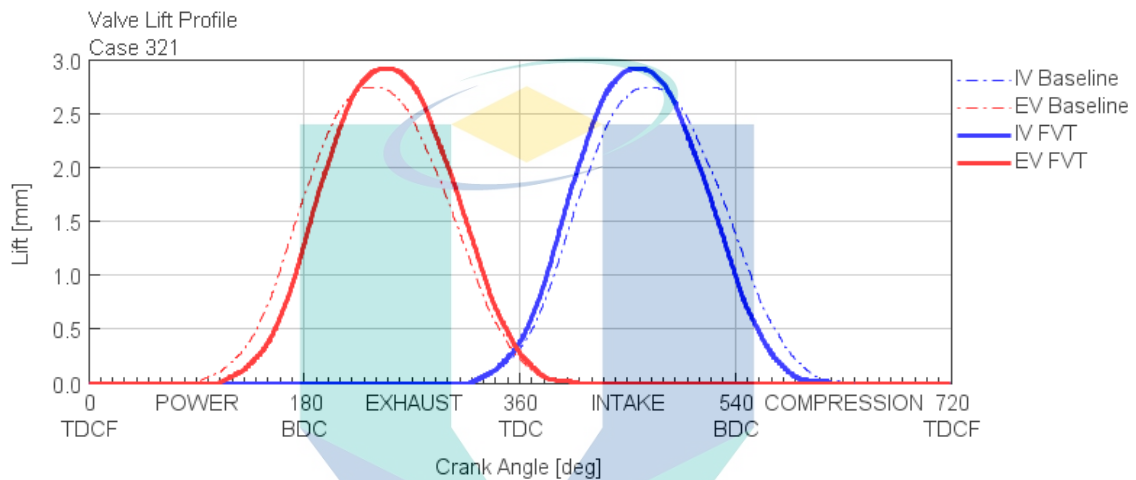


Figure 4.34 FVT Valve Lift Profile Curve from 4000 RPM to 5000 RPM

FVT profile at 6000 RPM

Figure 4.35 illustrates the valve lift profile of FVT against the crank angle degree at 6000 RPM. The FVT strategies applied at 6000 RPM are High-IVMAX, LEVO and High-IVMAX. The intake valve duration remains unchanged while the exhaust valve duration is reduced by 20 CAD. The amount of valve overlap remains unchanged.

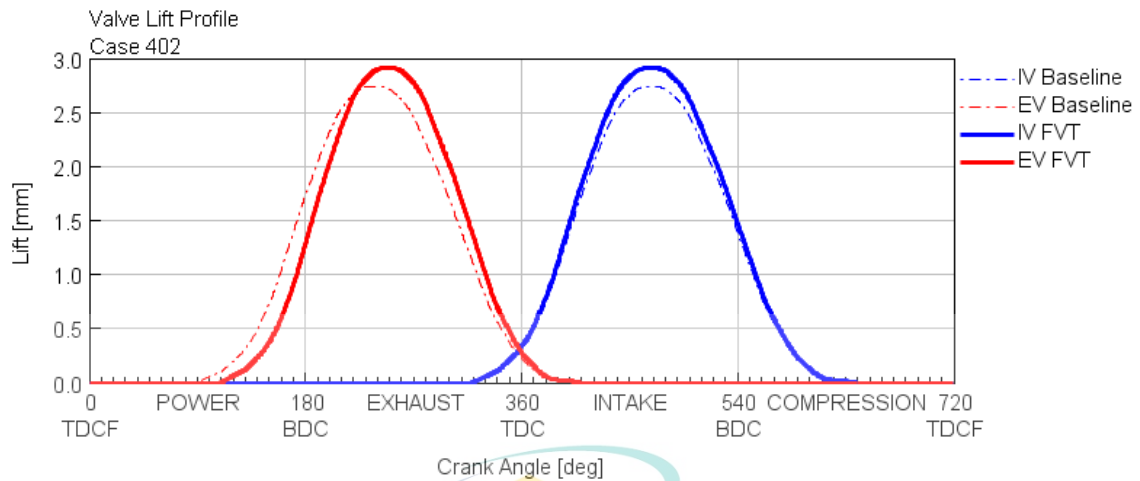


Figure 4.35 FVT Valve Lift Profile Curve at 6000 RPM

FVT profile at 7000 RPM and above

Figure 4.36 illustrates the valve lift profile of FVT against the crank angle degree 7000 RPM and above. The FVT strategies applied at 7000 RPM and above are EIVO, LIVC, High-IVMAX, LEVO, LEVC and High-EVMAX. The intake valve duration increases by 40 CAD, while the exhaust valve duration remains unchanged. The amount of valve overlap increases by 40 CAD. Early IVO and allows for a large exhaust valve overlap, which facilitates the internal exhaust gas flow into the cylinder (Stone, Kelly et al. 2017). The strategies such as early intake valve closing, late intake valve closing and variable valve lift are used to limit the pumping loss (Muzakkir and Hirani 2015). LIVC, which further decreases pumping losses by allowing further increased intake pressures by allowing the piston pushes some of the air back into the inlet system (Cairns, Zhao et al. 2013). LIVC has the potential of meeting all the performance, driveability and fuel economy where the intake valves can be phased relative to each other to extend the total intake opening period (Ma 1988). LIVC can be preferred rather than EIVC as it results in lower exhaust heat capacity reduction compared to EIVC (Basaran and Ozsoysal 2017). As engine speed increases, LEVC is advantageous, however it must be moderated to minimise the exhaust blow-down losses (Bonatesta, Altamore et al. 2016).

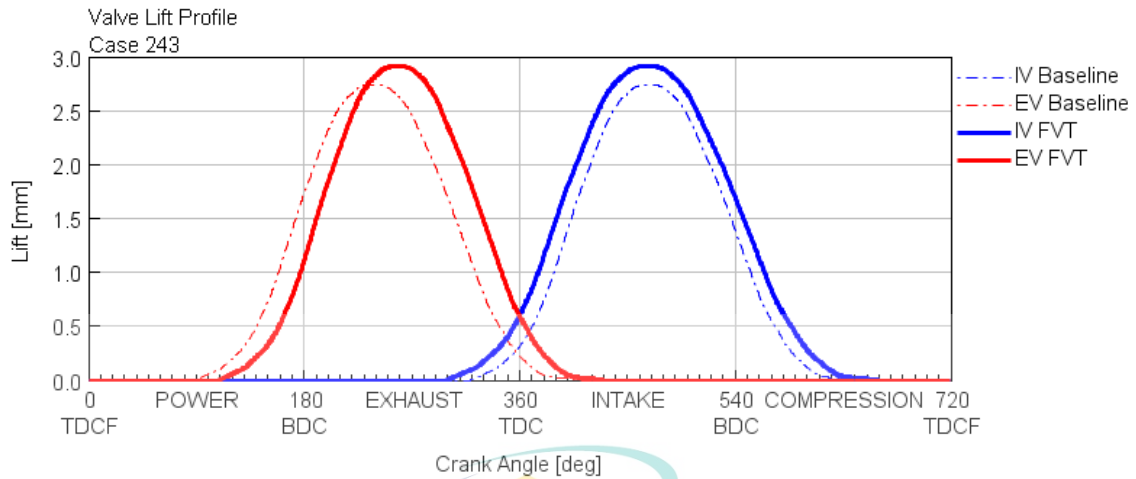


Figure 4.36 FVT Valve Lift Profile Curve at 7000 RPM above

4.5 FVT Model Performance Result

In this section, the selected FVT profiles from the previous section were applied to the baseline model to evaluate the performance boosting capability of the FVT model. The design of experiment has delivered results of optimum valve timing profiles that enhance the performance of the engine at every speed level. Five valve lift profiles have been identified as the FVT to be the optimum profiles for the engine performance boosting throughout ten levels of engine speed from 1000 RPM to 10 000 RPM. These profiles have demonstrated an improvement in the engine performance through the entire run. The same baseline model has shown a positive impact using the FVT profiles and produced a better engine performance compared to the baseline model. Table 5.3 shows the summary of the valve lift event parameter according to the identified FVT profiles at each engine speed level.

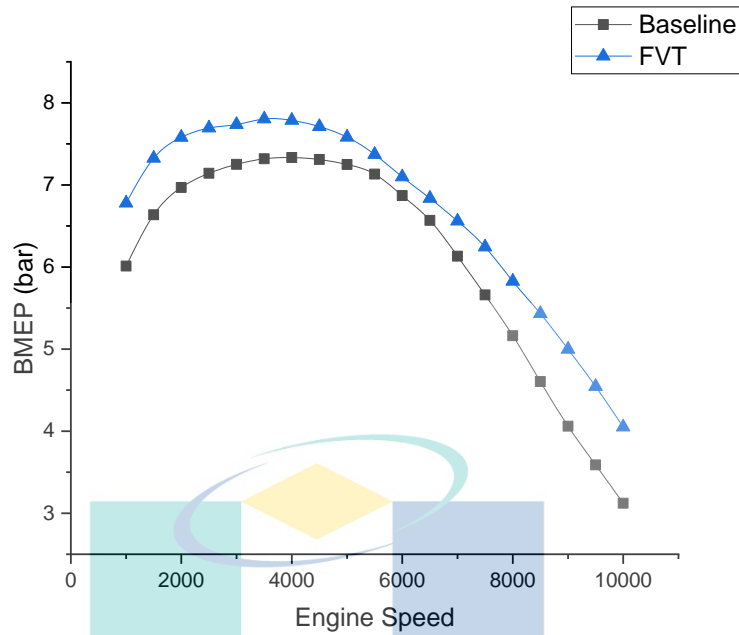


Figure 4.37 Brake Mean Effective Pressure (BMEP) of FVT Model

Figure 4.38 shows the BMEP comparison between the FVT and baseline model. A significant performance amplification is observed, which demonstrated the boosting potential of FVT application. Maximum BMEP is increased to 7.8 bar at 3500 RPM compared to baseline with 7.3 bar at 4000 RPM. BMEP of the entire engine speed has been improved at 11.49% on average using FVT profiles. The use of altering the exhaust valve is influential to the scavenging process. Even though the early opening of EV is not used, the power expansion produced by using EEVO increases the performance by eliminating the blowdown losses (Bonatesta, Altamore et al. 2016). Instead of a pure torque, BMEP is widely used as an indicator in engine performance assessment as it allows different types and capacities of the internal combustion engines to be compared.

Due to some elimination of pumping loss using FVT strategies, BMEP is boosted by consuming an excess of work produced by the engine.

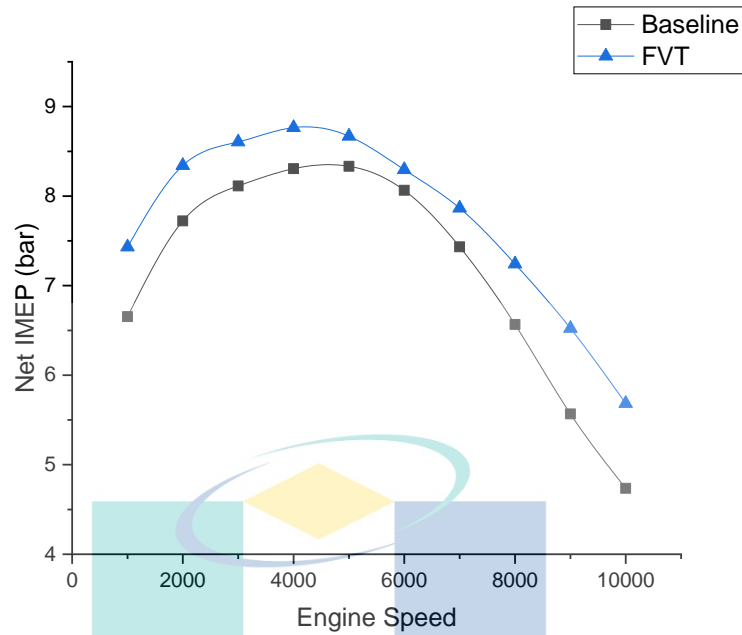


Figure 4.38 Net Indicated Mean Effective Pressure (IMEP720) of FVT Model

Figure 4.38 shows the IMEP720 comparison between the FVT and baseline model. A significant IMEP720 improvement is observed in the entire run by the FVT model, which demonstrated the boosting potential of FVT application. Maximum IMEP720 is increased to 8.76 bar at 4000 RPM from 8.33 bar at 4500 RPM. IMEP720 for the entire engine speed has been improved at 9.14% in average using FVT profiles. The improvement of IMEP using valve timing strategies also demonstrated from previous work (Samuel, Mithun et al. 2019).

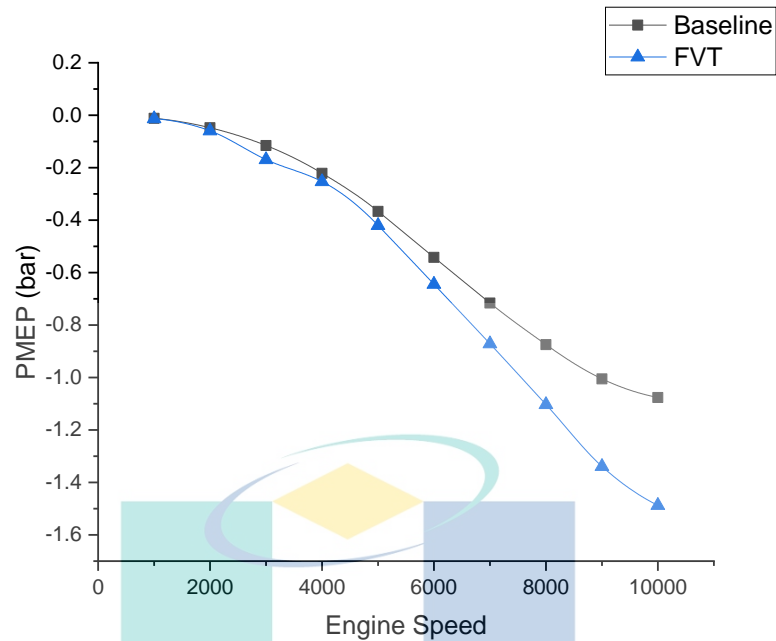


Figure 4.39 Pumping Mean Effective Pressure (PMEP) of FVT Model

Figure 4.39 illustrates the PMEP comparison between the FVT and baseline model. The pumping pressure assimilates the pumping work during the exhaust and intake of charge by the piston in the chamber. Larger pumping work deteriorates the engine performance theoretically because the work done by the engine will be contributed largely to pumping work. The improvement of pumping work can be observed starting at 3000 RPM. As engine speed increases, the FVT model has shown the reduction of PMEP value throughout the run. The PMEP improved at 5% on average. This result also demonstrated by intelligent valve actuation that able to improve pumping losses with a 5.3% reduction (Stone, Kelly et al. 2017). The reduction of pumping requirement compared to the traditional throttled engine, contribute to the improvement of engine efficiency (Muzakkir and Hirani 2015). Internal circulation of hot exhaust gas worked to reduce pumping loss and to improve combustion (Takemura, Aoyama et al. 2001). The advanced of IVC at 7000 RPM and above reduce the effective compression ratio, which had an additional effect on reducing pumping loss, which also led to a reduction in fuel consumption (Takemura, Aoyama et al. 2001). Increasing or delaying valve overlap increases trapped residuals and reduces engine pumping losses where the trapped residual gases occupy part of the cylinder volume and hence allow less vacuum to be used in the inlet system (Cairns, Zhao et al. 2013). By increasing the maximum lift of intake valve, the PMEP can be further reduced (Li, Liu et al. 2018). The reduction of PMEP using

valve timing strategies also demonstrated from previous work (Kohany and Sher 1999, Zhao, Xi et al. 2018).

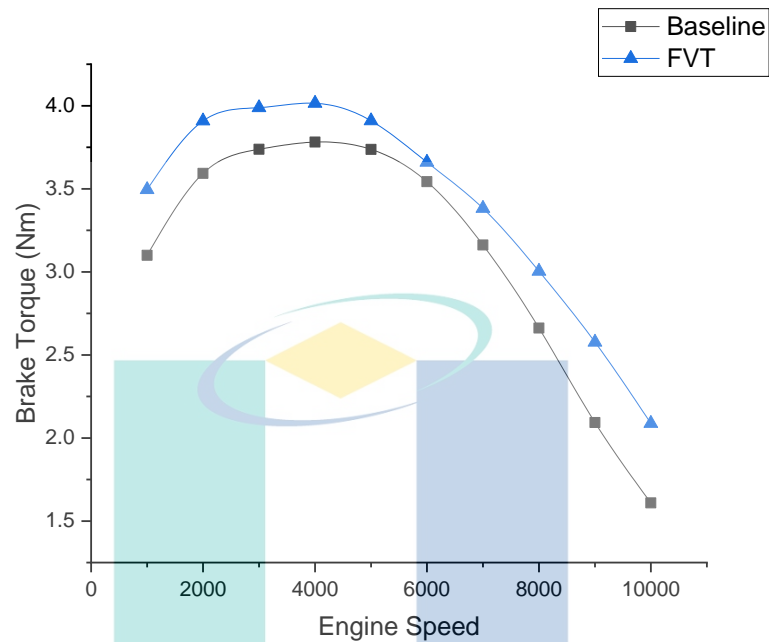


Figure 4.40 Brake Torque of FVT Model

Figure 4.40 shows the brake torque comparison between the FVT and baseline model. Significant brake torque is observed in the entire run by the FVT model, which demonstrated the boosting potential of the FVT application. The maximum brake torque is increased to 4.02 Nm at 3500 RPM from 3.75 Nm at 4000 RPM. Brake torque for the entire engine speed has been improved at 11.5% on average using FVT profiles. The amplification of brake torque using valve timing strategies also demonstrated from previous works (Kohany and Sher 1999, Li, Tao et al. 2001, Chen, Wang et al. 2016). When FVT is applied, the maximum torque produced is shifted towards a lower engine speed. This was also presented by previous research works on optimizing variable valve timing for maximizing performance (Sher and Bar-Kohany 2002).

Figure 4.41 and Figure 4.42 shows brake power comparison between FVT and baseline model in terms of kW and HP, respectively. A significant impact on the brake power is observed at high-speed region where higher maximum brake power is produced with 2.52kW (3.4HP) at 7500 RPM compared to the baseline model with 2.3kW (3HP) at 7200 RPM. However, improvement of brake power is observed in the entire engine speed, which demonstrated the boosting potential of FVT employment. Brake power for

the entire engine speed has been improved at 11.3% on average using FVT profiles. The amplification of brake power using valve timing strategies also demonstrated from previous works (Kohany and Sher 1999, Takemura, Aoyama et al. 2001, Ghazal, Najjar et al. 2013, Chen, Wang et al. 2016).

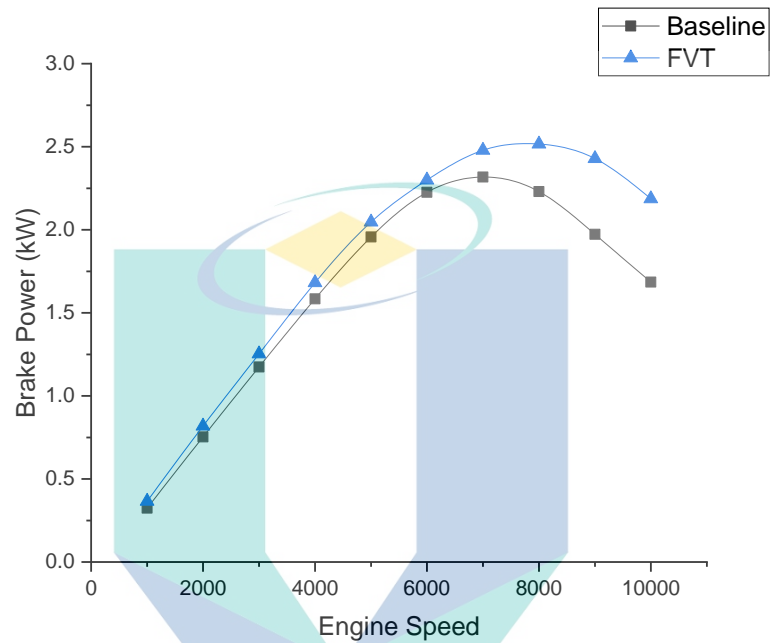


Figure 4.41 Brake Power of FVT Model

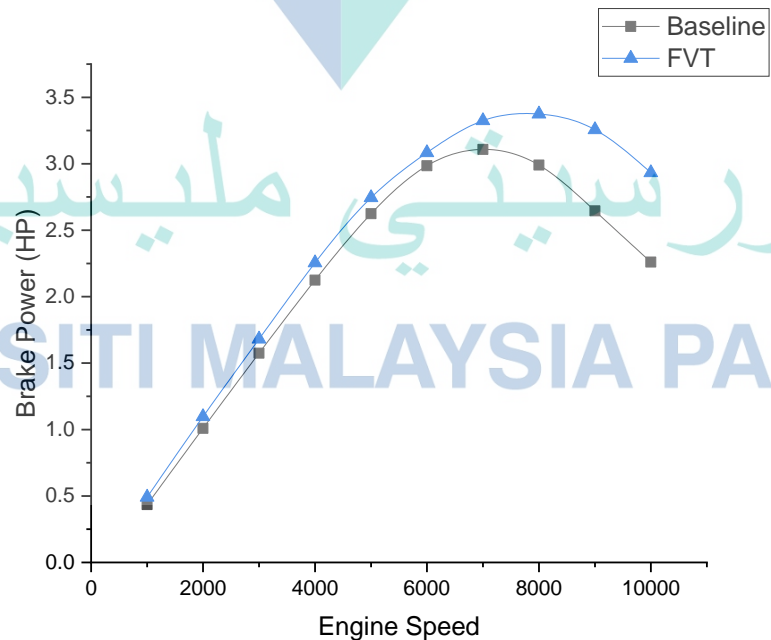


Figure 4.42 Brake Power (HP) of FVT Model

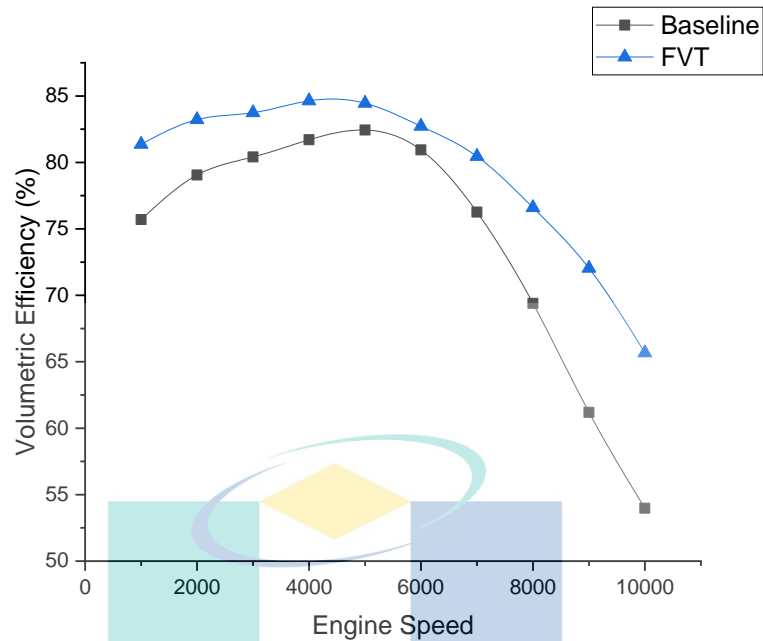


Figure 4.43 Volumetric Efficiency of FVT Model

Figure 4.43 displays the volumetric efficiency achieved by the FVT application is improved in the entire run. The maximum volumetric efficiency achieved is 84.69% at 4500 RPM compared to the baseline model which is 82.43% at 5000 RPM. The average improvement for the entire engine speed is 8% on average. The amplification of brake torque using valve timing strategies also demonstrated from previous work (Chen, Wang et al. 2016). Volumetric efficiency is high due to additional air with FVT strategies, which then causes a decrease in exhaust temperature, lead to low NO_x (Basaran and Ozsoysal 2017). The EIVO strategy used at 7000 RPM and above leads to a proven volumetric efficiency improvement with a significant amount as also demonstrated from previous work (Verhelst, Demuynck et al. 2010, Ghazal, Najjar et al. 2013). The IVC timing was found to influence the volumetric efficiency the most (Samuel, Mithun et al. 2019) as indicated in section 4.3.7. The increment valve overlap period improved the volumetric efficiency as speed increases (Khudhur, Saleh et al. 2015).

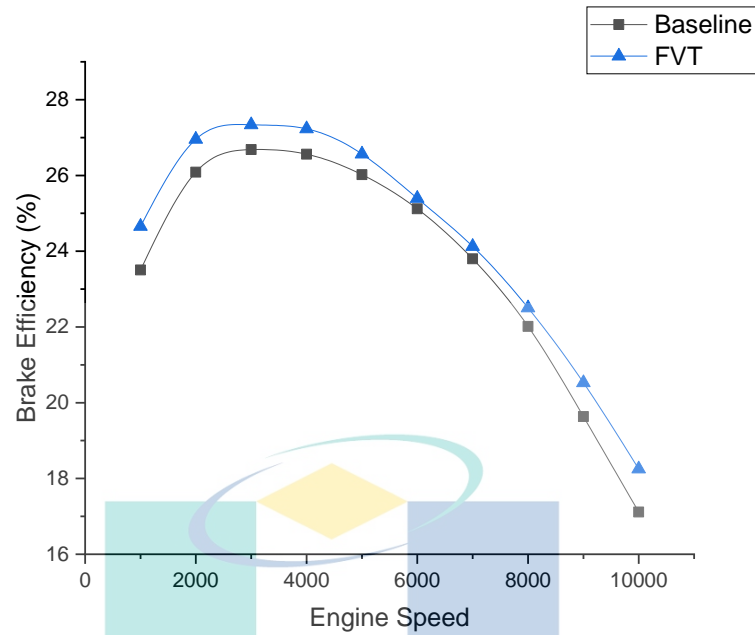


Figure 4.44 Brake Thermal Efficiency of FVT Model

Brake thermal efficiency is also improved in every engine speed by 3% on average as shown in Figure 4.44. The obvious improvement can be spotted at 1000 RPM to 5000 RPM. The maximum efficiency achieved by FVT is 27.4% at 3500 RPM compared to the baseline model which is 26.68% at 3000 RPM. Thermal efficiency is amplified by the adjustment of EVO timing, which influence the valve overlap and gas exchange process (Samuel, Mithun et al. 2019). EEVO is used at lower speed while LEVO at higher speed in FVT strategies. As speed increases, the valve overlap period affect the volumetric efficiency to increase (Khudhur, Saleh et al. 2015)

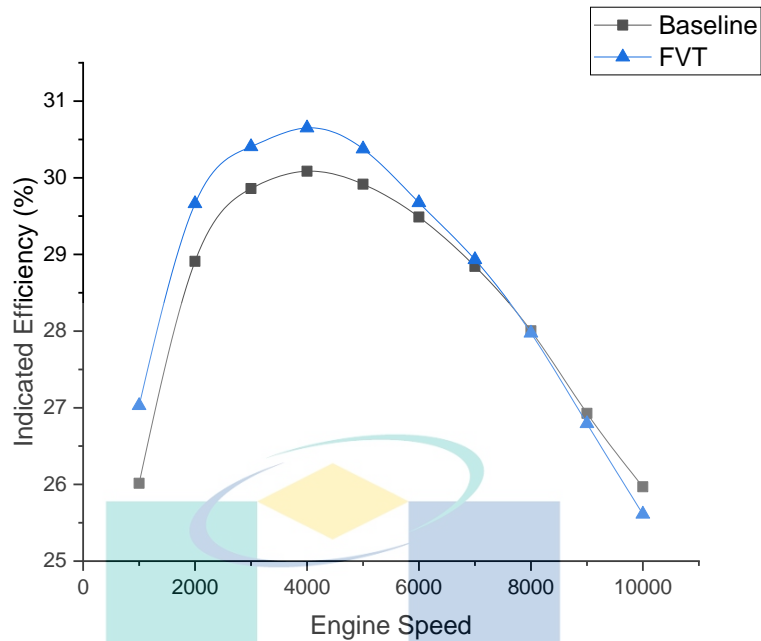


Figure 4.45 Indicated Efficiency of FVT Model

Figure 4.45 illustrates the comparison of the volumetric efficiency achieved by FVT with the baseline model. The maximum indicated efficiency achieved is improved by 30.65% at 4000 RPM compared to the baseline model, which is 30.08% at 4000 RPM. The improvement is achieved significantly from 1000 RPM to 7000 RPM, then the efficiency curve starts to deteriorate with the lowest value at 10 000 RPM. The maximum drop on indicated efficiency observed is 1.3%. The average improvement of indicated efficiency from 1000 RPM to 7000 RPM is 1.8% on average. Improvements in efficiency were achievable by reducing the residual mass fraction and knock sensitivity (Stone, Kelly et al. 2017).

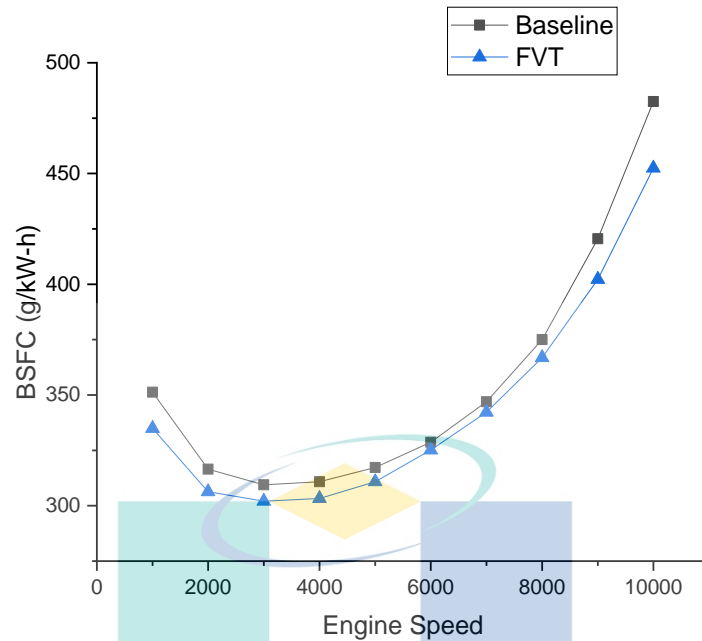


Figure 4.46 Brake Specific Fuel Consumption (BSFC) of FVT Model

Figure 4.46 displays the BSFC achieved by FVT compared with the baseline model. The BSFC is improved in the entire engine speed with a 3% reduction on average. The minimum BSFC produced by the FVT model is 302.06 g/kW-h at 3000 RPM, compared to the baseline model, which is 309.43 g/kW-h at 3000 RPM. This was also agreed by previous work on intelligent valve actuation with fuel economy improvements of up to 7.5% coincided with low pumping losses reduction from base engine levels (Stone, Kelly et al. 2017). The potential for improved fuel consumption and therefore reduced CO₂, in conjunction with further improvements in toxic emissions, is also presented in Intelligent Valve Technology (Stone and Douglas 2019). The reduction of BSFC using valve timing strategies also demonstrated from previous works (Takemura, Aoyama et al. 2001, Sher and Bar-Kohany 2002, Turner, Kenchington et al. 2004, Ghazal, Najjar et al. 2013, Kuruppu, Pesiridis et al. 2014, Chen, Wang et al. 2016, Dost and Getzlaff 2018, Zhao, Xi et al. 2018). Generally, the fuel economy is better with the variable IVC timing than the fixed IVC timing (Li, Tao et al. 2001). As speed increases, late closing of the exhaust valve results in an optimised BSFC (Kakaee, Keshavarz et al. 2016) as shown in section 4.3.7.

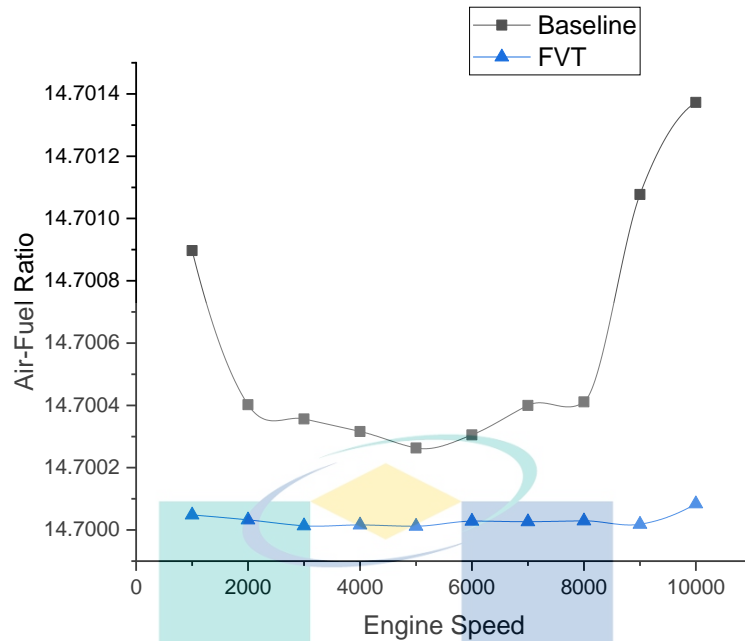


Figure 4.47 Air-Fuel Ratio of FVT Model

Simulation followed stoichiometric control of air-to-fuel ratio (D and A) at the injector. Figure 4.47 shows the plotted graphs of AFR produced by FVT in comparison with the baseline model. Even though stoichiometric gasoline AFR, which is 14.7:1 was set in the simulation, the baseline model shows the fluctuation of AFR value produced during the run. Compared to AFR produced by the FVT model, the values are levelled where a flat graph close to 14.7 is observed in the entire engine speed. Thus, the gas exchange performance is significantly influenced by the valve timing tuning and FVT application.

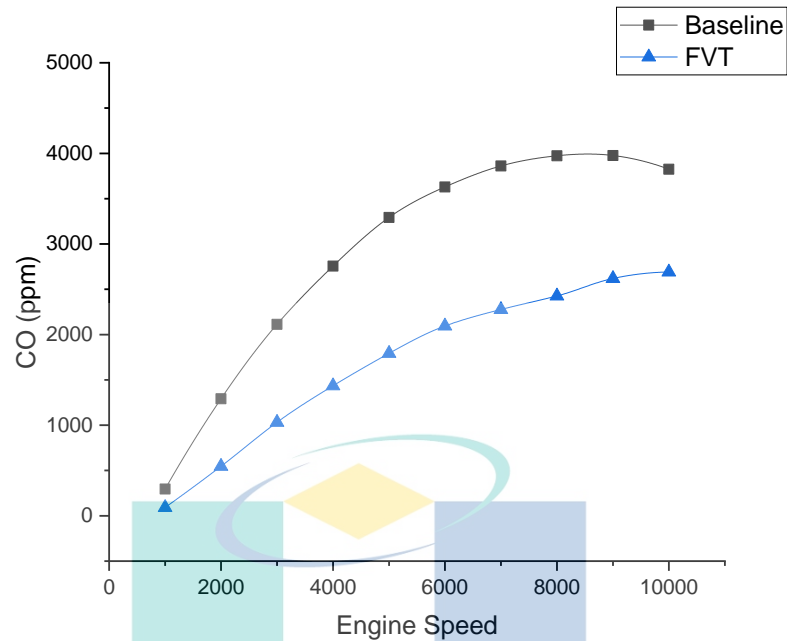


Figure 4.48 Carbon Monoxide Emission of FVT Model

Figure 4.48 shows the carbon monoxide level comparison between the FVT and baseline model. A very significant impact on the CO emission is observed in the entire run with a 45.75% improvement on average. The minimum CO produced by the FVT model is 91.73 ppm at 1000 RPM, compared to baseline model which is 295.4 ppm at 1000 RPM. The average CO emission produced by the FVT model is 1700.16 ppm, compared to the baseline model which is 2901.32 ppm. The reduction of CO using valve timing strategies also demonstrated from previous works (Li, Tao et al. 2001, Kuruppu, Pesiridis et al. 2014).

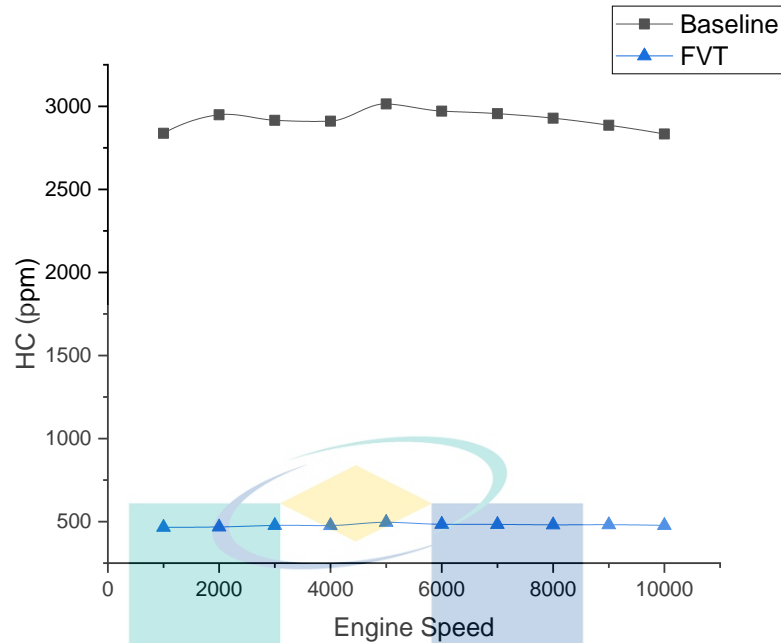


Figure 4.49 Hydrocarbon Emission of FVT Model

Figure 4.49 indicates the hydrocarbon level comparison between the FVT and baseline model. A very significant impact on the HC emission is observed in the entire run with a wide margin difference. The improvement is calculated at 83.61% on average. The value of HC emission produced by FVT is levelled in the entire run. The average HC emission produced by the FVT model is 478.42 ppm, compared to the baseline model, which is 2919.93 ppm. The improvement of HC emission using valve timing strategies also demonstrated from previous work (Takemura, Aoyama et al. 2001).

اونيورسيتي ملايسيا فھق

UNIVERSITI MALAYSIA PAHANG

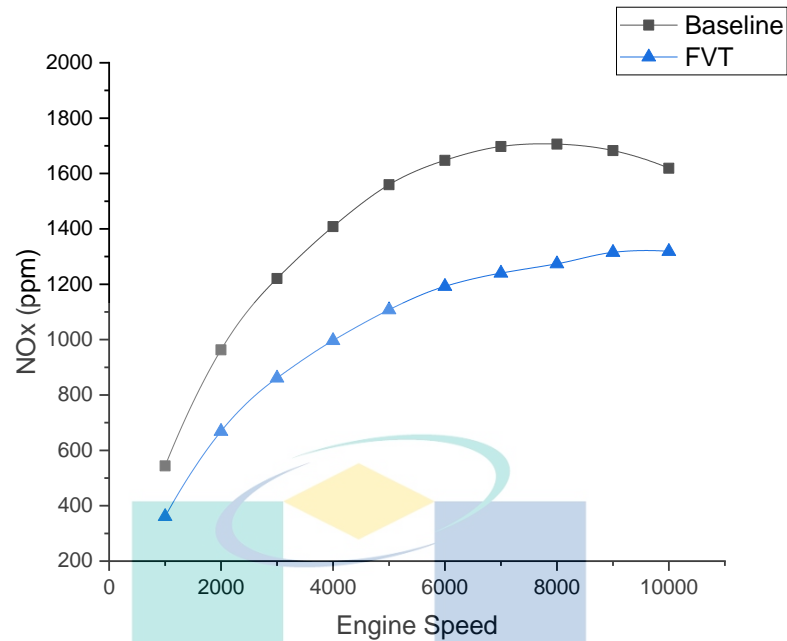


Figure 4.50 Nitrogen Oxide Emissions of FVT Model

A very significant impact on the NO_x emission is also observed in the entire run with a 27.21% improvement on average as shown in Figure 4.50. The minimum NO_x produced by the FVT model is 361.09 ppm at 1000 RPM, compared to the baseline model, which is 544.03 ppm at 1000 RPM. The average NO_x emission produced by the FVT model is 1404.73 ppm, compared to the baseline model, which is 2919.93 ppm. Minimum BSFC can be achieved with very low NO_x levels and long burn periods (Stone, Kelly et al. 2017). It was agreed that variable valve timing alone offered the greatest NO_x reduction potential (Cairns, Zhao et al. 2013). NO_x is performance generally improved with FVT. This is, however, at least partially due to the lower peak pressures present with the slower combustion that accompanies EIVC at speed below 7000 RPM (Pierik and Burkhard 2000). At above 700RPM, increased valve overlap leads to a higher amount of internal EGR. The higher amount of internal EGR leads to decreased NO_x emissions as peak temperatures are lowered. This is caused by exhaust gases being pushed back into the inlet manifold when the intake valves open (Verhelst, Demuyne et al. 2010). The reduction of NO_x using valve timing strategies also demonstrated from previous works (Li, Tao et al. 2001, Jia, Xie et al. 2011, Kuruppu, Pesiridis et al. 2014). EVC timing influenced combustion phasing by trapping less hot exhaust, thus lower cylinder temperature (Samuel, Mithun et al. 2019).

CHAPTER 5

CONCLUSION

5.1 Conclusion

A baseline model of a four-stroke spark-ignition engine has been developed in this study as a one-dimensional numerical model. The development consists of port flow assessment, cam profile measurement and numerical identification of other geometrical dimensions and parameters of the baseline engine. Port flow assessment shows the flow coefficient of intake port is comparable to SB Chevy data with an insignificant percentage of error. The flow coefficient of the exhaust port shows a significant difference compared to SB Chevy. However, the graph trend is comparable. The performance of the baseline model was evaluated and validated with the specification provided by the manufacturer and shows an acceptable agreement to replicate the baseline model using one-dimensional tool. The performance of the baseline model was investigated, thus accomplish the first objective of this research.

The design of experiment, which carries a full factorial method, has been conducted to test every possibility of valve event position and its impact on the engine performance in line with the idea of FVT strategies. ANOVA result of the DOE has shown a high R^2 coefficient value, which is an excellent indicator of goodness of fit of the data and ensures a satisfactory agreement between the calculated data and observed data in the tool. The P-value also indicated that all the models of the experiment are significant as they are less than 0.05.

The DOE has identified the effect of modification of intake and exhaust valve event on engine responses. Observing the main effect, which is the marginal effect caused solely by changing one variable at a time while other variables remain at baseline specification, intake valve timing have a larger impact on the engine responses at lower

engine speed compared to exhaust valve. At 1000 RPM to 4 000 RPM, the modification of IVC followed by IVO has caused a significant rate of impact. When engine speed reached 5000 RPM, the main effect has changed hands where the exhaust valve takes over the position. Up to 10 000 RPM, exhaust valve events, which are EVC followed by EVO affect the engine responses the most by their timing modification. The variation of maximum lift of both intake and exhaust valve has seen to produce no significant effect at a lower speed, and minimal effect at high-end RPM.

Interaction effects is the simultaneous effect of two or more independent variables that occur when the effect of one variable depends on the value of another variable. Interaction effects seem to provide more reliable results of valve timing philosophy because it evaluates the effect of all variables simultaneously and comprehensively. Intake valve events, which are IVO and IVC have shown the largest interaction effect at 1000 RPM and 2000 RPM engine speed. At 2000 RPM and above, exhaust valve events, which are EVO and EVC have taken place to become the most significant variable for interaction effects. Interaction effects of EVC and IVO carry the definition of valve overlap duration. The valve overlap duration is the third most significant variable of interaction effects after the intake and exhaust valve events in the entire run. This concludes that the modification intake valve events are impactful at 1000 RPM to 2000 RPM engine speed, while the modification of exhaust valve events is impactful above 2000 RPM to 10 000 RPM. Valve overlap duration possess a significant effect on engine response. As speed increases, the valve overlap effect increases. The maximum lift, however, contributed a small percent of interaction effect on the engine responses. The intake and exhaust philosophies for variable valve timing through an optimization technique were investigated, thus accomplish the second objective of this research.

Table 5.5 summarizes the positive impact of valve timing strategies used in this study on engine performance. The result of valve timing strategies is compared with previous work summarized in Table 5.6, which conducted the investigation on the main effects of variables without interaction.

Based on both tables, it is an agreement that LIVO strategy shows no positive impact on the engine as speed increases. This means the less valve overlapping is disadvantageous as engine speed increases. EIVO and LEVC strategies show a positive impact on the engine performance at higher speed. This concludes that more overlapping

is prompted as speed increases. The maximum lift of the intake and exhaust valves require lower lift at lower engine speed. As speed increases, a higher lift of intake and exhaust valves is beneficial to the engine performance. EIVC and EEVC are advantageous at lower engine speed, while LIVC, EIVO, and LEVC are advantageous at higher speed. LEVO and higher intake valve lift are beneficial at all speed. LIVO and EEVO show no positive impact on engine performance.

The DOE experiments have identified several optimum FVT profiles. The application of the FVT profiles has resulted in improvement of the engine performance by 11% on average. Furthermore, the emission rate is improved significantly at all speed levels with average of over 20% improvement overall. FVT profiles also proved the reduction of fuel consumption is achievable in line with the remarkable performance boosting, thus accomplish the third objective of this research.

5.2 Future recommendations

Firstly, a recommendation that needs to be issued for future works is to conduct a further optimization of the valve timings at every speed level as it seems the performance of the engine possesses a high potential to be refined further using FVT strategies.

Secondly, since the valve timing and lift modification is proved to enhance engine performance in the entire speed of the engine, a study to develop the actuation system in order to replicate the FVT actuation in real-time is proposed in the future.

Thirdly is to synchronize the valve actuation from a linear motor with the crankshaft angle in order to execute the application of the FVT system on a commercial internal combustion engine.

Fourthly, a study on performance investigation of the FVT system through experiment setup to validate the engine improvement since the FVT system has huge potential in variable valve timing application as well as the throttle-less engine, variable compression engine and cylinder deactivation.

REFERENCES

- Algieri, A. (2011). An Experimental Analysis of the Fluid Dynamic Efficiency of a Production Spark-Ignition Engine during the Intake and Exhaust Phase, ISRN Mechanical Engineering.
- Atkinson, J. (1887). US367496A. US.
- Auer, M. (2010). Erstellung phänomenologischer Modelle zur Vorausberechnung des Brennverlaufes von Magerkonzept-Gasmotoren, Technische Universität München.
- Ayala, F. A., M. D. Gerty and J. B. Heywood (2006). Effects of combustion phasing, relative air-fuel ratio, compression ratio, and load on SI engine efficiency, SAE Technical Paper.
- Basaran, H. U. and O. A. Ozsoysal (2017). "Effects of application of variable valve timing on the exhaust gas temperature improvement in a low-loaded diesel engine." Applied Thermal Engineering **122**: 758-767.
- Bernard, L., A. Ferrari, D. Micelli, A. Perotto, R. Rinolfi and F. J. M. w. Vattaneo (2009). "Electro-hydraulic valve control with multi-air technology." **70**(12): 4-10.
- Blair, G. and F. Drouin (1996). Relationship between discharge coefficients and accuracy of engine simulation, SAE Technical Paper.
- Bonatesta, F., G. Altamore, J. Kalsi and M. Cary (2016). "Fuel economy analysis of part-load variable camshaft timing strategies in two modern small-capacity spark ignition engines." Applied energy **164**: 475-491.
- Boretti, A. and J. Scalzo (2011). Exploring the advantages of atkinson effects in variable compression ratio turbo GDI engines, SAE Technical Paper.
- Braun, M., M. Klaas and W. Schröder (2018). "Influence of Miller Cycles on Engine Air Flow." SAE International Journal of Engines **11**(03-11-02-0011): 161-178.
- Brunt, M. F. and A. L. Emtage (1996). "Evaluation of IMEP routines and analysis errors." SAE transactions: 749-763.
- Brunt, M. F., H. Rai and A. L. Emtage (1998). "The calculation of heat release energy from engine cylinder pressure data." SAE transactions: 1596-1609.
- Cairns, A., H. Zhao, A. Todd and P. Aleiferis (2013). "A study of mechanical variable valve operation with gasoline-alcohol fuels in a spark ignition engine." Fuel **106**: 802-813.
- Çengel, Y. A. and M. A. Boles (2014). Thermodynamics: An Engineering Approach, McGraw-Hill.
- Chaichan, M. T. (2018). "Performance and emission characteristics of CIE using hydrogen, biodiesel, and massive EGR." International Journal of Hydrogen Energy **43**(10): 5415-5435.
- Chandras, P., J. McCarthy Jr, D. Stretch and B. Smith (2018). Effect of Intake Valve Profile Modulation on Passenger Car Fuel Consumption, SAE Technical Paper.

- Chen, J., Z. Wang and F. Tian (2016). "A New Hydraulic Variable Valve Timing and Lift System for Spark Ignition Engine." *Chemical Engineering Transactions* **51**.
- Clenci, A., A. Biziiac, P. Podevin and R. Niculescu (2013). "Variable intake valve lift on a port fuel injected engine and its effects on idle operation."
- Corti, E. and C. Forte (2011). Real-time combustion phase optimization of a PFI gasoline engine, SAE Technical Paper.
- Cox, D. R. (1984). "Interaction." *International Statistical Review / Revue Internationale de Statistique* **52**(1): 1-24.
- D, A. and A. A (2016). "Effect of Variable Valve Timing to Reduce Specific Fuel Consumption in HD Diesel Engine." *Journal of Applied Mechanical Engineering* **5**(6).
- de O. Carvalho, L., T. C. C. de Melo and R. M. de Azevedo Cruz Neto (2012). Investigation on the Fuel and Engine Parameters that Affect the Half Mass Fraction Burned (CA50) Optimum Crank Angle, SAE International.
- Dodge, Y. and D. Commenges (2006). *The Oxford dictionary of statistical terms*, Oxford University Press on Demand.
- Dost, T. and J. Getzlaff (2018). Cylinder Individually Gas Exchange Controlling: A Method for Improved Efficiency of Turbocharged SI Engines, SAE Technical Paper.
- Dresner, T. and P. Barkan (1989). *A Review of Variable Valve Timing Benefits and Modes of Operation*, SAE International.
- Ferguson, C. R. and A. T. Kirkpatrick (2015). *Internal combustion engines: applied thermosciences*, John Wiley & Sons.
- G. B. Parvate-Patil, H. H. a. B. G. (2003). "*An Assessment of Intake and Exhaust Philosophies for Variable Valve Timing*." Society of Automotive Engineers of Japan, Inc. **2003-32-0078**.
- Ghauri, A. (1999). *An Investigation into the Effects of Variable Valve Actuation on Combustion and Emissions in an SI Engine*, University of London.
- Ghazal, O. H., Y. S. Najjar and K. J. Al-Khishali (2013). "Modeling the Effect of Variable Timing of the Exhaust Valves on SI Engine Emissions for Greener Vehicles." *Energy and power engineering* **5**(03): 181.
- Gould, L. A., W. E. Richeson and F. L. Erickson (1991). Performance evaluation of a camless engine using valve actuators with programmable timing, SAE Technical Paper.
- Gupta, V. and R. Parsad (2005). "Fundamentals of Design of Experiments." 29.
- Hakansson, A. (2007). "CA50 estimation on HCCI engine using engine speed variations." Lund University: MSc Thesis.
- Halderman, J. D. and C. D. Mitchell (2014). *Automotive technology*, Pearson.
- Hanipah, M. R. B. (2015). Development of a spark ignition free-piston engine generator, University of Newcastle upon Tyne.

- Hanipah, M. R. B. H. (2008). Combustion process in a two-stroke, H₂-DI linear generator free-piston engine during starting, Universiti Teknologi Petronas.
- Hannibal, W., R. Flierl, L. Stiegler and R. Meyer (2004). Overview of Current Continuously Variable Valve Lift Systems for Four-Stroke Spark-Ignition Engines and the Criteria for their Design Ratings, SAE International.
- Hanrahan, G. and K. Lu (2006). "Application of Factorial and Response Surface Methodology in Modern Experimental Design and Optimization." *Critical Reviews in Analytical Chemistry* **36**(3-4): 141-151.
- Heywood, J. B. (1988). *Internal Combustion Engine Fundamentals*, McGraw-Hill.
- Heywood, J. B. (1988). *Internal Combustion Engine Fundamentals*, McGraw-Hill International.
- Hoglund, A., U. Carlson, C. Koenigsegg and L. Ivarsson (2017). Combustion engine with pneumatic valve return spring, Google Patents.
- Hou, S.-S. (2007). "Comparison of performances of air standard Atkinson and Otto cycles with heat transfer considerations." *Energy Conversion and Management* **48**.
- Hou, S.-S. (2007). "Comparison of performances of air standard Atkinson and Otto cycles with heat transfer considerations." *Energy Conversion and Management* **48**(5): 1683-1690.
- ICCT (2019). "CO₂ EMISSION STANDARDS FOR PASSENGER CARS AND LIGHT-COMMERCIAL VEHICLES IN THE EUROPEAN UNION." International Council on Clean Transportation **Policy Update**.
- Inoue, K., K. Nagahiro, Y. Ajiki and N. Kishi (1989). A high power, wide torque range, efficient engine with a newly developed variable-valve-lift and-timing mechanism, SAE Technical Paper.
- Jabbar, A. I., W. S. Vaz, H. A. Khairallah and U. O. Koylu (2016). "Multi-objective optimization of operating parameters for hydrogen-fueled spark-ignition engines." **41**(40): 18291-18299.
- Jacobs, T. J. (2017). *Internal Combustion Engines, Developments in. Encyclopedia of Sustainability Science and Technology*. R. A. Meyers. New York, NY, Springer New York: 1-53.
- Jankovic, M. and S. W. Magner (2002). "Variable cam timing: Consequences to automotive engine control design." *IFAC Proceedings Volumes* **35**(1): 271-276.
- Jia, M., M. Xie, T. Wang and Z. Peng (2011). "The effect of injection timing and intake valve close timing on performance and emissions of diesel PCCI engine with a full engine cycle CFD simulation." *Applied Energy* **88**(9): 2967-2975.
- Kakaee, A.-H., M. Keshavarz, A. Paykani and M. Keshavarz (2016). "Mathematical optimization of variable valve timing for reducing fuel consumption of A SI engine." *Engineering Review* **36**(1): 61-69.
- Karden, E., S. Ploumen, B. Fricke, T. Miller and K. Snyder (2007). "Energy storage devices for future hybrid electric vehicles." *Journal of Power Sources* **168**(1): 2-11.

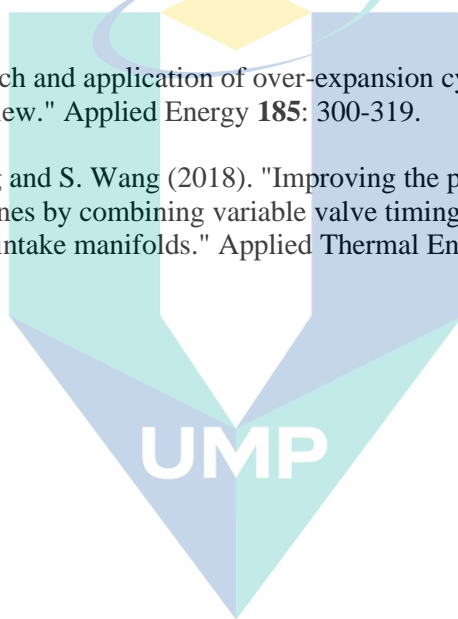
- Kesgin, U. (2005). "Efficiency improvement and NO_x emission reduction potentials of two-stage turbocharged Miller cycle for stationary natural gas engines." *International journal of energy research* **29**(3): 189-216.
- Kesner, A. L., P. J. Schleyer, F. Büther, M. A. Walter, K. P. Schäfers and P. J. Koo (2014). "On transcending the impasse of respiratory motion correction applications in routine clinical imaging—a consideration of a fully automated data driven motion control framework." *EJNMMI physics* **1**(1): 8.
- Khudhur, S. H., A. M. Saleh and M. T. Chaichan (2015). "The effect of variable valve timing on SIE performance and emissions." *International Journal of Scientific & Engineering Research* **6**(8): 173-179.
- Kim, C. and C. J. S. t. Bae (1999). "Hydrocarbon emissions from a gas fueled SI engine under lean burn conditions." 1551-1558.
- Knight, R. D. (2004). *Physics for Scientists and Engineers: A Strategic Approach with Modern Physics with Mastering Physics*, Benjamin Cummings.
- Kohany, T. and E. Sher (1999). *Using the 2nd Law of Thermodynamics to Optimize Variable Valve Timing for Maximizing Torque in a Throttled SI Engine*, SAE International.
- Kreuter, P., P. Heuser, J. Reinicke-Murmann, R. Erz, U. Peter and O. J. S. t. Böcker (2003). "Variable valve actuation—switchable and continuously variable valve lifts." 112-123.
- Kuruppu, C., A. Pesiridis and S. Rajoo (2014). *Investigation of cylinder deactivation and variable valve actuation on gasoline engine performance*, SAE Technical Paper.
- Lee, J. and H.-J. Chang (2017). *Multi-parametric model predictive control for variable valve timing*. 2017 17th International Conference on Control, Automation and Systems (ICCAS), IEEE.
- Leiviskä, K. (2013). "Introduction to Experiment Design." **5**.
- Li, L., J. Tao, Y. Wang, Y. Su and M. Xiao (2001). *Effects of intake valve closing timing on gasoline engine performance and emissions*, SAE Technical Paper.
- Li, Q., J. Liu, J. Fu, X. Zhou and C. Liao (2018). "Comparative study on the pumping losses between continuous variable valve lift (CVVL) engine and variable valve timing (VVT) engine." *Applied Thermal Engineering* **137**: 710-720.
- Li, Y., A. Khajepour and C. Devaud (2018). "Realization of variable Otto-Atkinson cycle using variable timing hydraulic actuated valve train for performance and efficiency improvements in unthrottled gasoline engines." *Applied Energy* **222**: 199-215.
- Lou, Z. D., Q. Deng, S. Wen, Y. Zhang, M. Yu, M. Sun and G. Zhu (2013). "Progress in Camless Variable Valve Actuation with Two-Spring Pendulum and Electrohydraulic Latching." *SAE International Journal of Engines* **6**(1): 319-326.
- Luo, Q.-h. and B.-g. Sun (2016). "Effect of the Miller cycle on the performance of turbocharged hydrogen internal combustion engines." *Energy Conversion and Management* **123**: 209-217.
- Luria, D., Y. Taitel and A. Stotter (1982). *The Otto-Atkinson engine—a new concept in automotive economy*, SAE Technical Paper.

- Ma, T. (1988). "Effect of variable engine valve timing on fuel economy." SAE transactions: 665-672.
- Martins, M. E. S. and T. D. M. Lanza (2015). "Full-load Miller cycle with ethanol and EGR: Potential benefits and challenges." Applied Thermal Engineering **90**: 274-285.
- Merker, G. P., P. Eckert, F. Otto, K. Christian, S. Rakowski, C. Reulein, G. Stiesch, R. Tatschl, B. Durst and A. Wimmer (2012). Grundlagen Verbrennungsmotoren: funktionsweise, simulation, messtechnik, Springer-Verlag.
- Middleton, R. J., L. K. M. Olesky, G. A. Lavoie, M. S. Wooldridge, D. N. Assanis and J. B. Martz (2015). "The effect of spark timing and negative valve overlap on Spark Assisted Compression Ignition combustion heat release rate." Proceedings of the Combustion Institute **35**(3): 3117-3124.
- Miller, R. (1947). "Supercharging and Internal Cooling Cycle for High Output." Trans. ASME **69**.
- Miller, R. (1956). US2817322A. US.
- Montgomery, D. C. and W. H. Woodall (2008). "An overview of six sigma." International Statistical Review **76**(3): 329-346.
- Moriya, Y., A. Watanabe, H. Uda, H. Kawamura, M. Yoshioka and M. Adachi (1996). A Newly Developed Intelligent Variable Valve Timing System-Continuously Controlled Cam Phasing as Applied to a New 3 Liter Inline 6 Engine, SAE Technical Paper.
- Muta, K., M. Yamazaki and J. Tokieda (2004). Development of new-generation hybrid system THS II-Drastic improvement of power performance and fuel economy, SAE Technical Paper.
- Muzakir, S. and H. Hirani (2015). "A magnetorheological fluid based design of variable valve timing system for internal combustion engine using axiomatic design." International Journal of Current Engineering Research **5**(2): 603-612.
- Neher, D. (2017). Miller Cycle and Exhaust Gas Recirculation for a Naturally Aspirated Lean-burn Gas Engine Doctoral, Universidad de Valladolid.
- Nithyanandan, K., H. Wu, M. Huo and C.-F. Lee (2014). A preliminary investigation of the performance and emissions of a port-fuel injected si engine fueled with acetone-butanol-ethanol (ABE) and gasoline, SAE Technical Paper.
- Noordin, M., V. Venkatesh, S. Sharif, S. Elting and A. Abdullah (2004). "Application of response surface methodology in describing the performance of coated carbide tools when turning AISI 1045 steel." Journal of materials processing technology **145**(1): 46-58.
- Obeng, D. P., S. Morrell and T. J. Napier-Munn (2005). "Application of central composite rotatable design to modelling the effect of some operating variables on the performance of the three-product cyclone." International Journal of Mineral Processing **76**(3): 181-192.
- Öztürk, N. and D. J. A. Kavak (2004). "Boron removal from aqueous solutions by adsorption on waste sepiolite and activated waste sepiolite using full factorial design." **10**(3): 245-257.

- Park, S. and S. Song (2017). "Model-based multi-objective Pareto optimization of the BSFC and NO_x emission of a dual-fuel engine using a variable valve strategy." *Journal of Natural Gas Science and Engineering* **39**: 161-172.
- Parvate-Patil, G., H. Hong and B. Gordon (2003). "An assessment of intake and exhaust philosophies for variable valve timing." *SAE transactions*: 2174-2189.
- Patel, R., N. Ladommatos, P. A. Stansfield, G. Wigley, C. P. Garner, G. Pitcher, J. W. G. Turner, H. Nuglisch and J. Helie (2010). "Un-throttling a direct injection gasoline homogeneous mixture engine with variable valve actuation." **11**(6): 391-411.
- Pertl, P., A. Trattner, A. Abis, S. Schmidt, R. Kirchberger and T. Sato (2012). Expansion to higher efficiency-investigations of the atkinson cycle in small combustion engines, SAE Technical Paper.
- Pierik, R. J. and J. F. Burkhard (2000). Design and development of a mechanical variable valve actuation system, SAE Technical Paper.
- Pulkrabek, W. W. (1997). *Engineering Fundamentals of the Internal Combustion Engine*, Prentice Hall.
- Rosli, M. H. A. (2018). Numerical Investigation of A Four Stroke Flexible Timings. Bachelor of Automotive Engineering, Universiti Malaysia Pahang.
- Ryan, T. P. and J. P. Morgan (2007). "Modern Experimental Design." *Journal of Statistical Theory and Practice* **1**(3-4): 501-506.
- Saied, G. M., S. Ahmad, S. A. Jazayeri and A. H. Shamekhi (2008). Modeling of variable intake valve timing in SI engine. ASME 2006 Internal Combustion Engine Division Spring Technical Conference, American Society of Mechanical Engineers Digital Collection.
- Samuel, J., S. Mithun, K. Panda, A. Ramesh, M. Wick, J. Andert, B. Lehrheuer and S. Pischinger (2019). Experimental Investigations on the Influence of Valve Timing and Multi-Pulse Injection on GCAI Combustion, SAE International.
- Sher, E. and T. Bar-Kohany (2002). "Optimization of variable valve timing for maximizing performance of an unthrottled SI engine—a theoretical study." *Energy* **27**(8): 757-775.
- Shojaeefard, M. H. and M. Keshavarz (2015). "Mathematical modeling of the complete thermodynamic cycle of a new Atkinson cycle gas engine." *Applied Thermal Engineering* **91**: 866-874.
- Siddiqui, M. S. (2017). Hydraulic Variable Valve Actuation on a Single Cylinder Engine, UWSpace.
- Singh, B. P., L. Besra and S. Bhattacharjee (2002). "Factorial design of experiments on the effect of surface charges on stability of aqueous colloidal ceramic suspension." *Colloids and Surfaces A: Physicochemical and Engineering Aspects* **204**(1): 175-181.
- Stone, C., T. Carden and I. Podmore (1993). "Analysis of the effect of inlet valve disablement on swirl, combustion and emissions in a spark ignition engine." *Proceedings of the Institution of Mechanical Engineers, Part D: Journal of Automobile Engineering* **207**(4): 295-305.

- Stone, R. (1992). Introduction to Internal Combustion Engines.
- Stone, R. and C. Douglas (2019). iVT, Intelligent Valve Technology: Development of a 16 Valve Cylinder Head. Symposium for Combustion Control 2019.
- Stone, R., D. Kelly, J. Geddes and S. Jenkinson (2017). Intelligent Valve Actuation-A Radical New Electro-Magnetic Poppet Valve Arrangement. Proceedings of the 26th Aachen Colloquium Automobile and Engine Technology, Germany.
- Sulaiman, S., S. Murad, I. Ibrahim and Z. A. Karim (2010). "Study of flow in air-intake system for a single-cylinder go-kart engine." **1**: 91-104.
- Takemura, S., S. Aoyama, T. Sugiyama, T. Nohara, K. Moteki, M. Nakamura and S. Hara (2001). "A study of a continuous variable valve event and lift (VEL) system." SAE Transactions: 118-125.
- Tavakoli, S., S. A. Jazayeri, M. Fathi and O. Jahanian (2016). "Miller cycle application to improve lean burn gas engine performance." *Energy* **109**: 190-200.
- Telford and J. K (2007). "A brief introduction to design of experiments." **27**(3): 224-232.
- Thompson, N. D. and J. S. Wallace (1994). "Effect of engine operating variables and piston and ring parameters on crevice hydrocarbon emissions." SAE transactions: 718-736.
- Turner, J., S. Kenchington and D. Stretch (2004). Production AVT development Lotus and Eaton's electrohydraulic closed-loop fully variable valve train system. 25th Vienna Motor Symposium, 2004, University of Bath.
- Unger, H., C. Schwarz, J. Schneider and K.-F. Koch (2008). "Die Valvetronic." *MTZ - Motortechnische Zeitschrift* **69**(7): 598-605.
- Van Basshuysen, R. and F. Schäfer (2004). Internal combustion engine handbook-basics, components, systems and perspectives.
- Venkatesan, L., A. Harris and M. Greyling (2014). "Optimisation of air rate and froth depth in flotation using a CCRD factorial design – PGM case study." *Minerals Engineering* **66-68**: 221-229.
- Verhelst, S., J. Demuyne, R. Sierens and P. Huyskens (2010). "Impact of variable valve timing on power, emissions and backfire of a bi-fuel hydrogen/gasoline engine." *International Journal of Hydrogen Energy* **35**(9): 4399-4408.
- Voelcker, J. (2009). "Top 10 tech cars." *IEEE Spectrum* **46**(4): 42-49.
- Wang, P.-Y. and S.-S. Hou (2005). "Performance analysis and comparison of an Atkinson cycle coupled to variable temperature heat reservoirs under maximum power and maximum power density conditions." *Energy Conversion Management* **46**(15-16): 2637-2655.
- Wang, T., D. Liu, G. Wang, B. Tan and Z. Peng (2015). "Effects of Variable Valve Lift on In-Cylinder Air Motion." *Energies* **8**(12): 13778-13795.
- Wang, Y., L. Lin, S. Zeng, J. Huang, A. P. Roskilly, Y. He, X. Huang and S. Li (2008). "Application of the Miller cycle to reduce NOx emissions from petrol engines." *Applied Energy* **85**(6): 463-474.

- Wang, Y., S. Zeng, J. Huang, Y. He, X. Huang, L. Lin and S. Li (2005). "Experimental investigation of applying Miller cycle to reduce NOx emission from diesel engine." *Proceedings of the Institution of Mechanical Engineers, Part A: Journal of Power Energy* **219**(8): 631-638.
- Wang, Y., B. Zu, Y. Xu, Z. Wang and J. Liu (2016). "Performance analysis of a Miller cycle engine by an indirect analysis method with sparking and knock in consideration." *Energy Conversion and Management* **119**: 316-326.
- Xu, Z., M. Jia, G. Xu and Y. Chang (2019). *Computational Optimization of Syngas/Diesel RCCI Combustion at Low Load in Different Engine Size*, SAE International.
- Zahidi, M. K., M. R. Hanipah, D. Ramasamy, M. Noor, K. Kadirgama and M. Rahman (2017). *The two-stroke poppet valve engine. Part 1: Intake and exhaust ports flow experimental assessments*. IOP Conference Series: Materials Science and Engineering, IOP Publishing.
- Zhao, J. (2017). "Research and application of over-expansion cycle (Atkinson and Miller) engines – A review." *Applied Energy* **185**: 300-319.
- Zhao, J., Q. Xi, S. Wang and S. Wang (2018). "Improving the partial-load fuel economy of 4-cylinder SI engines by combining variable valve timing and cylinder-deactivation through double intake manifolds." *Applied Thermal Engineering* **141**: 245-256.



اونيورسيتي ملايسيا قهغ

UNIVERSITI MALAYSIA PAHANG

APPENDIX A
PORT FLOW ASSESSMENT

Table 5.1 Intake Valve Flow Coefficient

Valve Lift, VL (m)	Valve Diameter, VD (m)	VL/VD	Flow Coefficient
0.0000	0.020	0.000	0.0000
0.0005	0.020	0.025	0.0264
0.0010	0.020	0.050	0.1054
0.0015	0.020	0.075	0.1659
0.0020	0.020	0.100	0.2466
0.0025	0.020	0.125	0.2993
0.0030	0.020	0.150	0.3365
0.0035	0.020	0.175	0.3582
0.0040	0.020	0.200	0.3768
0.0045	0.020	0.225	0.3877
0.0050	0.020	0.250	0.3970

Table 5.2 Exhaust Valve Flow Coefficient

Valve Lift, VL (m)	Valve Diameter, VD (m)	VL/VD	Flow Coefficient
0.0000	0.020	0.000	0.0000
0.0005	0.020	0.028	0.0651
0.0010	0.020	0.056	0.1320
0.0015	0.020	0.083	0.2083
0.0020	0.020	0.111	0.2790
0.0025	0.020	0.139	0.3403
0.0030	0.020	0.167	0.3738
0.0035	0.020	0.194	0.4017
0.0040	0.020	0.222	0.4184
0.0045	0.020	0.250	0.4134
0.0050	0.020	0.278	0.4407

اونیورسیتی ملیسیا قهغ

UNIVERSITI MALAYSIA PAHANG

APPENDIX B

Table 5.3 FVT Valve Lift Profile Parameters

Parameter	Unit	Baseline	FVT									
Engine Speed	RPM	Entire Speed	1000	2000	3000	4000	5000	6000	7000	8000	9000	10 000
Intake Valve	Opening	at CA°	319	319	319	319	319	319	299	299	299	299
	Closing	at CA°	639	619	619	619	619	639	659	659	659	659
	Maximum Lift	mm	2.74	2.57	2.57	2.57	2.91	2.91	2.91	2.91	2.91	2.91
	Duration	CA°	320	300	300	300	300	300	320	360	360	360
Exhaust Valve	Opening	at CA°	89	109	109	109	109	109	109	109	109	109
	Closing	at CA°	409	389	389	409	409	409	429	429	429	429
	Maximum Lift	mm	2.74	2.91	2.91	2.57	2.91	2.91	2.91	2.91	2.91	2.91
	Duration	CA°	320	280	280	300	300	300	300	320	320	320
Valve Overlap	mm	90	70	70	90	90	90	90	130	130	130	130

اونیورسیتی ملیسیا قهق

UNIVERSITI MALAYSIA PAHANG

APPENDIX C

Table 5.4 FVT Valve Lift Events Modification Attribute

Parameter		FVT									
Engine Speed		1000	2000	3000	4000	5000	6000	7000	8000	9000	10 000
Intake Valve	Opening	-	-	-	-	-	-	Advanced	Advanced	Advanced	Advanced
	Closing	Advanced	Advanced	Advanced	Advanced	Advanced	-	Retarded	Retarded	Retarded	Retarded
	Maximum Lift	Low-Lift	Low-Lift	Low-Lift	High-Lift	High-Lift	High-Lift	High-Lift	High-Lift	High-Lift	High-Lift
	Duration	Reduced	Reduced	Reduced	Reduced	Reduced	-	Increased	Increased	Increased	Increased
Exhaust Valve	Opening	Retarded	Retarded	Retarded	Retarded	Retarded	Retarded	Retarded	Retarded	Retarded	Retarded
	Closing	Advanced	Advanced	-	-	-	-	Retarded	Retarded	Retarded	Retarded
	Maximum Lift	High-Lift	High-Lift	Low-Lift	High-Lift	High-Lift	High-Lift	High-Lift	High-Lift	High-Lift	High-Lift
	Duration	Reduced	Reduced	Reduced	Reduced	Reduced	Reduced	-	-	-	-
Valve Overlap		Reduced	Reduced	-	-	-	-	Increased	Increased	Increased	Increased

اونیورسیتی ملیسیا قهق

UNIVERSITI MALAYSIA PAHANG

APPENDIX D

Table 5.5 Summary of Positive Impact of Valve Timing Strategies on FVT Engine Performance

Speed [RPM]	1000	2000	3000	4000	5000	6000	7000	8000	9000	10 000
Valve Timing Strategy	Positive Impact on Engine Performance									
EIVO	-	-	-	-	-	-	+	+	+	+
LIVO	-	-	-	-	-	-	-	-	-	-
EIVC	+	+	+	+	+	-	-	-	-	-
LIVC	-	-	-	-	-	-	+	+	+	+
High-Lift IV	-	-	-	+	+	+	+	+	+	+
Low-Lift IV	+	+	+	-	-	-	-	-	-	-
EEVO	-	-	-	-	-	-	-	-	-	-
LEVO	+	+	+	+	+	+	+	+	+	+
EEVC	+	+	-	-	-	-	-	-	-	-
LEVC	-	-	-	-	-	-	+	+	+	+
High-Lift EV	+	+	-	+	+	+	+	+	+	+
Low-Lift EV	-	-	+	-	-	-	-	-	-	-

Table 5.6 Summary of Positive Impact of Valve Timing Strategy on Engine Performance

Speed [RPM]	1000	2000	3000	4000	5000	6000	7000	8000	9000	10 000
Valve Timing Strategy	Positive Impact on Engine Performance									
EIVO	+	+	+	+	+	+	+	+	+	+
LIVO	-	-	-	-	-	-	-	-	-	-
EIVC	+	+	+	+	+	+	-	-	-	-
LIVC	-	-	-	-	-	+	+	+	+	+
EEVO	-	-	-	-	-	-	-	+	+	+
LEVO	-	-	-	-	-	+	+	+	+	+
EEVC	-	-	-	-	-	-	-	-	-	-
LEVC	-	-	-	+	+	+	+	+	+	+

Source: (Rosli 2018)